

Claremont Colleges

## Scholarship @ Claremont

---

KGI Theses and Dissertations

KGI Student Scholarship

---

Spring 5-13-2023

# The Development of a Primer Payload with Microparticles for UTI Pathogen Identification Using Polythymidine- Modified LAMP Primers in Droplet LAMP

Jonas Otoo

Follow this and additional works at: [https://scholarship.claremont.edu/kgi\\_theses](https://scholarship.claremont.edu/kgi_theses)



Part of the [Biotechnology Commons](#), [Computer-Aided Engineering and Design Commons](#), [Molecular, Cellular, and Tissue Engineering Commons](#), [Other Immunology and Infectious Disease Commons](#), and the [Pathogenic Microbiology Commons](#)

---

### Recommended Citation

Otoo, Jonas. (2023). *The Development of a Primer Payload with Microparticles for UTI Pathogen Identification Using Polythymidine- Modified LAMP Primers in Droplet LAMP*. KGI Theses and Dissertations, 29. [https://scholarship.claremont.edu/kgi\\_theses/29](https://scholarship.claremont.edu/kgi_theses/29).

This Open Access Dissertation is brought to you for free and open access by the KGI Student Scholarship at Scholarship @ Claremont. It has been accepted for inclusion in KGI Theses and Dissertations by an authorized administrator of Scholarship @ Claremont. For more information, please contact [scholarship@cuc.claremont.edu](mailto:scholarship@cuc.claremont.edu).



The Development of a Primer Payload with Microparticles  
for UTI Pathogen Identification Using Polythymidine-  
Modified LAMP Primers in Droplet LAMP

By

**Jonas Afotey Otoo**

A Dissertation submitted to the Faculty of Keck Graduate Institute  
of Applied Life Sciences in partial fulfillment of the requirements  
for the degree of

Doctor of Philosophy in Applied Life Sciences.

Keck Graduate Institute,

Claremont CA

2023

Approved by:

\_\_\_\_\_

Travis Schlappi, PhD

(Principal Investigator, Chair)

Copyright by Jonas Afotey Otoo, 2023

All Rights Reserved

## OFFICE OF THE REGISTRAR

# PhD Dissertation Completion Form

We, the undersigned, certify that we have read this dissertation of Jonas A. Otoo 972228576  
*Name and ID#*  
and approve it as adequate in scope and quality for the degree of Doctor of Philosophy.

Dissertation Committee:

**Travis Schlappi***(Typed name of Chair), Chair***Travis  
Schlappi***Signature*Digitally signed by Travis  
Schlappi  
Date: 2023.05.09 22:41:01  
-07'00'**Anna Hickerson***(Typed name), Member***Anna  
Hickerson***Signature*Digitally signed by Anna  
Hickerson  
Date: 2023.05.10 11:41:42  
-07'00'**Tochukwu D Anyaduba***(Typed name), Member***Tochukwu Dubem  
Anyaduba***Signature*Digitally signed by Tochukwu  
Dubem Anyaduba  
Date: 2023.05.10 11:58:51  
-07'00'**James Sterling***(Typed name), Visiting Examiner***James D.  
Sterling***Signature*Digitally signed by James D.  
Sterling  
Date: 2023.05.10 13:01:40  
-07'00'**James Sterling***(Typed name), PhD Program Director***James D.  
Sterling***Signature*Digitally signed by James D.  
Sterling  
Date: 2023.05.10 13:02:48  
-07'00'

Abstract

# The Development of a Primer Payload with Microparticles for UTI Pathogen Identification Using Polythymidine-Modified LAMP Primers in Droplet LAMP

By

Jonas Afotey Otoo

Keck Graduate Institute of Applied Life Sciences: 2023

Nucleic acid amplification tests (NAATs) are among the diagnostic tests with the highest sensitivity and specificity. However, they are more complex to develop than other diagnostic tests such as biochemical tests and lateral flow immunoassay tests. Polymerase chain reaction (PCR) is the gold standard for NAATs. PCR requires thermal cycling to achieve clonal amplification of the target pathogen DNA for diagnosis. Thermal cycling poses a challenge in the development of PCR diagnostics for point-of-care (POC) settings. Loop-mediated isothermal amplification (LAMP) offers an isothermal method for NAATs diagnostics. The advancement of the microfluidics field significantly enhances the development of LAMP diagnostics devices for POC testing. Another challenge with NAATs, is the limitation in the development of multiplex NAATs. Multiplexing however, occupies an important role in the efforts to address the antimicrobial resistance global crisis. Multiplexing will help to provide more thorough and complete diagnostics of

infections, and enable doctors to prescribe the most effective antibiotics to the patients. This will help slow the emergence of antibiotic resistant pathogens.

We are currently in a period of discovery void, with regards to antibiotics discovery. At this rate, more pathogens are becoming resistant to the antibiotics that we have, faster than we are developing new classes of antibiotics. According to the World Health Organization (WHO) interagency coordination group on AMR report to the secretary general of the United Nations, by 2050, there will be 10 million annual deaths globally, as a result of AMR-related events. There will also be \$55 billion productivity losses globally due to AMR. In addition, there will be a total of \$ 1 trillion in healthcare costs, and 28 million people will be living in poverty, as a result of the economic impact of uncontrolled AMR. Another area where multiplex diagnostics play a crucial role is infection control in the era of epidemics and pandemics. The increasing prevailing frequency of global pandemics stresses the need for the development of highly accurate and decentralized POC diagnostics. Over the last ten years, there have been more than 30 epidemics and pandemics around the world, including SARS-CoV-2, Monkey pox, India black fungus, Dengue fever, Measles, Zika, Avian influenza, Influenza A and Ebola. With advancing technology and international commerce and relations, we are now more connected than ever. This means that if there are no developments to make molecular tests more accessible at the POC, the future waves of epidemics and pandemics will have faster spread, further reach and more devastating impacts on the lives of the 8 billion people on our planet.

We have developed a diagnostic method for executing droplet microfluidics LAMP via a microparticle primer payload mechanism and have demonstrated it with urinary tract infection (UTI) pathogens. With inspiration from overhang PCR and RNA-Seq, we

engineered LAMP primers with 5' polythymidine (PolyT) oligonucleotide (PolyT is placed in the middle of the Forward inner primers and Backward inner primers). The PolyT sequence is recognized by a biotinylated capture oligonucleotide engineered with a polyadenylated (PolyA) polynucleotide on the 3' end. The streptavidin-coated microparticles functionalized with the PolyA oligonucleotide and PolyT primers, capture their specific target DNA and deliver the cargo into emulsion droplets of LAMP reagents for amplification. This platform provides the ability to multiplex by coding specific pathogen target DNA with different fluorescent signatures of the microparticles.

## Dedication

I dedicate this work to my loving family: to Mr. Roosevelt Otoo, Mrs. Sarah Otoo, Rebecca, Regina, and Gloria, for supporting me in every way possible, through a lifelong journey in school and in pursuit of my dreams. I also dedicate this work to Ebonee Rice, my wonderful fiancée, and her family for the overwhelming support I have received from them. In addition, I dedicate this work to Rev. Akrofi Otubuah, Dr. Priscilla Otubuah, and Mrs Grace Tackie-Yarboi, who have provided invaluable assistance for my spiritual and material needs throughout my doctoral program.

## Acknowledgments

Just like every worthwhile journey, this has not been an easy feat, and I could not have achieved this without the support of a myriad of people. I thank God for the grace and the strength to undertake this project.

I am deeply grateful to Dr. Schlappi, my PI, for his guidance, leadership, mentorship and support that was readily available to me as I embarked on this project. Thank you for believing in me.

I appreciate my committee, Dr. Sterling, Dr. Anyaduba and Dr. Hickerson, for guiding this work, lending their expertise, and for always providing feedback and support as I embarked on this project.

I acknowledge Natalie Barnard, Catharyne Magro, Kathryn McNevin, President Sheldon Schuster, and all the KGI professors, faculty, and staff for facilitating a conducive environment that fosters creativity and innovation.

I also thank my colleagues and friends like Bezalel, Jonathan, Uche, Ijeoma, Noa, Lydia, Elrmion, Divine, Tracy, Beatrice, Robert, Cephas, Albert, and Elliot, to name a few. This list goes on for miles, and I am grateful to each and every one of you for your support. I am also, very thankful for Victory Bible Church International Living Water City, for the community that I have enjoyed these past few years as I embarked on my studies.

Finally, I thank my family for always being there and for their incredible support.

## Published Content and My Contribution

J.A.O – Jonas A. Otoo

T.D.A – Tochukwu D. Anyaduba

K.W – Katie Wilson

T.S.S – Travis S. Schlappi

## Chapter 1

Chapter 1 covers the background of urinary tract infections and the technical background of the molecular biology tools in the infectious disease diagnostics landscape. There is an introduction of the scope and aims of this project.

## Chapter 2 (Published in MDPI Biosensors journal)

Otoo, J.A.; Schlappi, T.S. REASSURED Multiplex Diagnostics: A Critical Review and Forecast. *Biosensors* 2022, 12, 124. <https://doi.org/10.3390/bios12020124>

This paper summarizes the outlook of diagnostics devices that are on the market, and in research and academia, and the next generation of diagnostics devices that are capable of multiplex diagnostics. It also assesses the extent to which these devices meet the WHO's REASSURED criteria. Finally, it examines what the gaps are in the field of diagnostics and what the ideal diagnostic device presents. I am the first author of this manuscript.

## Author Contributions

Conceptualization, J.A.O.; methodology, J.A.O.; investigation, J.A.O.; resources, T.S.S.; data curation, J.A.O.; writing—original draft preparation, J.A.O.; writing—review and

editing, J.A.O. and T.S.S.; visualization, J.A.O.; supervision, T.S.S.; funding acquisition, T.S.S. All authors have read and agreed to the published version of the manuscript.

Chapter 3 (Published in MDPI Micromachines journal)

Anyaduba, T.D.; Otoo, J.A.; Schlappi, T.S. Picoliter Droplet Generation and Dense Bead-in-Droplet Encapsulation via Microfluidic Devices Fabricated via 3D Printed Molds.

Micromachines 2022, 13, 1946. <https://doi.org/10.3390/mi13111946>

This paper presents a 3D-printing method for the fabrication of a microfluidics cartridge for picoliter scale droplet generation. The device is used to develop a droplet digital LAMP assay. We also demonstrate dense bead encapsulation method with less than 2% percent of droplets having more than 1 bead. I am the second author of this manuscript.

Author Contributions

Conceptualization, T.D.A. and T.S.S.; methodology, T.D.A.; software, T.D.A.; validation, T.D.A. and J.A.O.; formal analysis, T.D.A., J.A.O. and T.S.S.; investigation, T.D.A. and J.A.O.; resources, T.S.S.; data curation, T.D.A. and J.A.O.; writing, T.S.S., T.D.A. and J.A.O.; visualization, T.D.A., T.S.S. and J.A.O.; supervision, T.S.S.; project administration, T.S.S. and T.D.A.; funding acquisition, T.S.S. and T.D.A. All authors have read and agreed to the published version of the manuscript.

Chapter 4

\*Not yet published

Primer payload with microparticles for pathogen identification using Polythymidine-modified LAMP primers in droplet LAMP

Jonas A. Otoo, Tochukwu D. Anyaduba, Katie Wilson, Travis S. Schlappi\*

This paper describes a droplet LAMP assay for pathogen identification. Polythymidine modifications of LAMP primers are employed as anchors to latch onto and deliver primers and target DNA into discrete droplets for amplification and detection.

Microparticles are serve as the primer payload carriers.

#### Author Contribution

The collaborators for this paper are T.D.A., K.W. and T.S.S. I am the first author of this paper. The roles that I held in this paper were the contribution to the conceptualization and development of the theoretical framework; the experimental design and execution and analysis of data.

## Contents

Acknowledgments.....	viii
Published Content and My Contribution .....	ix
Contents .....	xii
List of Abbreviations .....	xiv
List of Figures .....	xvi
List of Tables .....	xvii
List of Supplementary Figures.....	xvii
List of Supplementary Tables .....	xviii
Chapter 1 Introduction .....	1
1.1 Background of UTI.....	1
1.2 Technical Background .....	2
1.3 Project Aims: .....	7
1.4 References.....	8
Chapter 2 REASSURED Multiplex Diagnostics: A Critical Review and Forecast.....	12
2.1 Introduction.....	13
2.1.3 Clinically Available Multiplexed Diagnostics .....	20
2.1.4 Multiplexed Diagnostics in Research or Academia .....	26
2.1.5 Next Generation Multiplex Diagnostics .....	28
2.2 Discussion.....	30
2.3 References.....	34
2.4 Supplementary Information .....	51
Chapter 3 Picolitre Droplet Generation and Dense Bead-in-Droplet Encapsulation via Microfluidic Devices Fabricated via 3D Printed Molds .....	54
3.1 Introduction.....	55
3.2 Materials and Methods.....	59
3.3 Results and Discussion .....	65
3.4 Conclusions.....	71
3.4 References.....	75
3.5 Supplementary Information .....	87
Chapter 4 Primer payload with microparticles for pathogen identification using Polythymidine- modified LAMP primers in droplet LAMP .....	96
4.1 Introduction.....	96
4.2 Experimental section.....	101

4.3 Results and discussion .....	106
4.4 References.....	114
4.5 Supplementary Information .....	118
Chapter 5 Challenges and Other Projects .....	123
5.1 PMMA beads encapsulation .....	123
5.2 Gel beads primer payload delivery .....	125
5.3 Colorimetric droplet LAMP.....	126
5.4 Multiplexed bead-in-droplet LAMP .....	128
5.5 Reference .....	131
Chapter 6 Conclusion.....	132
6.1 Conclusion .....	132
6.2 Recommendation .....	133

## List of Abbreviations

Abbreviation	Meaning
AMR	Antimicrobial Resistance
ASSURED	Affordable, Sensitive, Specific, User-friendly, Rapid and Robust, Equipment-Free, and Deliverable
BiD	Bead-in-Droplet (also called Microparticle-in-Droplet)
BIP	Reverse Inner Primer
BOP	Reverse Outer Primer
CAD	Computer-aided Design
cDNA	Complementary Deoxyribonucleic Acid
CFU	Colony-Forming Unit
CLIA	Clinical Laboratory Improvement Amendments
COVID-19	Coronavirus Disease 2019
CRISPR	Clustered Regularly Interspaced Short Palindromic Repeats
DI	Deionized
dLAMP	Digital Loop-Mediated Isothermal Amplification
DNA	Deoxyribonucleic Acid
dNAAT	Digital Nucleic Acid Amplification and Testing
dNTPs	Deoxyribonucleotide Triphosphates
EDC	1-Ethyl-3-(3-Dimethylaminopropyl) Carbodiimide
ELISA	Enzyme-Linked Immunosorbent Assay
EUA	Emergency Use Authorization
FDA	Food and Drugs Administration
FIND	Foundation for Innovative New Diagnostics
FIP	Forward Inner Primers
fL	Femtoliter
FOP	Forward Outer Primer
GBS	Group B Streptococcus
HDA	Helicase-Dependent Amplification
LAMP	Loop-Mediated Isothermal Amplification
LFA	Lateral Flow Assay
LOD	Limit Of Detection
LoopB	Reverse Loop Primer
LoopF	Forward Loop Primer
MELISA	Mobile Enzyme-Linked Immunosorbent Assay
MES	M 2-(N-Morpholino)-Ethanesulfonic Acid
mL	Milliliter
NAAT	Nucleic Acid Amplification and Testing
NASBA	Nucleic Acid Sequence-Based Amplification
NEB	New England Biolabs
nL	Nanoliter
NTC	No Template Controls
PADs	Paper-Based Analytical Devices
PCR	Polymerase Chain Reaction

PDMS	Polydimethyl Siloxane
pL	Picoliter
PloyT	Polythymidine
PMMA	Polymethylmethacrylate
POC	Point-Of-Care
PolyA	Polyadenylated
qPCR	Quantitative Polymerase Chain Reaction
REASSURED	Real-time connectivity, Ease of specimen collection, Affordable, Sensitive, Specific, User-friendly, Rapid and Robust, Equipment-Free, and Deliverable
RFU	Relative Fluorescence Units
RNA	Ribonucleic Acid
RPA	Recombinase Polymerase Amplification
RPM	Revolutions per Minute
RT-PCR	Real-time Polymerase Chain Reaction
SARS-CoV-2	Severe Acute Respiratory Syndrome Coronavirus 2
SIMPLE	Self-powered Integrated Microfluidic Point-of-care Low-cost Enabling
SLA	Stereolithography
sp	Species
TBST	Tris-Buffered Saline with Tween 20
TE	Tris-EDTA Buffer
uL	Microliter
um	Micrometer
uTAS	Micro Total Analysis Systems
UTI	Urinary Tract Infection
VFA	Vertical Flow Assay
WHO	World Health Organization
wt	Weight

---

## List of Figures

Figure 2.1. Annual publications related to diagnostics compared to annual publications related to multiplex diagnostics from 1950 to 2021 from the PubMed database (National Center for Biotechnology Information).....	17
Figure 2.2 The timeline of antibiotics class discovery/development and onset of antimicrobial resistance reproduced from [29]. .....	18
Figure 2.3 Clinical diagnostics devices scored on the REASSURED scoring scheme: <b>A</b> Visby Medical Sexual Health reproduced with permission from Visby Medical ( <a href="https://www.visbymedical.com/">https://www.visbymedical.com/</a> ). <b>B</b> . Curo L7 reproduced with permission from Curofit ( <a href="https://curofit.com/">https://curofit.com/</a> ). .....	22
Figure 2.4 Multiplex diagnostics systems in research and academia. <b>A</b> . Smartphone ELISA plate reader system reproduced from [56] <b>B</b> . FGAS system reproduced from [76] with permission from the Royal Society of Chemistry <b>C</b> . Smartphone-based ELISA-on-a-chip reproduced from [74], with the permission of AIP Publishing. <b>D</b> . MELISA platform reproduced from [57] with permission from the Biosensors and Bioelectronics <b>E</b> . RespiDisk system reproduced from [77] <b>F</b> . IoT-based diagnostic system reproduced [78] with permission from the Biosensors and Bioelectronics. ....	27
Figure 3.1 Microfluidic device design and fabrication. <b>(A)</b> A solid master mold was designed with Solidworks CAD software and printed with FormLabs Form3 SLA printer. <b>(B)</b> PDMS device fabrication process.....	60
Figure 3.2 Picolitre-scale droplet generation. <b>(A)</b> Micrograph of the droplets retrieved from microfluidic cartridge outlet. <b>(B)</b> Droplet diameter distribution and CV at each flow condition. <b>(C)</b> The droplet diameter changes with volumetric flow rate of the oil phase. The volumetric flow rate of the aqueous phase was kept constant at 1 $\mu\text{L}/\text{min}$ . .....	67
Figure 3.3. Droplet digital LAMP. <b>(A)</b> Post-amplification micrographs of droplets. <b>(B)</b> Agreement between Poisson predicted positive droplet percentage and experimental data.....	68
Figure 3.4 Dense bead in droplet (BiD) encapsulation at varying bead concentrations ( $\lambda = 0.15, 0.2, 0.3$ ). <b>(A)</b> Microscope images of BiD. <b>(B)</b> Poisson-predicted bead in droplets distribution in comparison to the observed experimental data. ....	70
Figure 4.1 Schematic of functionalized microparticle for primer payload mechanism. ....	100
Figure 4.2 Schematic of a functionalized microparticle with captured DNA, encapsulated in a droplet of LAMP reagents for droplet LAMP reaction.....	106
Figure 4.3 The impact of the PolyT modification of <i>E. coli</i> primers on their sensitivity in a LAMP reaction. The placement of the PolyT modification in the FIP and BIP primers are crucial. ....	107
Figure 4.4 PCR reaction testing the ability of the functionalized microparticles to capture their target DNA.....	108
Figure 4.5 <b>A</b> . Pseudo-colored confocal microscopy fluorescent image of microparticles functionalized with ATTO 633 primers. <b>B</b> . Confocal image of microparticles that are not functionalized with ATTO 633 primers. <b>C</b> . Schematic of a microparticle functionalized with ATTO 633 polyT primers. ....	109
Figure 4.6 <b>A</b> . Fluorescent and <b>B</b> . Brightfield images of droplet LAMP with microparticles functionalized with <i>E. coli</i> DNA and <i>E. coli</i> primers. <b>C</b> . Fluorescent and <b>D</b> . Brightfield images of droplet LAMP with microparticles functionalized with <i>P. aeruginosa</i> DNA and <i>P. aeruginosa</i> primers. <b>E</b> . Fluorescent and <b>F</b> . Brightfield images of droplet LAMP with microparticles functionalized with GBS DNA and GBS primers. ....	110

Figure 4.7 A. Fluorescent and B. Brightfield images of droplet LAMP with microparticles functionalized with <i>E. coli</i> DNA (194 copies/uL) and <i>E. coli</i> primers. A. Fluorescent and B. Brightfield images of droplet LAMP with microparticles functionalized with <i>E. coli</i> DNA (9.71 x 10 <sup>3</sup> copies/uL) and <i>E. coli</i> primers.....	112
Figure 4.8 A. Fluorescent and B. Brightfield images of droplet LAMP with microparticles functionalized with GBS DNA (concentration) and <i>E. coli</i> primers. C. Fluorescent and D. Brightfield images of droplet LAMP with microparticles functionalized with <i>E. coli</i> DNA (concentration) and GBS primers. E. Fluorescent and F. Brightfield images of droplet LAMP with microparticles functionalized with <i>P. aeruginosa</i> DNA (concentration) and GBS primers. G. Fluorescent and H. Brightfield images of droplet LAMP with microparticles functionalized with GBS DNA (concentration) and <i>P. aeruginosa</i> primers. I. Fluorescent and J. Brightfield images of droplet LAMP with microparticles functionalized with <i>E. coli</i> DNA (concentration) and <i>P. aeruginosa</i> primers. K. Fluorescent and L. Brightfield images of droplet LAMP with microparticles functionalized with <i>P. aeruginosa</i> DNA (concentration) and <i>E. coli</i> primers. ....	113
Figure 5.1 A. Microfluidic cartridge channel clogged with 20 um PMMA beads. B. Broken PMMA beads in the microfluidic cartridge channel going into being encapsulated into droplets. ....	123
Figure 5.2 A. Comparing the sedimentation rate of microparticles in 16.5% Optiprep in water versus microparticles in just water. B One hour into Comparing the sedimentation rate of microparticles in 16.5% Optiprep in water versus microparticles in just water. C. Microparticle-in-droplet encapsulation with 16.5% Optiprep. ....	124
Figure 5.3 Dissolvable polyacrylamide gel beads. ....	126
Figure 5.4 A. Droplet LAMP using Eriochrome Black T (EBT) as indicator showing no color change. B. Droplet LAMP using NEB colorimetric LAMP master mix, showing faint pink (no DNA amplification) droplets and faint yellow (presence of DNA amplification) droplets.....	127
Figure 5.5 A. Streptavidin coated beads functionalized with biotinylated ATTO 633 primers and visualized under confocal microscopy. B. Non-functionalized bead visualized under fluorescent microscopy, for negative control. ....	129
Figure 5.6 Depicting the behavior of fluorescent beads in the reaction tube compared to the transparent beads.....	130

## List of Tables

Table 2-1 The REASSURED scoring scheme of 9 multiplex clinically available diagnostics. The scoring was assigned on a 1 to 3 scale based on developed criteria (Table S1, SX). The total score was obtained by finding the average score across all the elements of the REASSURED and expressing the value as a percentage of 3. ....	25
---	----

## List of Supplementary Figures

Figure S 3.1 . (A) Tube connecting syringe containing bead suspension to the droplet generation cartridge; red arrow shows region of bead sedimentation. (B) Syringe design for mechanical resuspension and homogenization of dense particles for vertical delivery. The DC motor is powered using a 3V battery. ....	88
---	----

Figure S 3.2 Without the syringe mixer in Fig. S1, bead sedimentation happens in the syringe and tubing, leading to the encapsulation of multiple beads per droplet.....	89
Figure S 3.3 . Denser fluids, such as glycerol, may improve bead buoyancy but it inhibits LAMP amplification (blue trace vs red trace). Bead Density = 1.18 g/ cm <sup>3</sup> , Glycerol Density = 1.26 g/cm <sup>3</sup> . .....	91
Figure S 3.4 Microcapillary lines imprinted by 3D printed mold. This is often due to printer-head misalignment that often occurred during prolonged prints. ....	93
Figure S 3.5 Micrograph showing curved vertices imprinted from 3D-printed mold .....	94
Figure S 3.6 Irregularities in chamber dimensions due to myriad factors, including incompletely cured PDMS and build-up PDMS deposit due to mold reuse. Note that the displayed images contain channels designed to have widths of 50 and 100 um .....	94
Figure S 3.7 Frosted PDMS molded on improperly cleaned 3D printed mold.....	95
Figure S 4.1 Testing the analytical specificity of E. coli polyT primers and P. aeruginosa polyT primer. B. Testing the analytical specificity of E. coli polyT primers and GBS polyT primer. C. Testing the analytical specificity GBS polyT primers and P. aeruginosa polyT primer.....	120
Figure S 4.2 Schematic LAMP reaction .....	121
Figure S 4.3 Schematic of LAMP reaction with PolyT primers. The reaction stops at step 9 when the PolyT modification of FIP and BIP are placed at the 5' end. ....	122

### List of Supplementary Tables

Table S 2-1 Scoring scheme for assessing diagnostics on the REASSURED criteria. The scoring ranges from 3 to 1, 3 being the highest score and 1 being the lowest score. ....	51
Table S 2-2 Scoring scheme of clinical diagnostics on the REASSURED criteria. Averages were calculated from the scores of the individual elements of the REASSURED criteria. The Overall score was calculated by expressing the average score as a percentage of 3, the highest achievable average score.....	52
Table S 4-1 Primer Sequences .....	118
Table S 4-2 Primer dilution for 100 uL final volume .....	119
Table S 4-3 PCR profile.....	119

# Chapter 1 Introduction

## 1.1 Background of UTI

Urinary tract infections (UTIs) are among the most common types of bacterial infections [1], [2]. They occur when bacteria enter and colonize the urinary tract. UTI can affect the bladder, urethra, and ureters [3]. The symptoms of UTI include a fever of  $\geq 38^{\circ}\text{C}$ , confusion, increased frequency and urgency of urination, pain or burning during urination, dysuria, pyuria, strong-smelling urine, and lower abdominal pain or back pain [2], [4]. These symptoms can be very subtle and are non-specific to UTI. Women are more predisposed to UTI infections than men due to the structure of the female anatomy. While anyone can develop the infection, studies show that older people are more susceptible to UTI. Some complications that can occur as a consequence of UTI are antimicrobial resistance, elevated risk of pyelonephritis, and fetal mortality during pregnancy. A study by Price et. al, stated that most antibiotic treatments are for UTIs [5]. This, therefore, has a significant impact on the current global AMR crisis.

Urinary tract infections are typically diagnosed through a combination of clinical symptoms, physical examination, and laboratory testing. A person is diagnosed with UTI when their urine sample yields a midstream urine culture of  $\geq 100,000$  CFU/mL [3]. There are about nine different groups of pathogens that can cause UTIs [6], [7]. They are Uropathogenic *E. coli*, *K. pneumoniae*, *Candida* sp., *S. aureus*, *P. mirabilis*, *P. aeruginosa*, *S. saprophyticus*, *Enterococcus* sp., and Group B *Streptococcus*. The gold standard for UTI diagnosis is midstream urine culture [8], [9]. Other methods for UTI diagnosis are urinalysis, the use of dipstick tests, diagnostics algorithms, and urine microscopy. These traditional methods have some limitations leading to a gap in accurate and timely diagnosis.

For example, urine cultures have long turnaround times and can miss infections in asymptomatic individuals, while dipstick tests may have limited accuracy and low specificity. Urine microscopy has low specificity, as it is not able to differentiate between pathogens. Furthermore, the results of urine microscopy are subjective as it depends on the observation and expertise of the technician [8]. There are currently no standardized diagnostic algorithms for UTI diagnosis as the algorithms are typically developed in-house by hospitals and clinics. In addition, diagnostic algorithms have low sensitivity and cannot provide any specificity. Central labs in hospitals and clinics have the capabilities to use Nucleic Acid Amplification Tests (NAATs) methods such as polymerase chain reaction (PCR) to diagnose UTIs. NAATs are expensive, and central labs are not readily accessible to many patients, especially patients in limited recourse settings. NAATs, also require upstream sample preparation steps, which adds additional levels of complexity for UTI diagnostics. Some NAATs have thermal cycling processes requiring additional instrumentation, increasing the costs of these tests. Isothermal NAATs with integrated sample preparation, are therefore better suited for use at the point-of-care (POC) or limited resource setting.

## 1.2 Technical Background

### *1.2.1 Polymerase Chain Reaction*

Quantitative polymerase chain reaction (qPCR) is the gold standard for NAATs [10]. It is a molecular biology technique used to clonally amplify and detect DNA sequences for diagnostic purposes. A master mix of certain components is required for a qPCR reaction. They include the template, which is the DNA of interest; pH buffers; short synthetic oligonucleotides known as primers; a heat-stable DNA polymerase, magnesium ions which

will serve as cofactors for the polymerase; and nuclease-free water. When the template of interest is an RNA instead of DNA, a variation of PCR known as reverse transcriptase PCR (RT-PCR) is used. In RT-PCR, complementary DNA (cDNA) is first synthesized from the RNA strand using reverse transcriptase enzyme. This is then followed by conventional PCR.

There are three main steps that occur in qPCR: denaturation, annealing, and extension. Denaturation is when the double-stranded DNA sample is heated to a high temperature, usually around 95°C, to separate the double strands. This is followed by annealing. In the annealing step, the primers are hybridized to single strands of DNA, by lowering the reaction temperature to about 55°C. These primers serve as starting points for DNA amplification. The third step is the extension. An enzyme called Taq polymerase synthesizes new DNA strands complementary to the original DNA strands. This step of the reaction is incubated at a higher temperature, usually around 72°C, which allows the DNA polymerase to efficiently synthesize the new DNA strands.

The cycles of denaturation, annealing, and extension are repeated several times, leading to exponential amplification of the target DNA. The end product is clonally amplified copies of the specific target DNA sequence, which will now be present at detectable concentrations. qPCR is widely used in diagnostics. However, it is not ideal for diagnostics in the POC setting because it requires thermal cycling. The additional instrumentational necessary for thermal cycling adds to the cost and complexity when developing diagnostics.

### *1.2.2 Loop-mediated isothermal amplification*

Loop-mediated isothermal amplification (LAMP) is a nucleic acid amplification technique that enables the amplification of DNA or RNA in a single reaction step under isothermal conditions [11]. LAMP reaction requires 4 to 6 primers. They are the two outer primers known as forward outer primer (FOP) and backward outer primer (BOP), two inner primers known as forward inner primer (FIP) and backward inner primer (BIP), and two loop primers known as forward loop (LOOPF) and backward loop (LOOPB) primers. The loop primers are optional since the reaction is able to proceed without their addition. LAMP also requires a heat-stable DNA polymerase to target a specific region of the genome and amplify it. The reaction is carried out at a constant temperature of around 65 - 68 °C, allowing for efficient strand displacement synthesis, resulting in exponential amplification of the target DNA. Since LAMP occurs at a lower temperature than the denaturation in qPCR, the DNA strands are separated enzymatically by the polymerase and single-strand binding proteins.

LAMP has been demonstrated to have some advantages over traditional PCR. It has faster reaction times. LAMP has the capability to amplify RNA as well as DNA in a single reaction. Moreover, the use of 4 – 6 primers increases the specificity of LAMP. It can also be performed in low-resource settings, such as in developing countries or in the field, as it does not require specialized equipment for thermal cycling. LAMP is also more robust than PCR [11], [12]. This is because the reaction is less sensitive to impurities than qPCR. As a result, LAMP can be performed on crude samples such as cell lysates, while PCR requires purified DNA.

Other isothermal nucleic acid amplification methods include Nucleic Acid Sequence-based Amplification (NASBA), Recombinase Polymerase Amplification (RPA), and Transcription-mediated Amplification (TMA). However, LAMP has shown more robustness and specificity, compared to qPCR

### *1.2.3 Microfluidics*

Microfluidics is the study and manipulation of fluids in micrometer volumes. Microfluidics applications are used in fields such as molecular biology, biosensing, and microelectronics. In the area of diagnostics, microfluidics applications such as lab-on-a-chip, present the possibility of automation, integration, and high-throughput analysis. There is also the potential for multiplexing, that is, detecting multiple biomarkers simultaneously in a single reaction. This can significantly improve accuracy, reduce costs, and make diagnostics more accessible for patients in the POC setting [13]– [15].

### *1.2.4 Droplet digital LAMP*

Digital Loop-Mediated Isothermal Amplification (dLAMP) is the application of microfluidics techniques in the LAMP by creating compartments of the LAMP reaction mixture and the target DNA, with each compartment serving as a unique reaction chamber. When the compartments used are droplets, it is known as droplet LAMP. Droplet LAMP involves the employment of droplet generation techniques to partition a mixture of LAMP reagents and target into discrete volumes of droplets in an immiscible phase, which is typically oil [16], [17]. This enables the compartmentalization of the LAMP reaction into discrete reactions. Droplet digital LAMP facilitates single molecule detection and can be used for quantification of the target DNA. Droplet digital LAMP is an avenue for massively parallel and high throughput analysis of samples. This, therefore, presents the potential for

multiplex applications in the analysis of samples for diagnostics. The types of droplet formation techniques used include crossflow, co-flow, and flow focusing.

Biological samples often have a limited number of copies of pathogen DNA. There is about 1 to 100,000 CFU/mL of pathogens in blood for sepsis diagnosis and about 100,000 CFU/mL in urine for UTI diagnosis [3], [18]. The distribution of target nucleic acids into droplets occurs stochastically. There is a certain probability that each droplet will receive zero or a discrete number of copies of the target nucleic acid. This probability distribution can be predicted or estimated by Poisson statistics.

#### *1.2.5 Fabrication of microfluidics with PDMS*

The process of fabrication of microfluidics devices falls under a technique called micro total analysis systems (uTAS). This is sometimes referred to as lab-on-a-chip. Some methods used in the fabrication of microfluidic devices are photolithography and soft lithography [19]. In photolithography, microchannels and structures are etched on a substrate such as a silicon wafer, by shooting light through a photomask onto the silicon wafer. In soft lithography, molds with microstructures are created, and those molds are used to create microchannels onto substrates like polydimethylsiloxane (PDMS). PDMS is a silicone-based polymer that is widely used as a material for microfluidic devices because of its unique properties [20]. It has a low surface tension, which makes it ideal for creating small fluidic channels in microfluidic devices. The material is soft and flexible, which allows it to conform to the shapes of the mold used to fabricate the device. Additionally, PDMS is transparent, which allows for visual inspection of the fluidic channels and the contents of the device. This makes it ideal for the fabrication of microfluidic devices. PDMS is also a biocompatible material, and hence, would not interfere with biomolecules

in bioassays. PDMS can be modified by adding other chemical groups to the polymer chain, which can produce properties such as an increase in its mechanical strength, and hydrophobicity [20], [21].

A major challenge in the development of NATs for UTI diagnostics is the development of the capability for multiplex detection of multiple pathogens. Multiplexing is particularly important because it saves cost and time. It also provides the capability for target differentiation and the ability to identify all the pathogens present in the same sample. This will ultimately equip doctors with the information to prescribe the most effective antibiotics to patients. Some studies have demonstrated diagnostic tests that are able to perform multiplex detection, by spatial multiplex [22]– [24]. However, spatial multiplex results in sample splitting, which reduces the number of available targets to be detected per reaction. This can lead to reduced sensitivity of the assay. A study by Padmavathy et. al, demonstrated a multiplex diagnostic test for UTI by PCR, without the use of spatial multiplex [25]. The challenge with these tests is that PCR requires thermal cycling, and hence there is a need for equipment components that are capable of thermal cycling.

### 1.3 Project Aims:

- To develop processes for isothermal nucleic acid amplification in droplet-bead emulsions.
- To create a POC-compatible microfluidic cartridge to execute the processes.
- To conduct preliminary verification of the device using extracted DNA.

#### 1.4 References

- [1] A. L. Flores-Mireles, J. N. Walker, M. Caparon, and S. J. Hultgren, “Urinary tract infections: epidemiology, mechanisms of infection and treatment options,” *Nat Rev Microbiol*, vol. 13, no. 5, pp. 269–284, May 2015, doi: 10.1038/nrmicro3432.
- [2] K. C. Claeys, N. Blanco, D. J. Morgan, S. Leekha, and K. V. Sullivan, “Advances and Challenges in the Diagnosis and Treatment of Urinary Tract Infections: The Need for Diagnostic Stewardship,” *Curr Infect Dis Rep*, vol. 21, no. 4, p. 11, Mar. 2019, doi: 10.1007/s11908-019-0668-7.
- [3] C. Wei Tan and M. P. Chlebicki, “Urinary tract infections in adults,” *Singapore Med J*, vol. 57, no. 9, pp. 485–490, Sep. 2016, doi: 10.11622/smedj.2016153.
- [4] N. M. Gilbert, V. P. O’Brien, S. Hultgren, G. Macones, W. G. Lewis, and A. L. Lewis, “Urinary Tract Infection as a Preventable Cause of Pregnancy Complications: Opportunities, Challenges, and a Global Call to Action,” *Glob Adv Health Med*, vol. 2, no. 5, pp. 59–69, Sep. 2013, doi: 10.7453/gahmj.2013.061.
- [5] T. K. Price, E. E. Hilt, T. J. Dune, E. R. Mueller, A. J. Wolfe, and L. Brubaker, “Urine trouble: should we think differently about UTI?,” *Int Urogynecol J*, vol. 29, no. 2, pp. 205–210, Feb. 2018, doi: 10.1007/s00192-017-3528-8.
- [6] M. Medina and E. Castillo-Pino, “An introduction to the epidemiology and burden of urinary tract infections,” *Ther Adv Urol*, vol. 11, May 2019, doi: 10.1177/1756287219832172.

- [7] Z. Tandogdu and F. M. E. Wagenlehner, “Global epidemiology of urinary tract infections,” *Current Opinion in Infectious Diseases*, vol. 29, no. 1, pp. 73–79, Feb. 2016, doi: 10.1097/QCO.0000000000000228.
- [8] G. Schmiemann, E. Kniehl, K. Gebhardt, M. M. Matejczyk, and E. Hummers-Pradier, “The Diagnosis of Urinary Tract Infection,” *Dtsch Arztebl Int*, vol. 107, no. 21, pp. 361–367, May 2010, doi: 10.3238/arztebl.2010.0361.
- [9] S. Sathiananthamoorthy et al., “Reassessment of Routine Midstream Culture in Diagnosis of Urinary Tract Infection,” *Journal of Clinical Microbiology*, vol. 57, no. 3, Mar. 2019, doi: 10.1128/JCM.01452-18.
- [10] T. Mosolygó, K. Laczi, G. Spengler, and K. Burián, “A Practical Approach for Quantitative Polymerase Chain Reaction, the Gold Standard in Microbiological Diagnosis,” *Sci*, vol. 4, no. 1, p. 4, Jan. 2022, doi: 10.3390/sci4010004.
- [11] T. Notomi, “Loop-mediated isothermal amplification of DNA,” *Nucleic Acids Research*, vol. 28, no. 12, pp. 63e–663, Jun. 2000, doi: 10.1093/nar/28.12.e63.
- [12] P. Francois et al., “Robustness of a loop-mediated isothermal amplification reaction for diagnostic applications,” *FEMS Immunol Med Microbiol*, vol. 62, no. 1, pp. 41–48, Jun. 2011, doi: 10.1111/j.1574-695X.2011.00785.x.
- [13] Y.-L. Lin, Y.-J. Huang, P. Teerapanich, T. Leichlé, and C.-F. Chou, “Multiplexed immunosensing and kinetics monitoring in nanofluidic devices with highly enhanced target capture efficiency,” *Biomicrofluidics*, vol. 10, no. 3, p. 034114, May 2016, doi: 10.1063/1.4953140.

- [14] X. Ye, Y. Li, L. Wang, X. Fang, and J. Kong, “All-in-one microfluidic nucleic acid diagnosis system for multiplex detection of sexually transmitted pathogens directly from genitourinary secretions,” *Talanta*, vol. 221, p. 121462, Jan. 2021, doi: 10.1016/j.talanta.2020.121462.
- [15] T. Mortelmans, D. Kazazis, C. Padeste, P. Berger, X. Li, and Y. Ekinci, “A nanofluidic device for rapid and multiplexed SARS-CoV-2 serological antibody detection,” In Review, preprint, May 2021. doi: 10.21203/rs.3.rs-537056/v1.
- [16] F. Schuler et al., “Digital droplet LAMP as a microfluidic app on standard laboratory devices,” *Analytical Methods*, vol. 8, no. 13, pp. 2750–2755, 2016, doi: 10.1039/C6AY00600K.
- [17] F. Hu et al., “Smartphone-Based Droplet Digital LAMP Device with Rapid Nucleic Acid Isolation for Highly Sensitive Point-of-Care Detection,” *Anal. Chem.*, vol. 92, no. 2, pp. 2258–2265, Jan. 2020, doi: 10.1021/acs.analchem.9b04967.
- [18] M. Sinha, J. Jupe, H. Mack, T. P. Coleman, S. M. Lawrence, and S. I. Fraley, “Emerging Technologies for Molecular Diagnosis of Sepsis,” *Clin Microbiol Rev*, vol. 31, no. 2, pp. e00089-17, Apr. 2018, doi: 10.1128/CMR.00089-17.
- [19] E. Ferrari, F. Nebuloni, M. Rasponi, and P. Occhetta, “Photo and Soft Lithography for Organ-on-Chip Applications,” in *Organ-on-a-Chip*, M. Rasponi, Ed., in *Methods in Molecular Biology*, vol. 2373. New York, NY: Springer US, 2022, pp. 1–19. doi: 10.1007/978-1-0716-1693-2\_1.

- [20] A. Shakeri, S. Khan, and T. F. Didar, “Conventional and emerging strategies for the fabrication and functionalization of PDMS-based microfluidic devices,” *Lab Chip*, vol. 21, no. 16, pp. 3053–3075, 2021, doi: 10.1039/D1LC00288K.
- [21] J. Zhou, A. V. Ellis, and N. H. Voelcker, “Recent developments in PDMS surface modification for microfluidic devices,” *Electrophoresis*, vol. 31, no. 1, pp. 2–16, Jan. 2010, doi: 10.1002/elps.200900475.
- [22] J. Chen et al., “Sensitive and rapid detection of pathogenic bacteria from urine samples using multiplex recombinase polymerase amplification,” *Lab Chip*, vol. 18, no. 16, pp. 2441–2452, Aug. 2018, doi: 10.1039/C8LC00399H.
- [23] K. J. Wojno et al., “Multiplex PCR Based Urinary Tract Infection (UTI) Analysis Compared to Traditional Urine Culture in Identifying Significant Pathogens in Symptomatic Patients,” *Urology*, vol. 136, pp. 119–126, Feb. 2020, doi: 10.1016/j.urology.2019.10.018.
- [24] N. Li, Y. Lu, J. Cheng, and Y. Xu, “A self-contained and fully integrated fluidic cassette system for multiplex nucleic acid detection of bacteriuria,” *Lab Chip*, vol. 20, no. 2, pp. 384–393, Jan. 2020, doi: 10.1039/C9LC00994A.
- [25] B. Padmavathy, R. Vinoth Kumar, A. Patel, S. Deepika Swarnam, T. Vaidehi, and B. M. Jaffar Ali, “Rapid and Sensitive Detection of Major Uropathogens in a Single-Pot Multiplex PCR Assay,” *Curr Microbiol*, vol. 65, no. 1, pp. 44–53, Jul. 2012, doi: 10.1007/s00284-012-0126-3.

# Chapter 2 REASSURED Multiplex Diagnostics: A Critical Review and Forecast

Jonas A. Otoo and Travis S. Schlappi \*

<sup>1</sup> Keck Graduate Institute; jotoo18@students.kgi.edu

<sup>2</sup> Keck Graduate Institute; tschlappi@kgi.edu

\* Correspondence: tschlappi@kgi.edu

**Abstract:** Diagnosis of infectious diseases is ineffective when the diagnostic test does not meet one or more of the necessary standards of affordability, accessibility, and accuracy. The World Health Organization further clarifies these standards with a set of criteria that has the acronym ASSURED. The advancement of the digital age has led to a revision of the ASSURED criteria to REASSURED: Real-time connectivity, Ease of specimen collection, Affordable, Sensitive, Specific, User-friendly, Rapid and robust, Equipment-free or simple, and Deliverable to end-users. Many diagnostic tests have been developed that aim to satisfy the REASSURED criteria, however most of them only detect a single target. With the progression of syndromic infections, coinfections and the current antimicrobial resistance challenges, the need for multiplexed diagnostics is now more important than ever. This review summarizes current diagnostic technologies for multiplexed detection and forecasts which methods have promise for detecting multiple targets and meeting all REASSURED criteria.

**Keywords:** diagnostics; multiplex; point-of-care diagnostics; REASSURED

## 2.1 Introduction

Clinical diagnostics are devices or methods that are used to detect biomarkers in the genome, proteome and metabolome for diagnosis, subclassification, prognosis, susceptibility risk assessment, treatment selection, and response to therapy monitoring[1], [2]. Biomarker analytes include nucleic acids, proteins, peptides, lipids, metabolites, and other small molecules[3], [4]. Diagnostic tests are generally carried out in central labs, clinics, hospitals, doctors' offices, and point of care (POC) settings. Thousands of diagnostic tests have been developed over the years, with varying levels of complexity, turnaround time, cost, and other factors. While diagnostics account for less than 5% of hospital costs and ~1.6% of all Medicare costs, they influence up to 60-70% of healthcare decision-making[5]. There are several stakeholders in diagnostics, each with their own priorities: patients, healthcare providers, payers, pharmaceutical companies, diagnostic device manufacturers, local and international health organizations, governments, public health agencies, and regulatory bodies[6], [7].

In order to be FDA approved, diagnostic tests need to meet certain standards for analytical and clinical validation. Analytical validation assesses the sensitivity, specificity, accuracy, and precision of the test. Clinical validation assesses the ability of the test to achieve its intended aim. Diagnostic tests in hospital or reference labs are able to meet analytical and clinical standards for accuracy and performance because complexity and cost are not an issue. It is much more difficult for point of care diagnostics, however, which must also minimize cost and complexity in their design and manufacturing. The World Health Organization Special Program for Research and Training in Tropical Diseases (WHO/TDR) concluded in a study in 2003, that POC diagnostics should meet the

ASSURED (Affordable, Sensitive, Specific, User-Friendly, Rapid, Equipment-Free, Delivered) criteria[8]. In 2006, the WHO/TDR further recommended the ASSURED criteria as a benchmark to decide whether diagnostic tests address disease control needs[9]. The ASSURED criteria represent three main attributes that are significant for a diagnostic test. These attributes are accessibility, affordability, and accuracy. While all three attributes are important, it is very challenging for any diagnostic test to adequately possess all three. The different stakeholders in diagnostics may have varying orders of priority among the three attributes. Patients may want diagnostic tests that are first, affordable, second, accessible, and third, accurate. Healthcare providers likely prefer accuracy, accessibility, and then affordability. Governments may prioritize accessibility over affordability and accuracy. Manufacturers of diagnostics that are maximizing profits probably emphasize accessibility, accuracy, and then affordability.

In the face of the SARS-CoV-2 pandemic, the role and importance of diagnostics has become increasingly apparent. Diagnostics help to track, contain, and control the spread of infectious diseases. Several diagnostic tests were developed in the wake of the SARS-CoV-2 pandemic[10]–[13], which guided the formulation and implementation of measures that were used to protect the public, find new variants, track the disease, and slow its spread. Diagnostics have also played a major role in non-infectious diseases. Early detection of biomarkers of cancer, cardiovascular disease and metabolic diseases such as diabetes and hypertension, have reduced the mortality rate of humans over the years[14]–[17].

### *2.1.1 Multiplexed Diagnostics*

Multiplexing is the process of simultaneously detecting or identifying multiple biomarkers in a single diagnostic test, which can be valuable for several different types of diseases. For

example, pharmacogenomic studies in patients with cardiovascular disease have indicated that the presence of polymorphisms affects patients' response to various drugs[18]. Therefore, the multiplex detection of relevant biomarkers will not only provide insight of the pathophysiology of cardiovascular disease, but also provide a guide for the most efficient treatment option. Most cancers have biomarkers in common with other cancers, hence detecting multiple biomarkers is needed for accurate differentiation of cancer types or location[19], [20]. Hermann et al.[21] demonstrated that several biomarkers are significantly elevated in breast cancer patients versus patients with benign breast tumor disease. Multiplexed detection of these biomarkers enables oncologists to accurately diagnose their patients and select the appropriate therapy, thus improving patient outcomes and decreasing healthcare costs.

Infectious disease is another area where multiplexed diagnostics are extremely valuable. Most infectious diseases such as urinary tract infections and respiratory infections have multiple causative pathogens, but the resulting symptoms do not indicate the causative pathogen. On the other hand, different types of infections which have shared symptoms could be misdiagnosed or incompletely diagnosed. For example, SARS-CoV-2 and influenza A or B present with many of the same symptoms and clinical features[22], [23]. Studies show that there is the prevalence of influenza coinfection among people with SARS-CoV-2 is 0.4% in the United States of America and 4.5% in Asia[24]. In a case study of 1986 patients that presented with Severe Acute Respiratory Infection (SARI), 14.3%, 8.8% and 0.3% had SARS-Cov-2, influenza and SARS-Cov-2/influenza coinfection respectively[25]. In another study, 40% of a cohort of Kenyans who sought treatment for fever were presumed to have malaria and received malaria medicines even

though they actually had HIV[26]. Incomplete diagnosis of infectious disease leads to inefficient treatments by exposing some pathogens to sub-lethal doses or the wrong antibiotics. This contributes to the emergence of antimicrobial resistance and recurrent infections as well as persistent secondary infections[27], [28]. The last two classes of antibiotics were discovered in 1987 and 2004[29], and since then, we are in a period of discovery void while there is rapid emergence of antimicrobial pathogens to the antibiotics that currently exist (Figure 2.2). According to O'Neil[30], 10 million people will die annually due to antimicrobial resistance (AMR) by 2050. Furthermore, AMR-related costs and the associated loss of productivity amount to about \$55 billion annually in the US alone[31]. Better diagnostics and treatment for tuberculosis could save 770,000 lives over the course of 2015 to 2025[30], while a malaria test could save ~2.2 million lives and prevent ~447 million unnecessary treatments per year[32]. The introduction of antibiotics increased the average lifespan of humankind by 23 years since the first introduction of antibiotics, thus showing the drastic consequences if we were to lose the use of antibiotics that we currently have[29]. Another instance where multiplexing is crucial is the diagnosis of blood infections. Sepsis resulting from blood infections can be caused by many pathogens and becomes increasingly fatal over time, with mortality increasing by 7.6% for every hour that goes by without receiving the correct antibiotic[33]. Accurately identifying which pathogen(s) is responsible for the blood infection is therefore a race against time to start the antibiotic therapy before sepsis becomes fatal[34]. The diagnosis of infections should therefore be approached by syndromic diagnosis, wherein all the potential pathogens for an infection or symptom are investigated rather than tested for just the most likely pathogen and then doing other tests if negative[35], [36]. Multiplexed diagnostic

tests—wherein one sample is simultaneously tested for multiple pathogens in the same device—are essential for blood infections now, and important to combat AMR for all types of infections in the future. A query on the PubMed database of the National Center for Biotechnology Information (NCBI) suggests that researchers have become increasingly more interested in multiplex diagnostics (Figure 2.1).

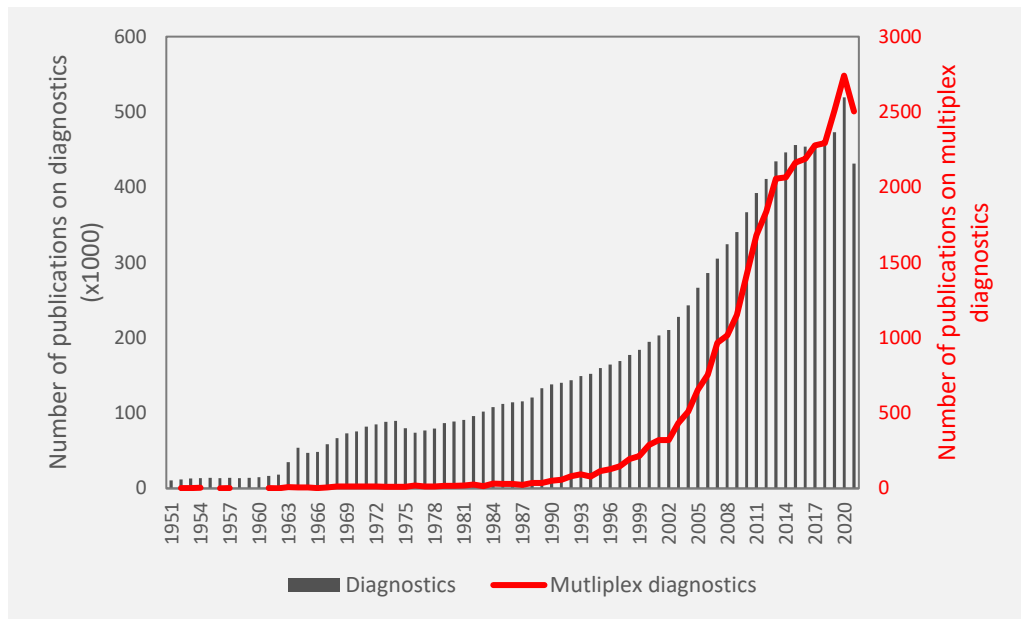


*Figure 2.1. Annual publications related to diagnostics compared to annual publications related to multiplex diagnostics from 1950 to 2021 from the PubMed database (National Center for Biotechnology Information)*

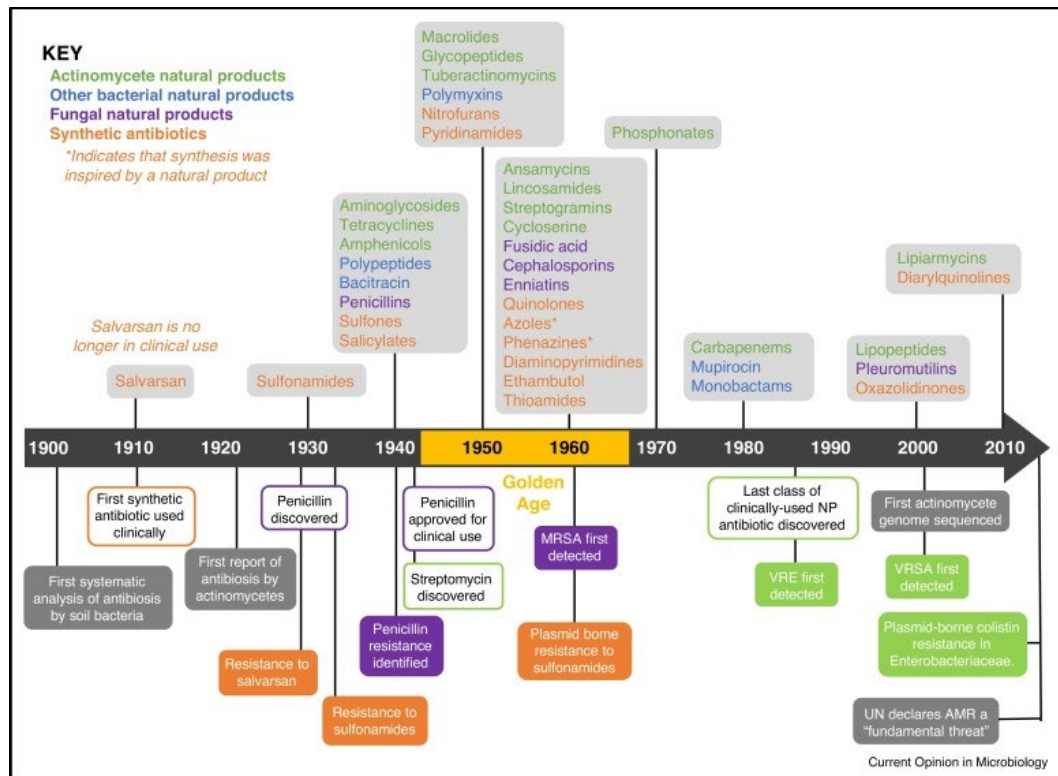


Figure 2.2 The timeline of antibiotics class discovery/development and onset of antimicrobial resistance reproduced from [29].

### 2.1.2. REASSURED Diagnostics

Considering the advances in digital technology and mobile health, a new REASSURED (Real-time connectivity, Ease of specimen collection, Affordable, Sensitive, Specific, User-Friendly, Rapid and Robust, Equipment free or simple Environmentally friendly, Deliverable to end-users) framework has been proposed as the benchmark for diagnostic systems[37]. Diagnosis of a disease is just the first step. The information from the diagnosis results needs to be used to inform actionable steps to treat or manage the disease. In a remote setting where a healthcare professional is not readily accessible, real-time connectivity provides the avenue to transmit the results to the healthcare professional for medical advice. Furthermore, having a reader that can provide the results of a diagnostic

test is important especially in ambiguous cases where there is uncertainty due to variation in the interpretation of the results. A reader will serve as a standardized way to state the results of the diagnostic test[38]–[40].

Development of diagnostic tests that meet all the ASSURED criteria but uses hard-to-obtain samples such as venous blood will not be very helpful in the absence of a trained professional to obtain the sample. It is therefore very crucial that, when possible, diagnostic tests should be developed to use easy-to-obtain and non-invasive samples such as finger pricks, nasal or oral swabs, or urine samples.

While all the elements of the REASSURED criteria are important for POC diagnostics, it is challenging for any diagnostic device to embody all of these elements and trade-offs are often made in one or more elements to achieve other elements. For instance, nucleic acid testing (NAT) is very sensitive and specific, but often requires purification or isolation of the nucleic acid, concentration of the nucleic acid, amplification, and detection of the nucleic acid[41]–[43]. These processes can be achieved by through user steps or by the introduction of equipment components that can execute them. On the other hand, antigen-based diagnostics such as a lateral flow assay, are not as sensitive and specific as NAT, but are far more user-friendly, affordable, rapid, and deliverable[44]. In these two scenarios, some degree of sensitivity and specificity could be traded for the affordability, user-friendliness, and equipment complexity of the diagnostic test by detecting antigens instead of nucleic acids.

Naseri *et al*[45] have summarized POC devices based on lateral flow assays (LFAs) and paper-based analytical devices (PADs) technology that were developed in the last 10 years for common human viral infection diagnostics. Dincer *et al.* [46] presented a survey of the

existing multiplexed POC tests in academia and industry, while Kim et al[47] summarized current POC tests for multiplex molecular testing of syndromic infections; however, these reviews focused mainly on POC diagnostics rather than summarizing devices that meet REASSURED criteria. Here, we present the current state of multiplexed diagnostic technology that meet REASSURED criteria based an in-house developed scoring scheme. This review will summarize multiplexed diagnostics in three categories: i) clinically used, ii) in academia or research only, and iii) next generation technology. We then discuss the limitations in developing multiplexed REASSURED diagnostics, present current gaps in technology, and describe needs for future research and development. For the purpose of this review, clinical diagnostics refer to diagnostics that have been approved by the FDA (including Emergency Use Authorization) or have a CE marking and are available for patient diagnosis.

### 2.1.3 Clinically Available Multiplexed Diagnostics

#### *2.1.3.1 Proteins and Peptides*

Multiplex detection of select protein or peptide biomarkers in human samples such as blood, serum, saliva and urine for clinical diagnosis, while very important, presents with a challenging puzzle: human samples typically have a myriad of diverse proteins and peptides[48], only some of which are the protein of interest. Accurately differentiating the select protein biomarkers out of the matrix is challenging due the occurrence of cross-reactivity[49]. Advancement in technology has made it possible for some immunoassays to be adapted to the point of care setting for multiplex peptide and protein biomarker detection. LFAs use a variety of detection techniques such as fluorescent immunoassays (FIA), chemiluminescence immunoassay[50] and colorimetric immune assays[51] for

detection of protein and peptide biomarkers. While LFAs have lower sensitivity compared to molecular diagnostic tests[52], they are rapid, and relatively cheaper to fabricate compared to other diagnostics[53]. LFAs were the first tests that meet the WHO ASSURED criteria[44], [54]. They are typically equipment free or are accompanied by a simple reader with a digital interface. When immunoassays such as LFAs have a colorimetric read-out, the interpretation of the results is subjective to the person who is reading the results. This may be problematic in cases where the biomarkers being detected are present in low concentrations. Utilizing a simple reader in conjunction with these LFAs will promote an objective and a more accurate interpretation of the results. This will also enable the LFAs to satisfy the REASSURED criteria.

Enzyme-Linked Immunosorbent Assays (ELISAs) are a highly sensitive method for the detection of protein and peptide biomarkers. ELISA are very prone to interferences[55] which pose challenges to developing multiplex test. This challenge is overcome through the use of spatial multiplexing approaches such as wells and microarrays[56], [57]. To avoid false positive tests as a result of non-specific interactions, there are multiple wash steps in ELISA assays. Automation of ELISAs for adoption to the POC and limited resource settings is therefore challenging because complex equipment components are required for fluid handling to execute wash steps. Furthermore, to avoid false negative tests, there are lengthy incubation periods in ELISA assays. It is therefore very challenging to adapt ELISAs for point of care diagnostics that fit the REASSURED criteria.

The BinaxNOW influenza A and B card 2 developed by Abbott is a multiplex immunochromatographic LFA that is able to provide rapid differential diagnosis of influenza A and B infection[58]. This test is designed to be read by the DIGIVAL reader

for results interpretation. The DIGIVAL reader is portable, and battery powered, making it suitable for limited resource settings. Becton and Dickinson's (BD) Veritor™ Flu A + B with analyzer distinguishes between influenzas A and B as well. The BD test analyzer is palm sized and battery powered and hence suitable for use at remote and limited resource settings[59]. Acucy influenza A and B test developed by Sekisui diagnostics comes with portable battery-powered reader as well[60]. Quidel's Sofia 2 Flu + SARS antigen FIA test is a multiplex fluorescent immunoassay for detection and differentiating SARS-Cov-2, influenzas A and B[61]. The Sofia 2 reader is portable but is not battery powered. It is suitable for a point of care settings but may not be fitting for a remote or limited resource setting. There appears to be a trend of LFA diagnostics being accompanied by readers and real-time connectivity[38]–[40], hence rapidly adapting and meeting the REASSURED criteria.

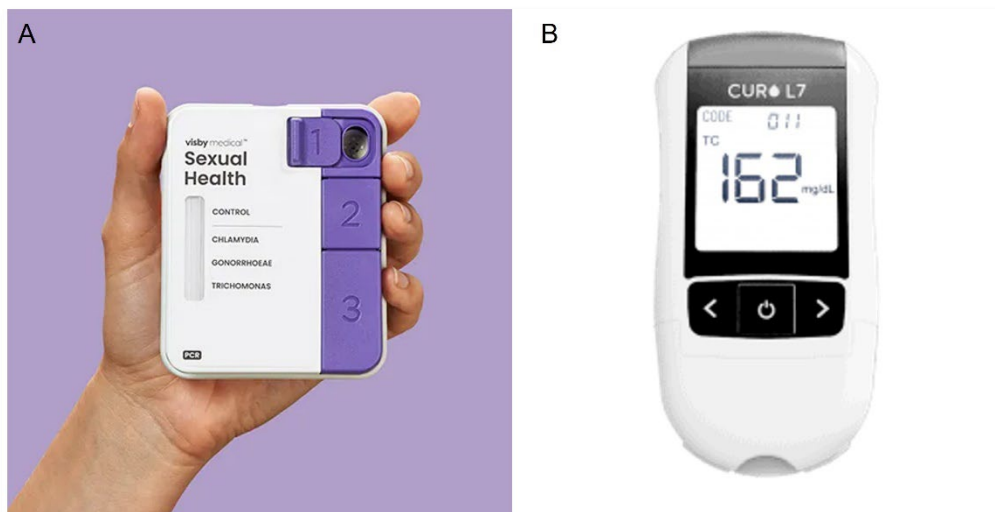


*Figure 2.3 Clinical diagnostics devices scored on the REASSURED scoring scheme: A Visby Medical Sexual Health reproduced with permission from Visby Medical*

(<https://www.visbymedical.com/>). **B. Curo L7** reproduced with permission from Curofit (<https://curofit.com/>).

### 2.1.3.2 Nucleic Acids

Polymerase chain reaction (PCR) is the gold standard amplification method for molecular diagnostic assays for clinical use. PCR based diagnostics assays are robust and can use crude samples such as blood[62]. The key obstacle preventing PCR NATs from meeting all of the ASSURED criteria is that multiple temperatures are required for the amplification of target NAs. Device components that can perform thermal cycling are therefore necessary when developing a PCR-based diagnostic device. On the other hand, isothermal amplification such as loop-mediated isothermal amplification (LAMP) and recombinase polymerase amplification (RPA) do not require thermal cycling[63], [64]. The sensitivity of LAMP is not affected when the nucleic acid sample is impure and has other crude components such as proteins and other cellular components[65].

The Accula dock developed by Mesa Biotech (now a part of Thermo Fisher Scientific), is a portable sample-to-answer molecular diagnostic device that uses Mesa Biotech's proprietary PCR technology OSCillating amplification reaction (OSCAR)[66]. The Accula systems operates with a test cassette in which the multiplexed nucleic acid detection occurs. The Accula Flu A and Flu B is CLIA waived multiplexed test for the detection of influenzas A and B, and the device has a 510K FDA clearance[67]. The disposable test cassette together with the dock are a portable system that checks nearly all the criteria for REASSURED diagnostics.

The Visby Medical Sexual Health (Figure 2.3A) developed by Visby Medical is a handheld device that is capable of rapid multiplexed PCR for the detection of *Chlamydia*

*trachomatis*, *Neisseria gonorrhoeae*, and *Trichomonas vaginalis*[68]. The Visby Medical Sexual Health device recently received CLIA waiver and FDA clearance. The device is a disposable sample-to-answer diagnostic which makes it adaptable for point of care testing and in remote setting. Visby medical's diagnostic device can be adaptable to any form of multiplexed molecular diagnostic test, as the Visby Medical COVID-19 test has been granted Emergency Use Authorization (EUA) by the FDA for use by authorized labs[69].

Biomeme's Franklin three9 is a rechargeable battery-operated mobile thermocycler which is capable of multiplexed detection of nucleic acids and adaptable to limited resource settings. It is capable of PCR, (Reverse Transcriptase PCR) RT-PCR, (quantitative) qPCR and isothermal amplification. Franklin is not a sample-to-answer platform as it requires upstream steps sample preparation. However, the sample preparation steps can be achieved in about 1-2 minutes using Biomeme's M1 sample-prep cartridge kits. The Franklin system has Bluetooth and wireless connection capability and is accompanied by an intuitive companion mobile App that facilitates wireless programing and managing of experiments[70].

#### *2.1.3.3 Small Molecules, Lipids, and Other Biomarkers*

CardioChek PA Analyzer by PTS Diagnostics is a portable handheld diagnostic device that is battery operated. It works in conjunction with panels test strips measure single and multiplex analytes. The CardioChek PA analyzer and test strips can measure total cholesterol, high density lipoproteins, triglycerides and glucose and provide results in 45 to 90 seconds. The test strips stable at room temperature[71].

Curofit's Curo L7 meter (Figure 2.3B) is capable of multiplex runs with up to 6 simultaneous tests with cholesterol test strip. The device is handheld and battery-powered

and is able to deliver results directly from sample. The Curo L7 meter is suitable for point of care and low resource settings[72].

*Table 2-1 The REASSURED scoring scheme of 9 multiplex clinically available diagnostics. The scoring was assigned on a 1 to 3 scale based on developed criteria (Table S1, SX). The total score was obtained by finding the average score across all the elements of the REASSURED and expressing the value as a percentage of 3.*

<b>TEST</b>	<b>R</b>	<b>E</b>	<b>A</b>	<b>S</b>	<b>S</b>	<b>U</b>	<b>R</b>	<b>E</b>	<b>D</b>	<b>SCORE</b>
<b>Accula dock Flu A/Flu B Test</b>	3	3	1	2	2	3	3	1	3	78%
<b>Visby Medical Sexual Health</b>	3	3	-	3	3	3	3	3	3	100%
<b>Franklin three9 Covid-19</b>	3	3	3	3	3	1	3	3	3	93%
<b>Binax Now Influenza A &amp; B with DIGIVAL</b>	3	3	1	1	2	3	3	3	3	81%
<b>BD Veritor™ Flu A + B with analyzer</b>	3	3	2	1	3	3	3	3	3	89%
<b>Sofia® 2 Flu + SARS antigen FIA</b>	3	2	1	1	2	3	3	3	3	81%
<b>Acucy influenza A and B</b>	3	3	2	1	3	3	3	3	3	89%
<b>CardioChek PA Analyzer with TOTAL+HDL+GLU Panel</b>	3	3	3	-	-	3	3	3	3	100%
<b>CuroL7</b>	3	3	3	-	-	3	3	3	3	100%

## 2.1.4 Multiplexed Diagnostics in Research or Academia

### 2.1.4.1 Proteins and Peptides

There are many multiplex immunoassays (MIAs) under development and only a few have been commercialized[73]. Chen *et al*[74] demonstrated the use of smartphone camera for reading ELISA-on-a-chip assays (Figure 2.4C). Berg *et al*[56] published a cellphone-based hand-held microplate reader (Figure 2.4A) that used optical fibers to transmit data from the ELISA plates to a cell-phone camera for diagnostics at the point of care. Mobile phone-based ELISA (MELISA) is a portable system published by Zhdanov *et al*[57] (Figure 2.4D). It is a miniature version of ELISA which is capable of executing all ELISA steps as well as provide a phone-based read-out of the results. The MELISA system has multiple reaction wells and has the potential to developed into a multiplexed system. According to the publishers, the total assembly of the MELISA system cost about \$35. The system does not require any complex instrumentation; however, it uses plasma and hence required an upstream sample preparation step. Ghosh *et al*[75]described a microchannel capillary flow assay that detected malaria by a smartphone-assisted chemiluminescence-based ELISA. Perhaps, mobile phone-based ELISA platforms are the future direction for REASSURED diagnostics for protein and peptide biomarker detection.

### 2.1.4.2 Nucleic Acids

Shu *et al* [76] proposed rapid multiplexed molecular diagnostic system dubbed flow genetic analysis system (FGAS) that is capable quantitative detection of nucleic acids (Figure 2.4B). FGAS is portable and battery powered, making it suitable for low resource settings. It is coupled with a smartphone which is used for fluorescent imaging. RespiDisk (Figure 4E) is a fully automated multiplex molecular diagnostic device for respiratory tract

infections[77]. The platform is based on RT-PCR and capable of automated sample-to-answer analysis, with a turnaround time of 3 hours and 20 minutes. The RespiDisk system operates by centrifugal microfluidics. An Internet of things (IoT) based diagnostic device is presented by Nguyen *et al*[78] (Figure 4F). This platform is accompanied by an integrated microfluidic chip that is capable of running a multiplexed reverse-transcriptase LAMP (RT-LAMP) reaction. In addition, this battery-powered portable device has optical detection capability and was able to accurately detect SARS-Cov-2 from clinical samples in 33 minutes. The advanced IoT based device can be operated with a smartphone and provides real-time data to the user. It is capable of sample-to-answer analysis and hence there are only few user steps. Carter *et al* [79] presented a multiplex lateral flow microarray platform for the detection nucleic acids. This platform combined the desirable qualities of an isothermal nucleic acid test (high sensitivity, high specificity, and no thermal cycling) with the best qualities LFAs (inexpensive, rapid, and equipment-free).

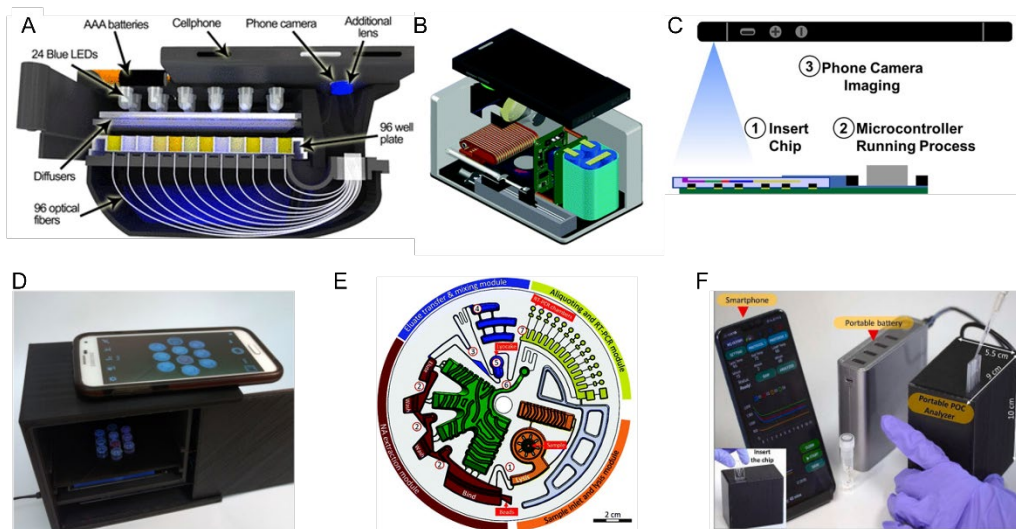


Figure 2.4 Multiplex diagnostics systems in research and academia. A. Smartphone ELISA plate reader system reproduced from [56] B. FGAS system reproduced from [76]

*with permission from the Royal Society of Chemistry* **C.** Smartphone-based ELISA-on-a-chip reproduced from [74], with the permission of AIP Publishing. **D.** MELISA platform reproduced from [57] with permission from the Biosensors and Bioelectronics **E.** RespiDisk system reproduced from [77] **F.** IoT-based diagnostic system reproduced [78] with permission from the Biosensors and Bioelectronics.

### 2.1.5 Next Generation Multiplex Diagnostics

The development of microfluidics and nanofluidics has inspired the emergence of several miniaturized platforms such as lab-on-a-chip and lab-on-a-disk. These platforms present the capabilities of molecular-scale sensitivity on low-cost and rapidly fabricated devices[80]–[82]. However, the adoption of these platforms into clinical diagnostics are yet to be realized. Yeh *et al*[83] presented a microfluidic chip called SIMPLE (Self-powered Integrated Microfluidic Point-of-care Low-cost Enabling). The SIMPLE chip is portable and completely integrated, allowing accurate quantitative detection of nucleic acids from whole blood in 30 minutes. The emergence of microfluidic technologies propelled the development of digital PCR (dPCR). dPCR offers advantages such as excellent precision[84], single copy detection, high sensitivity and absolute quantification[85]. Droplet microfluidics[86]–[88] and microarray[89], [90] are some of the techniques used to achieve multiplexing by dPCR. While not able to meet all REASSURED criteria, some dPCR techniques show potential by using a mobile phone for detection and using simple fluid handling methods[91], [92].

In recent years, a number of studies are migrating towards the application of CRISPR/Cas systems for multiplex molecular diagnostics[93]–[96]. Gootenberg *et al*[94] presents SHERLOCKv2, a multiplex platform for nucleic acid detection with high sensitivity and

specificity and is integrated with a lateral flow read out. This presents the potential for SHERLOCKv2 to be developed into a multiplex and portable platform for diagnostics. Recently, Ackerman *et al* [97] have proposed a high throughput multiplex nucleic acid detection microarray system called CARMEN-Cas13. The high sensitivity and specificity of CARMEN combined with its incredibly high throughput, endows it with the potential of being the ultimate point of care diagnostic device when integrated with upstream sample preparation and concentration steps. Rezaei *et al*[98] have recently developed a portable device for the screening of SARS-Cov-2 by RT-LAMP and followed by CRISPR/Cas12a reaction and FAM-biotin system to give a fluorescent readout in a LFA. The device is semiautomated and battery-operated. It has the potential for multiplexing and is able to produce results in about an hour. Yi *et al* presented a similar system termed CRICOLAP for detection of SARS-Cov-2 also employs an amplification step by RT-LAMP which is followed by a CRISPR/Cas12a collateral cleavage system for target recognition[99]. The paper reports a real-time parallel fluorescent readout system.

In the current digital age, next generation of diagnostics are combined with machine learning capabilities for high throughput and highly accurate results. Ballard *et al*.[100] demonstrated a multiplexed paper-based Vertical Flow Assay (VFA) platform that used a deep learning-based framework for sensing and quantifying high sensitivity C-Reactive Protein. This platform represents a low-cost device that can be adapted for molecular diagnostics at the POC and low resource settings. Machine learning-assisted dPCR has also improved diagnostic outcomes as demonstrated by Liu [101] and Miglietta [102].

## 2.2 Discussion

In the REASSURED scoring scheme (Table 1), LFAs with in-built or a combined reader had low sensitivity and specificity scores compared to molecular diagnostics but high overall scores. LFAs have been widely adopted for rapid diagnostics for decades and while they are more affordable and simpler to develop and/or use, they do not have good sensitivity and have low multiplex capacity. Most LFAs can only multiplex two or three types of biomarkers. The limitations to multiplexing capability of LFAs are due to technical and operational challenges such cross-reactivity and selection of appropriate diluents[53], [103]. Most proteins or peptides have unique charges and pH and hence, unique isoelectric points in different buffer conditions. There is therefore a challenge of selecting the appropriate buffer for the select protein and peptide biomarkers to multiplexed. In infectious diseases, acquired immune responses do not occur until several days after exposure, and the antibodies linger in the body for days after the pathogen has been cleared[104]. This makes it difficult for LFAs to distinguish between an active and inactive infection.

The reviewed molecular diagnostics demonstrated much higher multiplex capacity compared to the LFAs. Molecular diagnostics are easier to multiplex than LFAs because biomarker recognition is achieved through highly specific complementary hybridization of primers and/or probes. The quest to bring molecular diagnostic devices to the point of care setting has led to the increased focus on the miniaturization of the test systems. A major challenge that is often encountered by the miniaturization of the molecular diagnostic test platforms is the integration of sample preparation steps. Sample preparation include steps for isolation, purification, and concentration of nucleic acids from crude samples such as blood and saliva. While the execution of these steps increases the sensitivity and specificity

of molecular diagnostics, they are a major driver in the cost and complexity of these devices. Molecular diagnostics that had in-built readers or connectivity to smartphones, were completely integrated from sample to answer, and handheld and battery-powered generally scored the highest points on the multiplexed REASSURED scoring scheme.

There is a need for technology that is highly accurate but also affordable and accessible, especially in the developing world. Such a technology will not only help address the need for increased access to diagnostics but also ensure endemic and pandemic preparedness for the future. More funds need to be allocated to the development of multiplexed REASSURED diagnostics through funding by research and academic institutions, and incentivizing of research and development efforts of industry.

Point of care diagnostics development should gravitate towards more syndromic test panels such as respiratory infection panels, urinary tract infection panels, blood protein panel and STI panels. Multiplexed panel measurements rather than single panel measurements are important because they facilitate efficient and effective diagnosis of syndromic infections, accurately indicate the correct antibiotic or treatment, and minimize the number of tests that need to be run to diagnose coinfections.

Novel technologies in development that meet the REASSURED criteria should be incentivized by governments and international organizations to bring them to the market. Gene Xpert Omni, unveiled by Cepheid in 2015 and dubbed as the world's most portable molecular diagnostic system, was predicted to decentralize and increase access TB diagnosis[105], [106]. However, commercialization plans for the Gene Xpert Omni were aborted, and Cepheid has received petitions to reinstate the plan to commercialize the diagnostic system[107], [108]. The development of the Cepheid's Gene Xpert systems was

supported by the Foundation for Innovative New Diagnostics (FIND) and the National Institutes of Health (NIH), among other investors[109]. According to Gotham et al, FIND is currently evaluating the Gene Xpert Omni, and it is expected to be commercially available in 2022[109]. Cost is still an issue, however, as the lowest cost of the GeneXpert instrument is \$11,530 [111] and the per test cost averaged \$21 [112].

An ideal diagnostic case for SARS-CoV-2/Flu A & B would be a test of  $\leq$ \$1 that can simultaneously detect and differentiate between SARS-CoV-2/Flu A & B RNA in 15 to 60 minutes with a sensitivity and specificity of  $>98$  %. This test would have  $\leq 2$  user steps, all reagents prepackaged within, be equipment-free (or operated by a simple, portable, and handheld device  $\leq$ \$10), be made of environmentally friendly material, and disposable. Moreover, the device, test and its reagents would be stable at room temperature with a shelf-life of about a year. Finally, if a device is necessary beyond the disposable test itself, it would be battery or solar-powered, and able to transmit results remotely or by USB connection to a mobile phone.

Lateral flow assays meet the standards for affordability and accessibility, so improving their accuracy could be the answer. Molecular tests already have high accuracy, so a different approach would be adapting molecular tests into a REASSURED format and decreasing their cost/complexity. While there is currently no such diagnostic device, the rapid emergence of new technology such as machine-learning assisted diagnostics, CRISPR-based diagnostics and nanofluidic technology places such ideals in reach with further research and innovation.

**Author Contributions:** “Conceptualization, J.O.; methodology, J.O.; investigation, J.O.; resources, T.S.; data curation, J.O.; writing—original draft preparation, J.O.; writing—review and editing, J.O. and T.S.; visualization, J.O.; supervision, T.S.; funding acquisition, T.S. All authors have read and agreed to the published version of the manuscript.

**Funding:** This research and the APC was funded by the National Institute of Biomedical Imaging and Bioengineering of the National Institutes of Health under Award Number K01EB027718. The content is solely the responsibility of the authors and does not necessarily represent the official views of the National Institutes of Health.

**Data Availability Statement:** Not applicable.

**Conflicts of Interest:** The authors declare no conflict of interest. The funders had no role in the design of the study; in the collection, analyses, or interpretation of data; in the writing of the manuscript, or in the decision to publish the results.

### 2.3 References

- [1] G. P. Patrinos, W. Ansorge, and P. B. Danielson, Eds., *Molecular diagnostics*, Third edition. Amsterdam: Boston : Elsevier/Academic Press, 2017.
- [2] R. Mayeux, “Biomarkers: Potential uses and limitations,” *NeuroRX*, vol. 1, no. 2, pp. 182–188, Apr. 2004, doi: 10.1602/neurorx.1.2.182.
- [3] S. B. Nimse, M. D. Sonawane, K.-S. Song, and T. Kim, “Biomarker detection technologies and future directions,” *Analyst*, vol. 141, no. 3, pp. 740–755, Jan. 2016, doi: 10.1039/C5AN01790D.
- [4] P. D. Chandler *et al.*, “Lipid biomarkers and long-term risk of cancer in the Women’s Health Study,” *Am. J. Clin. Nutr.*, vol. 103, no. 6, pp. 1397–1407, Jun. 2016, doi: 10.3945/ajcn.115.124321.
- [5] The Lewin Group, Inc., “The Value of Diagnostics Innovation, Adoption and Diffusion into Health Care,” Jul. 2005. [Online]. Available: [https://www.lewin.com/content/dam/Lewin/Resources/Site\\_Sections/Publications/ValueofDiagnostics.pdf](https://www.lewin.com/content/dam/Lewin/Resources/Site_Sections/Publications/ValueofDiagnostics.pdf)
- [6] M. L. Mugambi, T. Peter, S. F. Martins, and C. Giachetti, “How to implement new diagnostic products in low-resource settings: an end-to-end framework,” *BMJ Glob. Health*, vol. 3, no. 6, p. e000914, Dec. 2018, doi: 10.1136/bmjgh-2018-000914.
- [7] Roundtable on Translating Genomic-Based Research for Health and Board on Health Sciences Policy; Institute of Medicine, “Genome-Based Diagnostics: Demonstrating Clinical Utility in Oncology: Workshop Summary. Washington (DC).”

National Academies Press (US), Dec. 27, 2013. [Online]. Available: <https://www.ncbi.nlm.nih.gov/books/NBK195902/>

[8] H. Kettler, K. White, and S. Hawkes, “Mapping the landscape of diagnostics for sexually transmitted infections: key findings and recommendations,” World Health Organization, 2004. [Online]. Available: <https://apps.who.int/iris/handle/10665/68990>

[9] R. W. Peeling, K. K. Holmes, D. Mabey, and A. Ronald, “Rapid tests for sexually transmitted infections (STIs): the way forward,” *Sex. Transm. Infect.*, vol. 82, no. suppl\_5, pp. v1–v6, Dec. 2006, doi: 10.1136/sti.2006.024265.

[10] A. Afzal *et al.*, “Rapid antibody diagnostics for SARS-CoV-2 adaptive immune response,” *Anal. Methods*, vol. 13, no. 36, pp. 4019–4037, Sep. 2021, doi: 10.1039/D1AY00888A.

[11] Y. Zhou, Y. Wu, L. Ding, X. Huang, and Y. Xiong, “Point-of-care COVID-19 diagnostics powered by lateral flow assay,” *Trends Anal. Chem.*, vol. 145, p. 116452, Dec. 2021, doi: 10.1016/j.trac.2021.116452.

[12] C. A. Hogan *et al.*, “Comparison of the Accula SARS-CoV-2 Test with a Laboratory-Developed Assay for Detection of SARS-CoV-2 RNA in Clinical Nasopharyngeal Specimens,” *J. Clin. Microbiol.*, vol. 58, no. 8, Jul. 2020, doi: 10.1128/JCM.01072-20.

[13] D. D. Rhoads, S. S. Cherian, K. Roman, L. M. Stempak, C. L. Schmotzer, and N. Sadri, “Comparison of Abbott ID Now, DiaSorin Simplexa, and CDC FDA Emergency Use Authorization Methods for the Detection of SARS-CoV-2 from Nasopharyngeal and

Nasal Swabs from Individuals Diagnosed with COVID-19,” *J. Clin. Microbiol.*, vol. 58, no. 8, Jul. 2020, doi: 10.1128/JCM.00760-20.

[14] C. V. Trinidad, A. L. Tetlow, L. E. Bantis, and A. K. Godwin, “Reducing Ovarian Cancer Mortality Through Early Detection: Approaches Using Circulating Biomarkers,” *Cancer Prev. Res. (Phila. Pa.)*, vol. 13, no. 3, pp. 241–252, Mar. 2020, doi: 10.1158/1940-6207.CAPR-19-0184.

[15] V. McCormack and A. Aggarwal, “Early cancer diagnosis: reaching targets across whole populations amidst setbacks,” *Br. J. Cancer*, vol. 124, no. 7, pp. 1181–1182, Mar. 2021, doi: 10.1038/s41416-021-01276-2.

[16] W. H. Herman *et al.*, “Early Detection and Treatment of Type 2 Diabetes Reduce Cardiovascular Morbidity and Mortality: A Simulation of the Results of the Anglo-Danish-Dutch Study of Intensive Treatment in People With Screen-Detected Diabetes in Primary Care (ADDITION-Europe),” *Diabetes Care*, vol. 38, no. 8, pp. 1449–1455, Aug. 2015, doi: 10.2337/dc14-2459.

[17] L. Capotosto, F. Massoni, S. De Sio, S. Ricci, and A. Vitarelli, “Early Diagnosis of Cardiovascular Diseases in Workers: Role of Standard and Advanced Echocardiography,” *BioMed Res. Int.*, vol. 2018, p. e7354691, Jan. 2018, doi: 10.1155/2018/7354691.

[18] M. Adamcova and F. Šimko, “Multiplex biomarker approach to cardiovascular diseases,” *Acta Pharmacol. Sin.*, vol. 39, no. 7, pp. 1068–1072, Jul. 2018, doi: 10.1038/aps.2018.29.

[19] M. H. Witte, M. T. Dellinger, C. M. Papendieck, and F. Boccardo, “Overlapping biomarkers, pathways, processes and syndromes in lymphatic development, growth and

neoplasia,” *Clin. Exp. Metastasis*, vol. 29, no. 7, pp. 707–727, Oct. 2012, doi: 10.1007/s10585-012-9493-1.

[20] S. Kumar, A. Mohan, and R. Guleria, “Biomarkers in cancer screening, research and detection: present and future: a review,” *Biomarkers*, vol. 11, no. 5, pp. 385–405, Jan. 2006, doi: 10.1080/13547500600775011.

[21] N. Hermann *et al.*, “Diagnostic relevance of a novel multiplex immunoassay panel in breast cancer,” *Tumor Biol.*, vol. 39, no. 6, p. 1010428317711381, Jun. 2017, doi: 10.1177/1010428317711381.

[22] J. W. Tang, P. A. Tambyah, and D. S. C. Hui, “Emergence of a novel coronavirus causing respiratory illness from Wuhan, China,” *J. Infect.*, vol. 80, no. 3, pp. 350–371, Mar. 2020, doi: 10.1016/j.jinf.2020.01.014.

[23] H. Khorramdelazad, M. H. Kazemi, A. Najafi, M. Keykhaee, R. Zolfaghari Emameh, and R. Falak, “Immunopathological similarities between COVID-19 and influenza: Investigating the consequences of Co-infection,” *Microb. Pathog.*, vol. 152, p. 104554, Mar. 2021, doi: 10.1016/j.micpath.2020.104554.

[24] M. Dadashi *et al.*, “COVID-19 and Influenza Co-infection: A Systematic Review and Meta-Analysis,” *Front. Med.*, vol. 8, p. 681469, Jun. 2021, doi: 10.3389/fmed.2021.681469.

[25] Z. Akhtar *et al.*, “SARS-CoV-2 and influenza virus coinfection among patients with severe acute respiratory infection during the first wave of COVID-19 pandemic in Bangladesh: a hospital-based descriptive study,” *BMJ Open*, vol. 11, no. 11, p. e053768, Nov. 2021, doi: 10.1136/bmjopen-2021-053768.

- [26] E. J. Sanders *et al.*, “Most adults seek urgent healthcare when acquiring HIV-1 and are frequently treated for malaria in coastal Kenya,” *AIDS*, vol. 25, no. 9, pp. 1219–1224, Jun. 2011, doi: 10.1097/QAD.0b013e3283474ed5.
- [27] A. Multani *et al.*, “Missed diagnosis and misdiagnosis of infectious diseases in hematopoietic cell transplant recipients: an autopsy study,” *Blood Adv.*, vol. 3, no. 22, pp. 3602–3612, Nov. 2019, doi: 10.1182/bloodadvances.2019000634.
- [28] I. Levin-Reisman, A. Brauner, I. Ronin, and N. Q. Balaban, “Epistasis between antibiotic tolerance, persistence, and resistance mutations,” *Proc. Natl. Acad. Sci.*, vol. 116, no. 29, pp. 14734–14739, Jul. 2019, doi: 10.1073/pnas.1906169116.
- [29] M. I. Hutchings, A. W. Truman, and B. Wilkinson, “Antibiotics: past, present and future,” *Curr. Opin. Microbiol.*, vol. 51, pp. 72–80, Oct. 2019, doi: 10.1016/j.mib.2019.10.008.
- [30] J. O’Neill, “Tackling drug-resistant infections globally: final report and recommendations,” May 2016. [Online]. Available: [https://amr-review.org/sites/default/files/160525\\_Final%20paper\\_with%20cover.pdf](https://amr-review.org/sites/default/files/160525_Final%20paper_with%20cover.pdf)
- [31] A. K. Nanayakkara, H. W. Boucher, V. G. Fowler Jr, A. Jezek, K. Outterson, and D. E. Greenberg, “Antibiotic resistance in the patient with cancer: Escalating challenges and paths forward,” *CA. Cancer J. Clin.*, vol. 71, no. 6, pp. 488–504, 2021, doi: 10.3322/caac.21697.
- [32] M. Urdea *et al.*, “Requirements for high impact diagnostics in the developing world,” *Nature*, vol. 444, no. 1, pp. 73–79, Nov. 2006, doi: 10.1038/nature05448.

- [33] A. Kumar *et al.*, “Duration of hypotension before initiation of effective antimicrobial therapy is the critical determinant of survival in human septic shock\*,” *Crit. Care Med.*, vol. 34, no. 6, pp. 1589–1596, Jun. 2006, doi: 10.1097/01.CCM.0000217961.75225.E9.
- [34] G. A. Westphal *et al.*, “Reduced mortality after the implementation of a protocol for the early detection of severe sepsis,” *J. Crit. Care*, vol. 26, no. 1, pp. 76–81, Feb. 2011, doi: 10.1016/j.jcrc.2010.08.001.
- [35] V. Wiwanitkit and H. Err, ““Syndromic approach” to diagnosis and treatment of critical tropical infections,” *Indian J. Crit. Care Med.*, vol. 18, no. 7, pp. 479–479, Jul. 2014, doi: 10.4103/0972-5229.136082.
- [36] G. Djomand *et al.*, “Genital infections and syndromic diagnosis among HIV-infected women in HIV care programmes in Kenya,” *Int. J. STD AIDS*, vol. 27, no. 1, pp. 19–24, Jan. 2016, doi: 10.1177/0956462415568982.
- [37] K. J. Land, D. I. Boeras, X.-S. Chen, A. R. Ramsay, and R. W. Peeling, “REASSURED diagnostics to inform disease control strategies, strengthen health systems and improve patient outcomes,” *Nat. Microbiol.*, vol. 4, no. 1, pp. 46–54, Jan. 2019, doi: 10.1038/s41564-018-0295-3.
- [38] T. Mahmoudi, M. Pourhassan-Moghaddam, B. Shirdel, B. Baradaran, E. Morales-Narváez, and H. Golmohammadi, “On-Site Detection of Carcinoembryonic Antigen in Human Serum,” *Biosensors*, vol. 11, no. 10, p. 392, Oct. 2021, doi: 10.3390/bios11100392.
- [39] C. Ruppert, N. Phogat, S. Laufer, M. Kohl, and H.-P. Deigner, “A smartphone readout system for gold nanoparticle-based lateral flow assays: application to monitoring

of digoxigenin,” *Microchim. Acta*, vol. 186, no. 2, p. 119, Feb. 2019, doi: 10.1007/s00604-018-3195-6.

[40] L. Saisin, R. Amarit, A. Somboonkaew, O. Gajanandana, O. Himananto, and B. Sutapun, “Significant Sensitivity Improvement for Camera-Based Lateral Flow Immunoassay Readers,” *Sensors*, vol. 18, no. 11, p. 4026, Nov. 2018, doi: 10.3390/s18114026.

[41] L. J. Scott, “Verigene® Gram-Positive Blood Culture Nucleic Acid Test: An In Vitro Diagnostic Assay for Identification of Gram-Positive Bacteria Associated with Bloodstream Infections and Bacterial Resistance Markers,” *Mol. Diagn. Ther.*, vol. 17, no. 2, pp. 117–122, Apr. 2013, doi: 10.1007/s40291-013-0021-z.

[42] C. Xie *et al.*, “Comparison of different samples for 2019 novel coronavirus detection by nucleic acid amplification tests,” *Int. J. Infect. Dis.*, vol. 93, pp. 264–267, Apr. 2020, doi: 10.1016/j.ijid.2020.02.050.

[43] H. V. Nguyen, V. D. Nguyen, H. Q. Nguyen, T. H. T. Chau, E. Y. Lee, and T. S. Seo, “Nucleic acid diagnostics on the total integrated lab-on-a-disc for point-of-care testing,” *Biosens. Bioelectron.*, vol. 141, p. 111466, Sep. 2019, doi: 10.1016/j.bios.2019.111466.

[44] F. Di Nardo, M. Chiarello, S. Cavalera, C. Baggiani, and L. Anfossi, “Ten Years of Lateral Flow Immunoassay Technique Applications: Trends, Challenges and Future Perspectives,” *Sensors*, vol. 21, no. 15, p. 5185, Jul. 2021, doi: 10.3390/s21155185.

- [45] M. Naseri, Z. M. Ziora, G. P. Simon, and W. Batchelor, “ASSURED-compliant point-of-care diagnostics for the detection of human viral infections,” *Rev. Med. Virol.*, vol. n/a, no. n/a, p. e2263, doi: 10.1002/rmv.2263.
- [46] C. Dincer, R. Bruch, A. Kling, P. S. Dittrich, and G. A. Urban, “Multiplexed Point-of-Care Testing – xPOCT,” *Trends Biotechnol.*, vol. 35, no. 8, pp. 728–742, Aug. 2017, doi: 10.1016/j.tibtech.2017.03.013.
- [47] H. Kim, H. J. Huh, E. Park, D.-R. Chung, and M. Kang, “Multiplex Molecular Point-of-Care Test for Syndromic Infectious Diseases,” *BioChip J.*, vol. 15, no. 1, pp. 14–22, Mar. 2021, doi: 10.1007/s13206-021-00004-5.
- [48] J. F. Rusling, “Multiplexed Electrochemical Protein Detection and Translation to Personalized Cancer Diagnostics,” *Anal. Chem.*, vol. 85, no. 11, pp. 5304–5310, Jun. 2013, doi: 10.1021/ac401058v.
- [49] A. C. Felix *et al.*, “Cross reactivity of commercial anti-dengue immunoassays in patients with acute Zika virus infection,” *J. Med. Virol.*, vol. 89, no. 8, pp. 1477–1479, 2017, doi: 10.1002/jmv.24789.
- [50] J. Deng, M. Yang, J. Wu, W. Zhang, and X. Jiang, “A Self-Contained Chemiluminescent Lateral Flow Assay for Point-of-Care Testing,” *Anal. Chem.*, vol. 90, no. 15, pp. 9132–9137, Aug. 2018, doi: 10.1021/acs.analchem.8b01543.
- [51] J. Park, “An Optimized Colorimetric Readout Method for Lateral Flow Immunoassays,” *Sensors*, vol. 18, no. 12, p. 4084, Nov. 2018, doi: 10.3390/s18124084.

- [52] I. Montesinos *et al.*, “Evaluation of two automated and three rapid lateral flow immunoassays for the detection of anti-SARS-CoV-2 antibodies,” *J. Clin. Virol.*, vol. 128, p. 104413, Jul. 2020, doi: 10.1016/j.jcv.2020.104413.
- [53] K. M. Koczula and A. Gallotta, “Lateral flow assays,” *Essays Biochem.*, vol. 60, no. 1, pp. 111–120, Jun. 2016, doi: 10.1042/EBC20150012.
- [54] K. Mohd Hanafiah, N. Arifin, Y. Bustami, R. Noordin, M. Garcia, and D. Anderson, “Development of Multiplexed Infectious Disease Lateral Flow Assays: Challenges and Opportunities,” *Diagnostics*, vol. 7, no. 3, p. 51, Sep. 2017, doi: 10.3390/diagnostics7030051.
- [55] S. Souf, “Recent advances in diagnostic testing for viral infections,” *Biosci. Horiz.*, 2016, doi: 10.1093/biohorizons/hzw010.
- [56] B. Berg *et al.*, “Cellphone-Based Hand-Held Microplate Reader for Point-of-Care Testing of Enzyme-Linked Immunosorbent Assays,” *ACS Nano*, vol. 9, no. 8, pp. 7857–7866, Aug. 2015, doi: 10.1021/acsnano.5b03203.
- [57] A. Zhdanov, J. Keefe, L. Franco-Waite, K. R. Konnaiyan, and A. Pyayt, “Mobile phone-based ELISA (MELISA),” *Biosens. Bioelectron.*, vol. 103, pp. 138–142, Apr. 2018, doi: 10.1016/j.bios.2017.12.033.
- [58] “BinaxNow™ influenza A&B card 2.”  
<https://www.globalpointofcare.abbott/en/product-details/binaxnow-influenza-a-and-b-2.html> (accessed Jan. 05, 2022).

- [59] “BD Veritor™ Plus System for Flu A + B.” <https://bdveritor.bd.com/en-us/main/rapid-antigen-testing/flu-a-b> (accessed Jan. 05, 2022).
- [60] “Acucy® Influenza A&B.” <https://sekisuidiagnostics.com/products-all/acucy-influenza-ab/> (accessed Jan. 05, 2022).
- [61] “Sofia SARS antigen FIA.” <https://www.quidel.com/immunoassays/rapid-sars-tests/sofia-sars-antigen-fia> (accessed Jan. 05, 2022).
- [62] M. B. Kermekchiev, L. I. Kirilova, E. E. Vail, and W. M. Barnes, “Mutants of Taq DNA polymerase resistant to PCR inhibitors allow DNA amplification from whole blood and crude soil samples,” *Nucleic Acids Res.*, vol. 37, no. 5, p. e40, Apr. 2009, doi: 10.1093/nar/gkn1055.
- [63] R. K. Daher, G. Stewart, M. Boissinot, and M. G. Bergeron, “Recombinase Polymerase Amplification for Diagnostic Applications,” *Clin. Chem.*, vol. 62, no. 7, pp. 947–958, Jul. 2016, doi: 10.1373/clinchem.2015.245829.
- [64] T. Notomi, “Loop-mediated isothermal amplification of DNA,” *Nucleic Acids Res.*, vol. 28, no. 12, pp. 63e–663, Jun. 2000, doi: 10.1093/nar/28.12.e63.
- [65] P. Francois *et al.*, “Robustness of a loop-mediated isothermal amplification reaction for diagnostic applications,” *FEMS Immunol. Med. Microbiol.*, vol. 62, no. 1, pp. 41–48, Jun. 2011, doi: 10.1111/j.1574-695X.2011.00785.x.
- [66] “Actionable. Accessible. Affordable. SARS-CoV-2 (COVID-19) Rapid PCR Testing.” <https://www.mesabiotech.com/> (accessed Jan. 05, 2022).

- [67] “510(k) Substantial equivalence determination decision summary: Accula Flu A/Flu B Test,” *U.S. Food and Drug Administration*. [https://www.accessdata.fda.gov/cdrh\\_docs/reviews/K171641.pdf](https://www.accessdata.fda.gov/cdrh_docs/reviews/K171641.pdf) (accessed Jan. 05, 2022).
- [68] “Visby Medical Sexual Health Test.” <https://www.visbymedical.com/sexual-health-test/>
- [69] “Visby Medical COVID-19 Test Fast, accurate, and actionable PC.” <https://www.visbymedical.com/covid-19-test/> (accessed Jan. 05, 2022).
- [70] “Mobile qPCR Thermocyclers.” <https://info.biomeme.com/mobile-qpcr-thermocyclers> (accessed Jan. 05, 2022).
- [71] “CardioChek PA Analyzer.” <https://ptsdiagnostics.com/cardiochek-pa-analyzer/> (accessed Jan. 05, 2022).
- [72] “Curo L7.” <https://curofit.com/s/lipidocare-17-cholesterol-test-kit/> (accessed Jan. 05, 2022).
- [73] S. K. Vashist, P. B. Lupta, L. Y. Yeo, A. Ozcan, and J. H. T. Luong, “Emerging Technologies for Next-Generation Point-of-Care Testing,” *Trends Biotechnol.*, vol. 33, no. 11, pp. 692–705, Nov. 2015, doi: 10.1016/j.tibtech.2015.09.001.
- [74] A. Chen, R. Wang, C. R. S. Bever, S. Xing, B. D. Hammock, and T. Pan, “Smartphone-interfaced lab-on-a-chip devices for field-deployable enzyme-linked immunosorbent assay,” *Biomicrofluidics*, vol. 8, no. 6, p. 064101, Nov. 2014, doi: 10.1063/1.4901348.

- [75] S. Ghosh, K. Aggarwal, V. T. U., T. Nguyen, J. Han, and C. H. Ahn, “A new microchannel capillary flow assay (MCFA) platform with lyophilized chemiluminescence reagents for a smartphone-based POCT detecting malaria,” *Microsyst. Nanoeng.*, vol. 6, no. 1, p. 5, Dec. 2020, doi: 10.1038/s41378-019-0108-8.
- [76] B. Shu, C. Zhang, and D. Xing, “A handheld flow genetic analysis system (FGAS): towards rapid, sensitive, quantitative and multiplex molecular diagnosis at the point-of-care level,” *Lab. Chip*, vol. 15, no. 12, pp. 2597–2605, Jun. 2015, doi: 10.1039/C5LC00139K.
- [77] M. Rombach *et al.*, “RespiDisk: a point-of-care platform for fully automated detection of respiratory tract infection pathogens in clinical samples,” *The Analyst*, vol. 145, no. 21, pp. 7040–7047, 2020, doi: 10.1039/D0AN01226B.
- [78] H. Q. Nguyen, H. K. Bui, V. M. Phan, and T. S. Seo, “An internet of things-based point-of-care device for direct reverse-transcription-loop mediated isothermal amplification to identify SARS-CoV-2,” *Biosens. Bioelectron.*, vol. 195, p. 113655, Jan. 2022, doi: 10.1016/j.bios.2021.113655.
- [79] D. J. Carter and R. B. Cary, “Lateral flow microarrays: a novel platform for rapid nucleic acid detection based on miniaturized lateral flow chromatography,” *Nucleic Acids Res.*, vol. 35, no. 10, pp. e74–e74, Apr. 2007, doi: 10.1093/nar/gkm269.
- [80] Y.-L. Lin, Y.-J. Huang, P. Teerapanich, T. Leïchlé, and C.-F. Chou, “Multiplexed immunosensing and kinetics monitoring in nanofluidic devices with highly enhanced target capture efficiency,” *Biomicrofluidics*, vol. 10, no. 3, p. 034114, May 2016, doi: 10.1063/1.4953140.

- [81] X. Ye, Y. Li, L. Wang, X. Fang, and J. Kong, “All-in-one microfluidic nucleic acid diagnosis system for multiplex detection of sexually transmitted pathogens directly from genitourinary secretions,” *Talanta*, vol. 221, p. 121462, Jan. 2021, doi: 10.1016/j.talanta.2020.121462.
- [82] T. Mortelmans, D. Kazazis, C. Padeste, P. Berger, X. Li, and Y. Ekinci, “A nanofluidic device for rapid and multiplexed SARS-CoV-2 serological antibody detection,” In Review, preprint, May 2021. doi: 10.21203/rs.3.rs-537056/v1.
- [83] E.-C. Yeh, C.-C. Fu, L. Hu, R. Thakur, J. Feng, and L. P. Lee, “Self-powered integrated microfluidic point-of-care low-cost enabling (SIMPLE) chip,” *Sci. Adv.*, vol. 3, no. 3, p. e1501645, doi: 10.1126/sciadv.1501645.
- [84] J. Kuypers and K. R. Jerome, “Applications of Digital PCR for Clinical Microbiology,” *J. Clin. Microbiol.*, vol. 55, no. 6, pp. 1621–1628, Jun. 2017, doi: 10.1128/JCM.00211-17.
- [85] X. Mao, C. Liu, H. Tong, Y. Chen, and K. Liu, “Principles of digital PCR and its applications in current obstetrical and gynecological diseases,” *Am. J. Transl. Res.*, vol. 11, no. 12, pp. 7209–7222, Dec. 2019.
- [86] S. Badran, M. Chen, and J. E. Coia, “Multiplex Droplet Digital Polymerase Chain Reaction Assay for Rapid Molecular Detection of Pathogens in Patients With Sepsis: Protocol for an Assay Development Study,” *JMIR Res. Protoc.*, vol. 10, no. 12, p. e33746, Dec. 2021, doi: 10.2196/33746.

- [87] Y. Wouters *et al.*, “Droplet digital polymerase chain reaction for rapid broad-spectrum detection of bloodstream infections,” *Microb. Biotechnol.*, vol. 13, no. 3, pp. 657–668, May 2020, doi: 10.1111/1751-7915.13491.
- [88] B. Chen, Y. Jiang, X. Cao, C. Liu, N. Zhang, and D. Shi, “Droplet digital PCR as an emerging tool in detecting pathogens nucleic acids in infectious diseases,” *Clin. Chim. Acta*, vol. 517, pp. 156–161, Jun. 2021, doi: 10.1016/j.cca.2021.02.008.
- [89] T. Gheit *et al.*, “Development of a Sensitive and Specific Assay Combining Multiplex PCR and DNA Microarray Primer Extension To Detect High-Risk Mucosal Human Papillomavirus Types,” *J. Clin. Microbiol.*, vol. 44, no. 6, pp. 2025–2031, Jun. 2006, doi: 10.1128/JCM.02305-05.
- [90] M. Tian *et al.*, “Microarray Multiplex Assay for the Simultaneous Detection and Discrimination of Influenza A and Influenza B Viruses,” *Indian J. Microbiol.*, vol. 54, no. 2, pp. 211–217, Jun. 2014, doi: 10.1007/s12088-013-0432-x.
- [91] D. A. Selck, M. A. Karymov, B. Sun, and R. F. Ismagilov, “Increased Robustness of Single-Molecule Counting with Microfluidics, Digital Isothermal Amplification, and a Mobile Phone versus Real-Time Kinetic Measurements,” *Anal. Chem.*, vol. 85, no. 22, pp. 11129–11136, Nov. 2013, doi: 10.1021/ac4030413.
- [92] F. Shen *et al.*, “Multiplexed Quantification of Nucleic Acids with Large Dynamic Range Using Multivolume Digital RT-PCR on a Rotational SlipChip Tested with HIV and Hepatitis C Viral Load,” *J. Am. Chem. Soc.*, vol. 133, no. 44, pp. 17705–17712, Nov. 2011, doi: 10.1021/ja2060116.

- [93] S. Agrawal *et al.*, “Rapid, point-of-care molecular diagnostics with Cas13.” p. 2020.12.14.20247874, Apr. 04, 2021. Accessed: Dec. 16, 2021. [Online]. Available: <https://www.medrxiv.org/content/10.1101/2020.12.14.20247874v2>
- [94] J. S. Gootenberg, O. O. Abudayyeh, M. J. Kellner, J. Joung, J. J. Collins, and F. Zhang, “Multiplexed and portable nucleic acid detection platform with Cas13, Cas12a, and Csm6,” *Science*, vol. 360, no. 6387, pp. 439–444, Apr. 2018, doi: 10.1126/science.aaq0179.
- [95] J. Quan *et al.*, “FLASH: a next-generation CRISPR diagnostic for multiplexed detection of antimicrobial resistance sequences,” *Nucleic Acids Res.*, vol. 47, no. 14, pp. e83–e83, Aug. 2019, doi: 10.1093/nar/gkz418.
- [96] B. C. Dhar, N. Steimberg, and G. Mazzoleni, “Point-of-Care Pathogen Detection with CRISPR-based Programmable Nucleic Acid Binding Proteins,” *ChemMedChem*, vol. 16, no. 10, pp. 1566–1575, May 2021, doi: 10.1002/cmdc.202000782.
- [97] C. M. Ackerman *et al.*, “Massively multiplexed nucleic acid detection with Cas13,” *Nature*, vol. 582, no. 7811, pp. 277–282, Jun. 2020, doi: 10.1038/s41586-020-2279-8.
- [98] M. Rezaei *et al.*, “A Portable RT-LAMP/CRISPR Machine for Rapid COVID-19 Screening,” *Biosensors*, vol. 11, no. 10, p. 369, Oct. 2021, doi: 10.3390/bios11100369.
- [99] Z. Yi *et al.*, “Rational Programming of Cas12a for Early-Stage Detection of COVID-19 by Lateral Flow Assay and Portable Real-Time Fluorescence Readout Facilities,” *Biosensors*, vol. 12, no. 1, p. 11, Dec. 2021, doi: 10.3390/bios12010011.

- [100] Z. S. Ballard *et al.*, “Deep learning-enabled point-of-care sensing using multiplexed paper-based sensors,” *Npj Digit. Med.*, vol. 3, no. 1, p. 66, Dec. 2020, doi: 10.1038/s41746-020-0274-y.
- [101] C. Liu *et al.*, “Multiplexed analysis of small extracellular vesicle-derived mRNAs by droplet digital PCR and machine learning improves breast cancer diagnosis,” *Biosens. Bioelectron.*, vol. 194, p. 113615, Dec. 2021, doi: 10.1016/j.bios.2021.113615.
- [102] L. Miglietta *et al.*, “Coupling Machine Learning and High Throughput Multiplex Digital PCR Enables Accurate Detection of Carbapenem-Resistant Genes in Clinical Isolates,” *Front. Mol. Biosci.*, vol. 8, p. 775299, Nov. 2021, doi: 10.3389/fmolb.2021.775299.
- [103] A. A. Ellington, I. J. Kullo, K. R. Bailey, and G. G. Klee, “Antibody-Based Protein Multiplex Platforms: Technical and Operational Challenges,” *Clin. Chem.*, vol. 56, no. 2, pp. 186–193, Feb. 2010, doi: 10.1373/clinchem.2009.127514.
- [104] Institute of Medicine (US) Forum on Microbial Threats and Global Infectious Disease Surveillance and Detection, *Assessing the Challenges—Finding Solutions, Workshop Summary. Washington (DC)*. National Academies Press (US), 2007. Accessed: Dec. 20, 2021. [Online]. Available: <https://www.ncbi.nlm.nih.gov/books/NBK52875/>
- [105] “World’s most portable molecular diagnostics system unveiled at AACC,” Jul. 28, 2015. <https://www.tbonline.info/posts/2015/7/28/worlds-most-portable-molecular-diagnostics-system-/> (accessed Jan. 06, 2022).
- [106] “Cepheid Targets Development of a Point of Care HIV Viral Load Test From a Few Drops of Blood,” Sep. 08, 2016. <https://www.prnewswire.com/news->

releases/cepheid-targets-development-of-a-point-of-care-hiv-viral-load-test-from-a-few-drops-of-blood-300324397.html (accessed Jan. 06, 2022).

[107] “Advocates urge Cepheid to reinstate plans to commercialize GeneXpert Omni,” Oct. 14, 2021. <https://www.tbonline.info/posts/2021/10/14/advocates-urge-cepheid-reinstate-plans-commerciali/> (accessed Jan. 06, 2022).

[108] D. Branigan, “Time for \$5 Coalition Urges Cepheid to Reinstate Plans to Launch GeneXpert Omni.” Oct. 14, 2021. Accessed: Jan. 06, 2022. [Online]. Available: [https://www.tbonline.info/media/uploads/documents/time\\_for\\_\\$5\\_coalition\\_open\\_letter\\_to\\_cepheid\\_14oct2021.pdf](https://www.tbonline.info/media/uploads/documents/time_for_$5_coalition_open_letter_to_cepheid_14oct2021.pdf)

[109] D. Gotham, L. McKenna, S. Deborggraeve, S. Madoori, and D. Branigan, “Public investments in the development of GeneXpert molecular diagnostic technology,” *PLOS ONE*, vol. 16, no. 8, p. e0256883, Aug. 2021, doi: 10.1371/journal.pone.0256883.

[110] “Covid-19 testing.” <https://info.biomeme.com/covid-19> (accessed Jan. 06, 2022).

[111] “GeneXpert.” <https://www.finddx.org/pricing/genexpert/> (accessed Jan. 08, 2022).

[112] E. Hsiang et al., “Higher cost of implementing Xpert(®) MTB/RIF in Ugandan peripheral settings: implications for cost-effectiveness,” *Int J Tuberc Lung Dis*, vol. 20, no. 9, pp. 1212–1218, Sep. 2016, doi: 10.5588/ijtld.16.0200.

2.4 Supplementary Information

## REASSURED Multiplex Diagnostics: A Critical Review and Forecast

Jonas A. Otoo <sup>1</sup> and Travis S. Schlappi <sup>2,\*</sup>

<sup>1</sup> Keck Graduate Institute; jotoo18@students.kgi.edu

<sup>2</sup> Keck Graduate Institute; tschlappi@kgi.edu

\* Correspondence: tschlappi@kgi.edu

*Table S 2-1 Scoring scheme for assessing diagnostics on the REASSURED criteria. The scoring ranges from 3 to 1, 3 being the highest score and 1 being the lowest score.*

	<b>High (3)</b>	<b>Medium (2)</b>	<b>Low (1)</b>
<b>R</b>	Test has a portable battery reader system or can be connected to mobile phone. The reader has real-time connectivity and can transmit results data	Test has a portable battery reader system which is does not have real-time connectivity or cannot transmit results.	Test has a reader system which is not battery operated.
<b>E</b>	Saliva, urine, stool, nasal swab, cheek swab, vaginal swab, nasopharyngeal swab, throat swab	Finger prick, sputum	Venous blood, serum
<b>A</b>	$x < \$5$	$\$5 < x < \$20$	$x > \$20$
<b>S</b>	$x > 95\%$	$90\% < x < 95\%$	$x < 90\%$
<b>S</b>	$x > 95\%$	$90\% < x < 95\%$	$x < 90\%$

<b>U</b>	x < 2 minutes, CLIA waived	2 < x < 5 minutes, moderate complexity	x > 5 minutes, high complexity
<b>R</b>	x < 1 hr	1 < x < 3 hrs	x > 3 hrs
<b>E</b>	Portable, handheld, disposable device or cartridge, battery or solar powered.	Portable, disposable device or cartridge, that can potentially be powered by a power pack.	Portable device or cartridge, potentially powered by power pack.
<b>D</b>	Reagents can be stored at room temp	Reagents are stable at room temp but for a few hours	Reagents require refrigeration

Table S 2-2 Scoring scheme of clinical diagnostics on the REASSURED criteria. Averages were calculated from the scores of the individual elements of the REASSURED criteria. The Overall score was calculated by expressing the average score as a percentage of 3, the highest achievable average score.

<i>Multiplex diagnostic</i>	<i>Test type</i>	<i>CLIA</i>	<i>Cost of device</i>	<i>≈Cost per test</i>	<i>Test duration (min)</i>	<i>Hands-on time (min)</i>	<i>Sensitivity</i>	<i>Specificity</i>	<i>PPA</i>	<i>NPA</i>	<i>Temp</i>	<i>Sample</i>
<i>Accula system flu A+B[67]</i>	Nucleic Acid	Waived	\$350	\$63	30	1	94%	94%	-	-	RT	Nasal Swab
<i>Visby Medical Sexual Health Click Test chlamydia, gonorrhoeae and trichomonas[68]</i>	Nucleic Acid	Waived	-	-	28	1	98.80%	95.80%	97.40%	96.70%	RT	Vaginal swab
<i>Franklin three9 Covid-19[110]</i>	Nucleic Acid	High	\$9,950	\$1.15	60	2	97.46%	98.51%	-	-	RT	NPS

<i>Acucy influenza A+B[60]</i>	Immunoassay	Waived	\$1,454	\$14.52	15	1	82.30%	96.00%	-	-	RT	NPS
<i>Binaxnow influenza A+B with digival[58]</i>	Immunoassay	Waived	\$5,192	\$28.68	15	1	-	-	81%	93.60%	RT	NPS
<i>BD Veritor™ Flu A + B with analyzer[59]</i>	Immunoassay	Waived	\$411.55	\$15.15	11	1	-	-	81.30%	97.60%	RT	NPS
<i>Sofia 2 Flu + SARS antigen FIA[61]</i>	Immunoassay	Waived	\$2,080	\$51.04	15	1	-	-	89%	94.60%	RT	NPS
<i>CardioChek PA Analyzer[71]</i>	Chemistry	Waived	\$778	\$10.53	-	1	-	-	-	-	RT	Finger pick
<i>CuroL7 Blood profile test strips[72]</i>	Chemistry	-	\$289	\$7.90	3	1	-	-	-	-	RT	Finger prick

RT = Room Temperature, NPS = Nasopharyngeal Swab

# Chapter 3 Picolitre Droplet Generation and Dense Bead-in-Droplet Encapsulation via Microfluidic Devices Fabricated via 3D Printed Molds

Tochukwu D. Anyaduba <sup>1,2</sup> Jonas A. Otoo <sup>1</sup> and Travis S. Schlappi <sup>1</sup>

<sup>1</sup> Keck Graduate Institute, Riggs School of Applied Life Sciences, Claremont, CA 91711, USA

<sup>2</sup> Abbott Rapid Diagnostics, 4545 Towne Center Ct, La Jolla, San Diego, CA 92121, USA

\* Correspondence: [travis\\_schlappi@kgi.edu](mailto:travis_schlappi@kgi.edu)

**Abstract:** Picolitre-scale droplets have many applications in chemistry and biology, such as biomolecule synthesis, drug discovery, nucleic acid quantification, and single cell analysis. However, due to the complicated processes used to fabricate microfluidic channels, most picolitre (pL) droplet generation methods are limited to research in laboratories with cleanroom facilities and complex instrumentation. The purpose of this work is to investigate a method that uses 3D printing to fabricate microfluidic devices that can generate droplets with sizes <100 pL and encapsulate single dense beads mechanistically. Our device generated monodisperse droplets as small as ~48 pL and we demonstrated the usefulness of this droplet generation technique in biomolecule analysis by detecting *Lactobacillus acidophillus* 16s rRNA via digital loop-mediated isothermal amplification (dLAMP). We also designed a mixer that can be integrated into a syringe to overcome dense bead sedimentation and found that the bead-in-droplet (BiD) emulsions

created from our device had <2% of the droplets populated with more than 1 bead. This study will enable researchers to create devices that generate pL-scale droplets and encapsulate dense beads with inexpensive and simple instrumentation (3D printer and syringe pump). The rapid prototyping and integration ability of this module with other components or processes can accelerate the development of point-of-care microfluidic devices that use droplet-bead emulsions to analyze biological or chemical samples with high throughput and precision.

**Keywords:** microfluidics; picolitre droplets; rapid prototyping; bead encapsulation; 3D printing

### 3.1 Introduction

Droplet microfluidics uses devices with channels dimensions tens or hundreds of microns wide to generate and manipulate discrete  $\mu\text{L}$  or less volumes. Dividing a sample of interest into fL to  $\mu\text{L}$  scale volumes reduces reagent usage, increases the sensitivity of chemical analyses, and provides enhanced control over reagent delivery, mixing, and chemical interactions [1]. There are many applications of droplet microfluidics in chemistry, biology, and biomedical engineering, such as therapeutic agent delivery, biomedical imaging, biomolecule synthesis, diagnostic chips, drug discovery, cell culture, biochemical characterization, and single cell analysis [2]. The implementation of droplet microfluidics in these applications are accomplished through lab-on-a-chip devices. These lab-on-a-chip devices may require droplet manipulation processes such as mixing, fission and/or fusion, sorting, and transportation of droplets [3,4], which can be accomplished via electrowetting, magnetic actuation, dielectrophoresis, surface acoustic waves, optical methods, or thermal methods [3–7]. However, due to the complicated processes used to fabricate channels that

are tens or hundreds of microns wide, most droplet microfluidic methods are limited to research in laboratories with cleanroom facilities and complex instrumentation (e.g., photolithography with silicon wafers [8–10] or wet etching [11–13]). The few droplet generation technologies commercially available for diagnostic use are expensive (\$89 k–\$100 k

for an instrument and \$24–\$240 per disposable cartridge) and not integrated with other assay steps such as chemical reaction incubation and droplet analysis [14].

To make the droplet generation process simpler, less time-intensive, and less expensive, many innovative methods have been created. Some researchers have used glass capillaries to generate pL-scale droplets. For example, Li et al. bonded microscope glass slides to pulled glass capillaries to generate monodisperse multiple emulsions [15], Gu et al. created and manipulated pL droplets for single cell assays with a 75  $\mu\text{m}$  fused-silica capillary [16], and Li et al. used an asymmetrical beveled capillary to generate pL to nL droplets and execute a digital PCR assay [17]. While the instrumentation costs for these devices are lower than for photolithography, devices made from glass capillaries are difficult to integrate into other upstream or downstream modules and not amenable to rapid prototyping due to the intricate procedures for fabricating capillaries  $<1$  mm in diameter. Other groups rely on micromachining to generate droplets, such as direct milling of polycarbonate [18,19] or micromachining in PMMA [20]. These methods have demonstrated consistent and controllable droplet generation; however, the droplet sizes are large ( $>1$  nL) or when ply- sized droplets are achieved, a centrifuge is needed to create the

droplets in a reaction tube, which precludes its ability to be integrated into other microfluidic modules [20].

3D printing is now commonly used to create molds for PDMS devices, which eliminates the need for cleanroom facilities, photolithography, or etching and enables rapid prototyping and fabrication [21–24]. Researchers have also used 3D printers to build monolithic devices out of resin for droplet generation, albeit with larger channel dimensions and therefore larger droplets (>1 nL) [25–31]. Picolitre-scale droplets are important for several applications, such as increasing the precision, sensitivity and dynamic range of digital PCR [32], or preventing cross contamination and target dilution in single cell analysis [16,33]. The small channel sizes required for pL-scale droplets are typically fabricated with complex processes inside a cleanroom, usually photolithography [8–10], and have not been made with 3D printed molds or 3D printed monolithic devices. The methods described above have significantly advanced droplet generation for the picolitre scale via photolithography or glass capillaries, and the nanoliter scale via 3D printing; however, there remains a need for <100 pL droplet generation from a rapid prototyping method (e.g., 3D printed molds) that can be easily integrated into other sample preparation, analysis, and detection modules.

An important area of investigation in droplet microfluidics are methods that encapsulate a single bead in a droplet (BiD). These BiD platforms have enabled exciting advancements in biomedical research and diagnostics, including genome sequencing [34], enzyme evolution and screening [35,36], detecting rare genetic mutations [37,38] single cell analysis [39], and molecular diagnostics [40]. While these devices have high throughput and multiplexing capabilities, they are limited to laboratories with sophisticated

instrumentation for photolithography and bead encapsulation. Additionally, they have shown Poisson or better distributions of BiDs for particles with a similar density to water, such as gel particles [41], polystyrene beads [42–44], agarose beads [39], or biological cells [39,44,45]. Particles with a higher density than water sediment to the bottom before being encapsulated in droplets and cause the first fraction of droplets to have more than 1 bead per droplet and the remaining fraction to not have any beads. To use beads of varying densities in BiD platforms, this sedimentation effect must be overcome.

The purpose of this work is to overcome current limitations of droplet microfluidic devices by creating a droplet generation device with the following features: (i) a simple and inexpensive fabrication process that is amenable to rapid prototyping and integration with other modules, (ii) droplet volumes <100 pL, and (iii) the ability to encapsulate dense beads in aqueous droplets with a Poisson-like distribution. We found that using 3D printing to create a mold instead of photolithography or etching is a suitable fabrication method to accomplish this purpose. Our device generated monodisperse droplets as small as ~48 pL and we demonstrated the usefulness of this droplet generation technique in biomolecule detection by quantifying nucleic acids via digital loop-mediated isothermal amplification (dLAMP). We also designed a mixer that can be integrated into a syringe to overcome dense bead sedimentation and found that the BiD emulsions created from our device had less than 2% of the droplets populated with more than 1 bead when the average input concentration was 0.15 beads/droplet, in line with Poisson statistical projections. This study will enable researchers to create devices that generate pL-scale droplets and encapsulate dense beads with inexpensive and simple instrumentation (3D printer and syringe pump). The rapid prototyping and integration ability of this method can accelerate

the development of point-of-care microfluidic devices that generate droplet-bead emulsions and analyze samples with high throughput and precision.

## 3.2 Materials and Methods

### *3.2.1 Device Fabrication*

3D models of the master molds were designed using SolidWorks CAD software (Dassault Systems, Velizy-villacoublay, France) to have flow channel dimensions of  $100\ \mu\text{m} \times 100\ \mu\text{m}$  and inlet/outlet ports of  $750\ \mu\text{m}$  (Figure 3.1A). Stereolithography (SLA) files were prepared for 3D printing by orienting them at a  $45^\circ$  angle and avoiding cups and overhangs in Form Labs' Preform software. The models were then printed using the Form3 SLA 3D printer (Form Labs) in Clear resin (FLGPCL04) at a layer thickness of  $25\ \mu\text{m}$ . The printed master molds were thoroughly cleaned with isopropyl alcohol to remove excess resin, then UV-cured for 30 min.

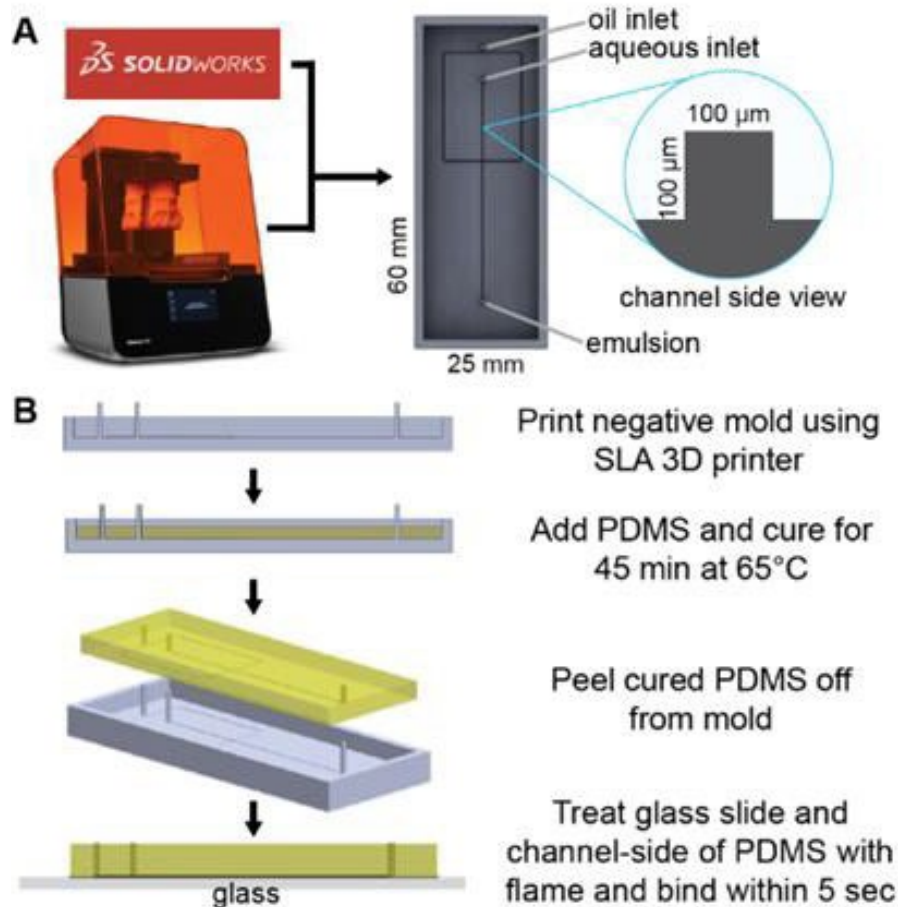


*Figure 3.1 Microfluidic device design and fabrication. (A) A solid master mold was designed with Solidworks CAD software and printed with FormLabs Form3 SLA printer. (B) PDMS device fabrication process.*

To make polydimethylsiloxane (PDMS), SYLGARD™ 184 Silicone Elastomer Base and SYLGARD™ 184 Silicone Elastomer Curing Agent (Dow Corning, Midland, MI, USA) are combined at 10:1 w/w ratio to make up ~3 gm needed to fill each mold. Prior to pouring the mixture into the mold, it is degassed in a Cole Parmer Diblock oven at room temperature until no bubbles can be seen in the PDMS mixture. After filling the molds with the degassed PDMS, the degassing process is repeated to ensure complete filling of the corners of the channels before curing at 65 °C for 45 min. Once cured, the PDMS is gently

peeled from the master mold and bonded onto glass microscope slides (Amscope BS-72P 100S-22) after surface activation using flame treatment as an alternative to oxygen plasma bonding [46] (Figure 3.1B). The device is then placed in an 85 °C oven overnight to allow the PDMS to harden. Next, the devices are examined for binding strength of the PDMS by gently prying at them. They are also checked for channel dimensions under a microscope. A  $\pm 10\%$  tolerance is allowed for the channel widths measured from micrographs prior to the attachment of the flow tubing (Scientific Commodities, Lake Havasu City, AZ, USA, BB31695 PE/3). The tubing is attached to the chip by plumbing them into the inlet and outlet ports, making sure to leave a clearance space between the tubing nozzle and the slide surface. The tubing is further held in place using cold weld steel-reinforced epoxy (JB Weld, Marietta, GA, USA).

### *3.2.2 Droplet Generation*

Droplets were generated using the designed flow-focusing PDMS microfluidic devices described above. The oil phase consisted of mineral oil (Sigma Aldrich M3516-1L), 0.1 wt% Triton X-100 (Fisher Scientific, Waltham, MA, USA), and 3 wt% ABIL EM 90 (Evonik, Essen, Germany), and was pumped at various volumetric flow rates (20, 25, 50, 75, 100  $\mu\text{L}/\text{min}$ ). The aqueous phase (DI water) was maintained at a volumetric flow rate of 1  $\mu\text{L}/\text{min}$ . The oil and aqueous phases were pumped to an intersection in the device by syringe pumps (KD Scientific, Holliston, MA, USA), at which point droplets were generated and subsequently collected from the outlet in Eppendorf tubes. A fraction of the droplets was imaged using confocal imaging (Leica SP5, Wetzlar, Germany) and the respective planar areas of the droplets were deduced using ImageJ software after

segmentation processing. The spherical diameter of each droplet is calculated from the deduced area.

### 3.2.3 Droplet Digital Loop-Mediated Isothermal Amplification for DNA Quantification

*Lactobacillus acidophilus* (*L. acid.*) obtained from MicroKwik vials (Carolina Biological Supply, Burlington, NC, USA) was cultured in de Man, Rogosa and Sharpe (MRS) agar formulated in-house using Millipore-Sigma formulation (CCW4691). The QuickExtract™ one-step DNA extraction kit (Lucigen, Middleton, WI, USA) was used to extract DNA from the colonies. Extracted genomic DNA was quantified via absorbance measurements from a Nanodrop One instrument (ThermoFisher Scientific, Waltham, MA, USA) and diluted in nuclease-free water to concentrations ranging from 0 to  $9.5 \times 10^6$  copies/mL.

LAMP master mix was prepared with final concentrations of  $1 \times$  isothermal amplification buffer (New England Biolabs, NEB), 8 mM of MgSO<sub>4</sub> (NEB), 1.4 mM dNTPs (NEB), 320 U/ mL Bst 2.0 WarmStart polymerase (NEB), primer mix, and  $1 \times$  SybrGreen (Life Technologies). The primer mix was designed in-house to target the *L. acidophilus* 16S rRNA gene and consisted of 1.6  $\mu$ M each of forward inner primer (CTGCACTCAA-GAAAAACAGTTTCCGAGTCTGATGTGAAAGCCCTC) and backward inner primer (AA-GAGGAGAGTGGA ACTCCATGTGAGACCAGAGAGCCGCCTT), 0.2  $\mu$ M each of forward outer primer (TAAAGCGAGCGCAGGC) and backward outer primer (CCTCAGCGTCAGTTGC),

0.4  $\mu\text{M}$  each of forward loop primer (GCAGTTCCTCGGTTAAGCC) and backward loop primer (ATGCGTAGATATATGGAAGAACACC) (Integrated DNA Technologies, Clarville, IA, USA). *L. acid* DNA dilutions were added to LAMP master mix to yield final concentrations of 0,  $1.0 \times 10^7$ ,  $2.5 \times 10^7$ ,  $5.0 \times 10^7$ ,  $4.0 \times 10^8$  DNA copies/mL (quantified by Nanoquant absorbance measurements). Four replicates of each dilution (10  $\mu\text{L}$ /well) were amplified at 68 °C for 60 min using a LightCycler®96 Instrument (Roche, Basel, Switzerland) as positive controls.

The LAMP mix + *L. acid* DNA samples were infused into a droplet generation device as described in “Droplet Generation”, with oil flow rate 75  $\mu\text{L}/\text{min}$  and aqueous flow rate 1  $\mu\text{L}/\text{min}$ . Droplets from the microfluidic devices were collected in amber SepCap vials (Thermoscientific, Waltham, MA, USA C4015-99) and incubated at 68°C for 60 min using a Multi-Therm shaker (Benchmark Scientific, Sayreville, NJ, USA). After incubation, the droplets were imaged using a Leica SP5 confocal microscope, and images were analyzed with Image J to determine the relative fluorescence intensity (RFI) of each droplet. A threshold was determined by computing  $\mu_{NTC} + 3 \cdot \sigma_{NTC}$ , where  $\mu_{NTC}$  is the mean and  $\sigma_{NTC}$  is the standard deviation of the RFI of the 0 cop/mL sample droplets. Droplets with RFI greater than the threshold were classified as positive while the droplets less than or equal to the threshold are classified as negative. One can then use Poisson statistics with the number of positive and negative droplets to calculate a concentration for each sample [47].

#### 3.2.4 Bead Mixer

A blind hole with a diameter of about 9 mm was drilled into the side of a 3 mL plastic syringe (CareTouch, Westminster, CO, USA) at the 0.5 mL mark. A small DC motor with a plastic impeller which was originally designed for a bead-beating sample preparation

device (Claremont Bio 01.340.48 OmniLyse®Kit) was retrieved and carefully positioned into the syringe through the blind hole. The motor with the impeller was affixed to the syringe with cold weld steel-reinforced epoxy (JB Weld, Marietta, GA, USA) such that the blind hole was completely sealed and airtight. The epoxy was allowed to set for 48 to 72 h. The impeller mixer was powered by a 1.5 V DC power supply (SI, Figure S1).

### *3.2.5 Bead-in-Droplet Emulsions*

Hard shell Polymethyl Methacrylate (PMMA) beads (PolyAn Microshperes Po-105 00 020 and Alpha Nanotech colloidal PMMA) of 20  $\mu\text{m}$  in diameter were used in the bead encapsulation experiment. A mixture of the beads and 0.1 %v/v Tween 20 in nuclease-free water at working concentrations of 0.15, 0.2 and 0.3 beads/droplet ( $\lambda$ ) were used as the dispersed phase for the experiments. A mixture of mineral oil (Sigma Aldrich-M3516-1L), 0.1 wt% Triton X-100 (Fisher Scientific, Waltham, MA, USA) and 3 wt% ABIL EM 90 (Evonik, Essen, Germany) was used as the continuous phase. The dispersed phase (bead suspension) was aspirated into a modified syringe and loaded onto a syringe pump (KD Scientific, Holliston, MA, USA, KDS100). A 1.5 V DC power supply was connected to the mixer to keep the beads solution homogenous. The continuous phase was put into a 10 mL plastic syringe (CareTouch, Westminster, CO, USA) and loaded onto a syringe pump. The continuous and dispersed phases were introduced into the droplet generation device using syringe pumps at flow rates of 30  $\mu\text{L}/\text{min}$  and 1–7  $\mu\text{L}/\text{min}$ , respectively. A period of about 5 min was allowed for the cartridge to be primed and for the droplet generation to be stabilized. The droplets were collected from the cartridge into 1 mL amber SepCap vials (Thermoscientific, Waltham, MA, USA, C4015-99). The excess oil from the continuous phase was poured off and the droplets were put onto a microscope slide and mounted onto

a microscope (Omax microscope 3152102) for imaging. Micrographs of the droplets were taken using the Amscope microscope camera md35 and Amsocpe software version 4.

### 3.2.6 Image Analysis

The images were opened in Image J. The scale was set according to the scale bar on the images and the unit was set to  $\mu\text{m}$ . The images were converted to 8-bit gray scale images and speckles and noise were filtered from the images. The threshold of the images was adjusted to convert them to binary images. The images were converted to mask to invert the black to white, making the droplets appear white. The droplets were then analyzed to calculate the area of each droplet. The diameter and volume of each droplet were calculated from the area of the droplets. The droplets containing beads were manually counted and the number of beads in each droplet was recorded. The data were compiled in Excel (Microsoft Office) and parsed into Python 3.0 for further analysis and visual presentation.

## 3.3 Results and Discussion

### 3.3.1 Picolitre-Scale Droplet Generation

The physics of droplet generation via flow focusing has been well documented with theory and experiments showing an inverse logarithmic relationship between Capillary number ( $Ca = \mu_{ave}(2Q_o + Q_w)/\sigma hw$ ) and non-dimensionalized droplet diameter,  $D_d/D_h$ , where  $\mu_{ave}$  is the average viscosity of the two fluids,  $Q_o$  is the oil flow rate,  $Q_w$  is the water flow rate,  $\sigma$  is the surface tension,  $h$  is the channel height,  $w$  is the channel width,  $D_d$  is the diameter of the droplet, and  $D_h$  is the hydraulic diameter of the channel,  $2hw/(h + w)$  [48,49]. These flow focusing studies demonstrate that  $<100$  pL droplets can theoretically be generated with  $Ca > 0.001$  (faster flow rates ( $Q_o, Q_w$ ) relative to channel dimensions ( $h, w$ )) and  $144 \mu\text{m} > D_h > 39 \mu\text{m}$ , or with  $Ca < 0.001$  (slower flow rates ( $Q_o, Q_w$ ) relative to channel

dimensions  $(h,w)$ ) and  $14 \mu\text{m} < D_h < 39 \mu\text{m}$  [48] (SI, Section S2). Experimentally, the authors test devices with maximum channel heights of  $27 \mu\text{m}$  [48] or widths of  $71 \mu\text{m}$  [49]. In these studies and others [8–13], pL droplets are generated by using small channel widths ( $<100 \mu\text{m}$ ) facilitated by photolithographic processes in cleanrooms. As our objective was to develop a device that generates pL droplets without complex fabrication processes, we were limited to the channel widths  $100 \mu\text{m}$  or greater that an SLA 3D printer is capable of printing in a mold. Therefore, our device design would need to be in the  $Ca > 0.001$  regime with faster flow rates relative to channel dimensions.

With the limits on our device’s physical features established, we 3D printed a mold and made a PDMS cast of  $100 \mu\text{m}$  channel width and  $100 \mu\text{m}$  channel height without a cleanroom, photolithography processes, or complex instrumentation (Figure 3.1). We chose oil and water flow rates such that the droplet generation device would have  $Ca \gg 0.001$ , with  $Q_o = 25$  to  $100 \mu\text{L}/\text{min}$  and  $Q_w = 1 \mu\text{L}/\text{min}$  (SI, Section S2), which resulted in droplets of diameters  $45$  to  $112 \mu\text{m}$  ( $48$  to  $736 \text{ pL}$ ) (Figure 3.2). The droplets generated from this device are monodisperse (Figure 3.2B, coefficient of variation (CV) from 2–12%), which is in the range of droplets generated from other devices [50,51]. As expected, there is an inverse power relationship between droplet volume and oil flow rate [49], showing that devices fabricated with 3D printed molds give similar consistency and expected performance at the picolitre scale as devices made with photolithography in a cleanroom. Because this device is made from a 3D printed mold, researchers can iterate prototypes rapidly without undergoing the time and resource-consuming processes of photolithography; additionally, the droplet generation module can be part of a larger 3D

printed mold that includes modules for executing other upstream or downstream assay processes.

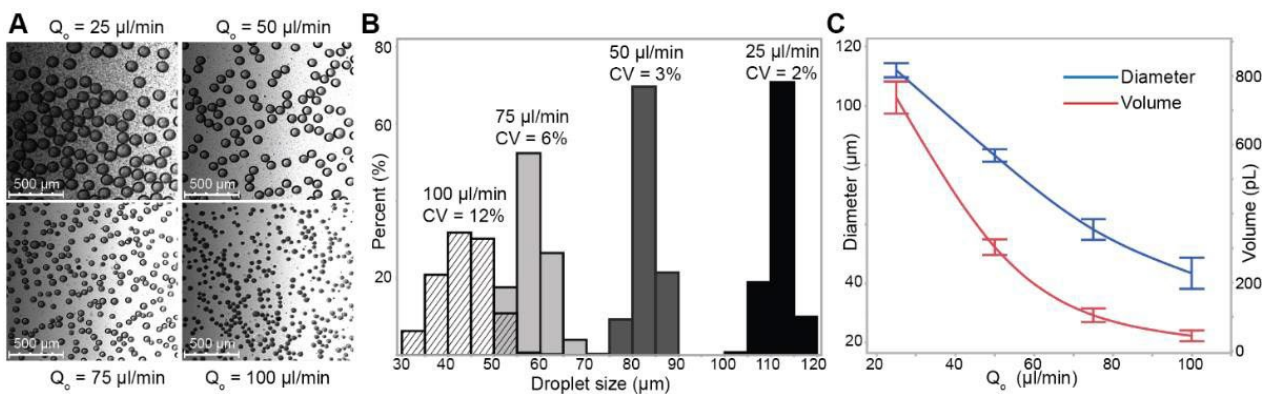


*Figure 3.2 Picolitre-scale droplet generation. (A) Micrograph of the droplets retrieved from microfluidic cartridge outlet. (B) Droplet diameter distribution and CV at each flow condition. (C) The droplet diameter changes with volumetric flow rate of the oil phase. The volumetric flow rate of the aqueous phase was kept constant at  $1 \mu\text{L/min}$ .*

### 3.3.2 Droplet Digital Loop-Mediated Isothermal Amplification

To explore the utility of this droplet generation device in molecular diagnostic applications, droplet digital loop-mediated isothermal amplification (ddLAMP) was performed to detect and quantify a DNA target. Digital LAMP is an emerging nucleic acid (NA) amplification method that can quantify the NA concentration of a sample with high accuracy and precision, even in the midst of temperature, reaction time, or imaging variance [52]. NA quantification via dLAMP is useful in several applications, such as viral load measurements for HIV [53], hepatitis C virus genotyping [54], and rapid antibiotic susceptibility testing [55]. Current dLAMP methods partition the sample into pL to nL droplets with microfluidic devices made using photolithography [56,57], wet etching [52–55], or fused-silica capillaries [58]. Our droplet generation device made from a 3D printed

mold could make dLAMP more accessible by eliminating the need for complex facilities or instruments and enabling integration with other amplification or detection modules.

We tested the feasibility of encapsulating LAMP reagents with target DNA and primers into droplets with our device (Materials and Methods). After generation, the droplets were incubated at 68 °C for 60 min for amplification of DNA via LAMP and SybrGreen fluorescence was measured to indicate the presence or absence of amplification product within each droplet (Figure 3.3A). Five DNA dilutions were tested, and the positive droplet percentage was plotted against the prediction from Poisson statistics (Figure 3.3B), assuming a 10% LAMP efficiency and 300 pL droplet volume (SI, Section S3).

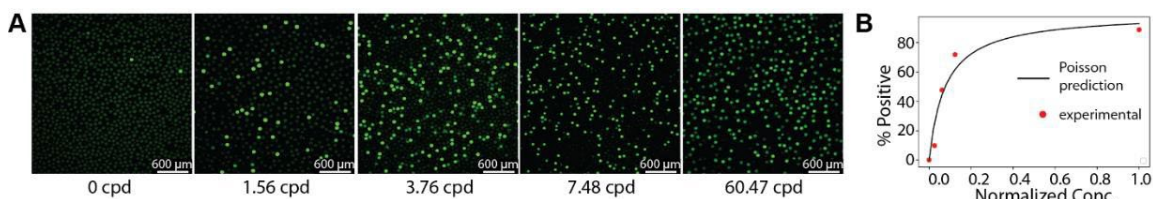


*Figure 3.3. Droplet digital LAMP. (A) Post-amplification micrographs of droplets. (B) Agreement between Poisson predicted positive droplet percentage and experimental data.*

### 3.3.4 Dense Bead-in-Droplet Emulsions

Interest in using microparticles as delivery systems in various technologies has been widely researched, especially in combination with microdroplets for biological applications [59–62]. This is due to the high surface-to-volume ratio and the ease of immobilizing biorecognition molecules on them, as well as the potential for compartmentalized single-molecule assays [63–65]. Single particle encapsulation in droplets, however, faces two major challenges: sedimentation due to particle density [62], and mechanistic single particle encapsulation [41,66].

Particle density poses a challenge when loading microparticles into encapsulation devices because the higher density particles ( $>1$  gm/mL) sediment in the syringe and delivery tubing, causing nonhomogeneous distribution of microparticles in droplets (SI, Figures S 3.1A and S 3.2). This can be solved by the dissipation of the bead density by suspending them in denser fluids such as glycerol [62]; however, such fluids may not be compatible with the intended bio-application. For example, glycerol at 50% v/v inhibits NA amplification, thereby defeating the purpose of using microbeads for NA applications (SI, Figure S4). To circumvent this challenge, researchers used gel beads with similar density to water, which ensured a binary distribution of beads in the droplets [65,67–69]. However, this method is time-consuming, requiring a particle velocity of  $\sim 50$   $\mu\text{m}/\text{h}$  [41] to achieve single- particle encapsulation; furthermore, some multiplexed nucleic acid detection methods are not compatible with beads made in gel form [70–72]. Price et al. presented a potentially simple solution by exploiting the sedimentation potential of the beads using a hopper system [62]. They, however, showed that it took

0.8 h (17  $\mu\text{m}$  Tetangel resin beads) and 3.8 h (2.8  $\mu\text{m}$  magnetic beads) for bead introduction before achieving single bead encapsulation. Kim et al. successfully developed a pneumatic system which is capable of trapping and releasing beads, thus creating a deterministic encapsulation of a defined number of beads per droplet [62]. This system is not simple to develop or operate, thus, unfit for low-cost point-of-care devices that can integrate with other modules.

Our goal was to present a simple, easy-to-fabricate method to encapsulate single dense beads in droplets that can be used for further downstream analysis. It is important to encapsulate single beads as opposed to multiple beads to avoid cross-contamination or

confusion of which target molecule or bead is in the droplet. The idea is to vertically orient the syringe pump while keeping the beads suspended by mechanical agitation (which prevents loss of beads due to sedimentation in the flow tubing and in the syringe) (Figure S 3.1B), then pump the contents directly into the droplet generation cartridge (Figure 3.1B). Using this principle, we set up bead encapsulation with the droplet generation device such that  $\lambda \approx 0.15, 0.2$  and  $0.3$  beads/droplet, where  $\lambda$  represents the average number of beads per droplet input into the device (Figure 3.4). We observed that our dense bead encapsulation method agreed well with Poisson predictions (Figure 3.4B). Importantly, the droplet generation device resulted in  $<2\%$  of droplets containing more than 1 bead at  $\lambda \approx 0.15$ ,  $<4\%$  of droplets containing more than 1 bead at  $\lambda \approx 0.2$ , and  $<6\%$  of droplets containing more than 1 bead at  $\lambda \approx 0.3$ .

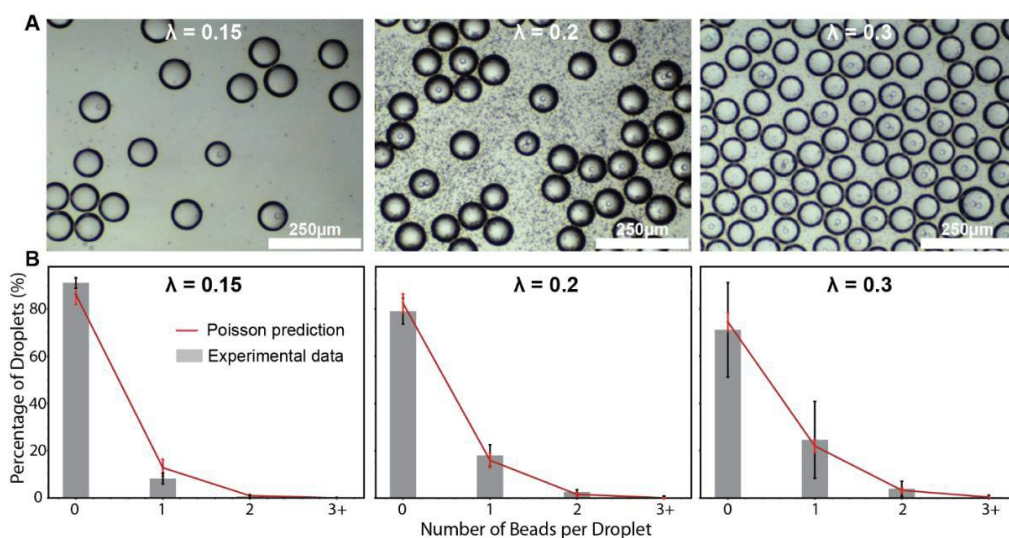


Figure 3.4 Dense bead in droplet (BiD) encapsulation at varying bead concentrations ( $\lambda = 0.15, 0.2, 0.3$ ). (A) Microscope images of BiD. (B) Poisson-predicted bead in droplets distribution in comparison to the observed experimental data.

### 3.4 Conclusions

Using design principles from droplet microfluidic device literature, we designed and developed a microfluidic device fabricated without complex equipment or cleanroom facilities that can generate sub-100 pL droplets and encapsulate dense beads with a Poisson-like distribution. Because the device is made from a 3D printed mold, researchers can iterate prototypes rapidly without undergoing the time and resource-consuming processes of photolithography; additionally, the droplet generation module can be part of a larger 3D printed mold that includes modules for executing other upstream or downstream assay processes, such as sample preparation, NA amplification, or single cell analysis.

While simple instrumentation was used to fabricate the microfluidic device, we still needed a syringe pump for operation of the device to generate consistent and controlled droplet sizes. Further improvements need to be made to our design to make it more amenable to point-of-care settings, such as a pumping lid [73], or other equipment-free pumping mechanisms [74]. Another limitation is that due to the 3D printer's minimum channel dimension ( $\sim 100 \mu\text{m}$ ), the lowest droplet diameter achieved was  $45 \mu\text{m}$  (48 pL).

Lower sizes could be possible in the future with the next generation of 3D printers that print channels down to  $15 \mu\text{m}$  [75].

Other microfluidic devices have encapsulated beads in a non-random distribution and thus have a much higher percentage of droplets with a single bead [41,43], though the beads in those studies have a similar density to water. While the phenomenon for the non-random distribution is unexplained, similar designs could potentially be used with the

dense bead mixing method studied here for higher percentages of droplets with single beads. In its current form, this device enables research and innovation into assays or methods that need to use beads with a density greater than water and thus overcome the sedimentation effect, such as PMMA or magnetic beads. Because it can easily be printed and combined with others as part of a larger device, microfluidic sorting mechanisms can also be used to concentrate the beads downstream if desired [76].

Future research directions from this work can include: eliminating the need for a syringe pump for <100 pL droplet generation, adapting the device to other biological assay applications beyond digital LAMP, beating Poisson encapsulation statistics for dense beads to reduce the waste of empty droplets, or adapting the BiD method for tagging multiple biomarkers. Due to the simple instrumentation used, this work enables rapid prototyping for a variety of biological applications of droplet microfluidic devices and dense bead encapsulation.

**Supplementary Materials:** The following supporting information can be downloaded at: [https:](https://www.mdpi.com/article/10.3390/mi13111946/s1)

[//www.mdpi.com/article/10.3390/mi13111946/s1](https://www.mdpi.com/article/10.3390/mi13111946/s1), Section S1: Syringe with mixer to overcome sedimentation effect of dense beads; Section S2: Capillary number calculations for picolitre-scale droplet generation design; Section S3: Poisson prediction of positive droplet percentage; Section S4: Effect of Glycerol on LAMP Amplification; Section S5: Pitfalls of 3D Printing Fabrication of Microfluidic Cartridges. Figure S1: (A) Tube connecting syringe containing bead suspension to the droplet generation cartridge; red arrow shows region of bead sedimentation. (B) Syringe design for mechanical resuspension and homogenization of dense particles for vertical delivery. The DC motor is powered

using a 3V battery. Figure S2: Without the syringe mixer in Figure S1, bead sedimentation happens in the syringe and tubing, leading to the encapsulation of multiple beads per droplet. Figure S3: Denser

fluids, such as glycerol, may improve bead buoyancy but it inhibits LAMP amplification (blue trace vs. red trace). Bead Density = 1.18 g/cm<sup>3</sup>, Glycerol Density = 1.26 g/cm<sup>3</sup>.

Figure S4: Microcapillary lines imprinted by 3D printed mold. This is often due to printer-head misalignment that often occurred

during prolonged prints. Figure S5: Micrograph showing curved vertices imprinted from 3D-printed mold. Figure S6: Irregularities in chamber dimensions due to myriad factors, including incompletely cured PDMS and build-up PDMS deposit due to mold reuse. Note that the displayed images contain channels designed to have widths of 50 and 100 μm.

Figure S7: Frosted PDMS molded on improperly cleaned 3D printed mold. Figure S8: Image of final fabricated PDMS device and 3D printed mold.

**Author Contributions:** Conceptualization, T.D.A. and T.S.S.; methodology, T.D.A.; software, T.D.A.; validation, T.D.A. and J.A.O.; formal analysis, T.D.A., J.A.O. and T.S.S.; investigation, T.D.A. and J.A.O.; resources, T.S.S.; data curation, T.D.A. and J.A.O.; writing, T.S.S., T.D.A. and J.A.O.; visualization, T.D.A., T.S.S. and J.A.O.; supervision, T.S.S.; project administration, T.S.S. and T.D.A.; funding acquisition, T.S.S. and T.D.A. All authors have read and agreed to the published version of the manuscript.

**Funding:** Research reported in this publication was supported by the National Institute of Biomedical Imaging and Bioengineering of the National Institutes of Health under Award

Number K01EB027718. The content is solely the responsibility of the authors and does not necessarily represent the official views of the National Institutes of Health.

**Data Availability Statement:** The data presented in this study are available in this article and Supplementary Materials.

**Conflicts of Interest:** The authors declare no conflict of interest.

### 3.4 References

1. Teh, S.Y.; Lin, R.; Hung, L.H.; Lee, A.P. Droplet microfluidics. *Lab Chip*. **2008**, *8*, 198–220. [[CrossRef](#)] [[PubMed](#)]
2. Sohrabi, S.; Kassir, N.; Keshavarz Moraveji, M. Droplet microfluidics: Fundamentals and its advanced applications. *RSC Adv*. **2020**, *10*, 27560–27574. [[CrossRef](#)]
3. Zhu, G.P.; Wang, Q.Y.; Ma, Z.K.; Wu, S.H.; Guo, Y.P. Droplet Manipulation under a Magnetic Field: A Review. *Biosensors* **2022**, *12*, 156. [[CrossRef](#)] [[PubMed](#)]
4. Yang, C.G.; Xu, Z.R.; Wang, J.H. Manipulation of droplets in microfluidic systems. *TrAC—Trends Anal. Chem.* **2010**, *29*, 141–157. [[CrossRef](#)]
5. Park, S.Y.; Kalim, S.; Callahan, C.; Teitell, M.A.; Chiou, E.P.Y. A light-induced dielectrophoretic droplet manipulation platform. *Lab Chip*. **2009**, *9*, 3228–3235. [[CrossRef](#)]
6. Hartmann, J.; Schür, M.T.; Hardt, S. Manipulation and control of droplets on surfaces in a homogeneous electric field. *Nat. Commun.* **2022**, *13*, 289. [[CrossRef](#)]
7. Zaman, M.A.; Padhy, P.; Ren, W.; Wu, M.; Hesselink, L. Microparticle transport along a planar electrode array using moving dielectrophoresis. *J. Appl. Phys.* **2021**, *130*, 034902. [[CrossRef](#)]
8. Mazutis, L.; Araghi, A.F.; Miller, O.J.; Baret, J.-C.; Frenz, L.; Janoshazi, A.; Taly, V.; Miller, B.J.; Hutchison, J.B.; Link, D.; et al. Droplet-based microfluidic systems

- for high-throughput single DNA molecule isothermal amplification and analysis. *Anal. Chem.* **2009**, *81*, 4813–4821. [[CrossRef](#)]
9. Zhang, K.; Kang, D.K.; Ali, M.M.; Liu, L.; Labanieh, L.; Lu, M.; Riazifar, H.; Nguyen, T.N.; Zell, J.A.; Digman, M.A.; et al. Digital quantification of miRNA directly in plasma using integrated comprehensive droplet digital detection. *Lab Chip.* **2015**, *15*, 4217–4226. [[CrossRef](#)]
  10. Kintsjes, B.; Hein, C.; Mohamed, M.F.; Fischlechner, M.; Courtois, F.; Lainé, C.; Hollfelder, F. Picoliter cell lysate assays in microfluidic droplet compartments for directed enzyme evolution. *Chem. Biol.* **2012**, *19*, 1001–1009. [[CrossRef](#)]
  11. Perroud, T.D.; Meagher, R.J.; Kanouff, M.P.; Renzi, R.F.; Wu, M.; Singh, A.K.; Patel, K.D. Isotropically etched radial micropore for cell concentration, immobilization, and picodroplet generation. *Lab Chip.* **2009**, *9*, 507–515. [[CrossRef](#)] [[PubMed](#)]
  12. Beer, N.R.; Hindson, B.J.; Wheeler, E.K.; Hall, S.B.; Rose, K.A.; Kennedy, A.I.M.; Colston, B.W. Reaction in Picoliter Droplets. *Anal. Chem.* **2007**, *79*, 8471–8475. [[CrossRef](#)] [[PubMed](#)]
  13. Zhu, Y.; Zhang, Y.X.; Cai, L.F.; Fang, Q. Sequential operation droplet array: An automated microfluidic platform for picoliter-scale liquid handling, analysis, and screening. *Anal. Chem.* **2013**, *85*, 6723–6731. [[CrossRef](#)]
  14. Baker, M. Digital PCR hits its stride. *Nat. Methods* **2012**, *9*, 541–544. [[CrossRef](#)]
  15. Li, E.Q.; Zhang, J.M.; Thoroddsen, S.T. Simple and inexpensive microfluidic

- devices for the generation of monodisperse multiple emulsions. *J. Micromech. Microeng.* **2014**, *24*, 015019. [CrossRef]
16. Gu, S.Q.; Zhang, Y.X.; Zhu, Y.; Du, W.B.; Yao, B.; Fang, Q. Multifunctional picoliter droplet manipulation platform and its application in single cell analysis. *Anal. Chem.* **2011**, *83*, 7570–7576. [CrossRef]
  17. Li, H.T.; Wang, H.F.; Wang, Y.; Pan, J.Z.; Fang, Q. A minimalist approach for generating picoliter to nanoliter droplets based on an asymmetrical beveled capillary and its application in digital PCR assay. *Talanta* **2020**, *217*, 120997. [CrossRef] [PubMed]
  18. Postek, W.; Kaminski, T.; Garstecki, P. A passive microfluidic system based on step emulsification allows to generate libraries of nanoliter-sized droplets from microliter droplets of varying and known concentration of sample. *Lab Chip.* **2017**, *17*, 1323–1331. [CrossRef]
  19. Churski, K.; Nowacki, M.; Korczyk, P.M.; Garstecki, P. Simple modular systems for generation of droplets on demand. *Lab Chip.* **2013**, *13*, 3689. [CrossRef]
  20. Schulz, M.; Probst, S.; Calabrese, S.; Homann, A.R.; Borst, N.; Weiss, M.; Von Stetten, F.; Zengerle, R.; Paust, N. Versatile tool for droplet generation in standard reaction tubes by centrifugal step emulsification. *Molecules* **2020**, *25*, 1914. [CrossRef]
  21. Mohamed, M.G.A.; Kumar, H.; Wang, Z.; Martin, N.; Mills, B.; Kim, K. Rapid and inexpensive fabrication of multi-depth microfluidic device using high-resolution LCD stereolithographic 3D printing. *J. Manuf. Mater. Process.*

- 2019**, 3, 26. [CrossRef]
22. Hwang, Y.; Paydar, O.H.; Candler, R.N. 3D printed molds for non-planar PDMS microfluidic channels. *Sens. Actuators A Phys.* **2015**, 226, 137–142. [CrossRef]
23. Saggiomo, V.; Velders, A.H. Simple 3D Printed Scaffold-Removal Method for the Fabrication of Intricate Microfluidic Devices. *Adv. Sci.* **2015**, 2, 1500125. [CrossRef] [PubMed]
24. Li, Z.; Yang, J.; Li, K.; Zhu, L.; Tang, W. Fabrication of PDMS microfluidic devices with 3D wax jetting. *RSC Adv.* **2017**, 7, 3313–3320. [CrossRef]
25. Zhang, J.M.; Li, E.Q.; Aguirre-Pablo, A.A.; Thoroddsen, S.T. A simple and low-cost fully 3D-printed non-planar emulsion generator. *RSC Adv.* **2016**, 6, 2793–2799. [CrossRef]
26. Zhang, J.M.; Aguirre-Pablo, A.A.; Li, E.Q.; Buttner, U.; Thoroddsen, S.T. Droplet generation in cross-flow for cost-effective 3D-printed “plug-and-play” microfluidic devices. *RSC Adv.* **2016**, 6, 81120–81129. [CrossRef]
27. Bhargava, K.C.; Thompson, B.; Malmstadt, N. Discrete elements for 3D microfluidics. *Proc. Natl. Acad. Sci. USA* **2014**, 111, 15013–15018. [CrossRef]
28. Shallan, A.I.; Smejkal, P.; Corban, M.; Guijt, R.M.; Breadmore, M.C. Cost-effective three-dimensional printing of visibly transparent microchips within minutes. *Anal. Chem.* **2014**, 86, 3124–3130. [CrossRef]
29. Donvito, L.; Galluccio, L.; Lombardo, A.; Morabito, G.; Nicolosi, A.; Reno, M. Experimental validation of a simple, low-cost, T-junction droplet generator

- fabricated through 3D printing. *J. Micromech. Microeng.* **2015**, *25*, 035013.  
[CrossRef]
30. Jiao, Z.; Zhao, L.; Tang, C.; Shi, H.; Wang, F.; Hu, B. Droplet-based PCR in a 3D-printed microfluidic chip for miRNA-21 detection. *Anal. Methods.* **2019**, *11*, 3386–3393. [CrossRef]
31. Ji, Q.; Zhang, J.M.; Liu, Y.; Li, X.; Lv, P.; Jin, D.; Duan, H. A Modular Microfluidic Device via Multimaterial 3D Printing for Emulsion Generation. *Sci. Rep.* **2018**, *8*, 4791. [CrossRef] [PubMed]
32. Heyries, K.A.; Tropini, C.; Vaninsberghe, M.; Doolin, C.; Petriv, O.I.; Singhal, A.; Leung, K.; Hughesman, C.B.; Hansen, C.L. Megapixel digital PCR. *Nat. Methods* **2011**, *8*, 649–651. [CrossRef] [PubMed]
33. Chiu, D.T.; Lorenz, R.M.; Jeffries, G.D.M. Droplets for ultrasmall-volume analysis. *Anal. Chem.* **2009**, *81*, 5111–5118. [CrossRef] [PubMed]
34. Margulies, M.; Egholm, M.; Altman, W.E.; Attiya, S.; Bader, J.S.; Bembien, L.A.; Berka, J.; Braverman, M.S.; Chen, Y.-J.; Chen, Z.; et al. Genome sequencing in microfabricated high-density picolitre reactors. *Nature* **2005**, *437*, 376–380. [CrossRef]
35. Tawfik, D.S.; Griffiths, A.D. Man-made cell-like compartments for molecular evolution. *Nat. Biotechnol.* **1998**, *16*, 291–294. [CrossRef]
36. Griffiths, A.D.; Tawfik, D.S. Miniaturising the laboratory in emulsion droplets. *Trends Biotechnol.* **2006**, *24*, 395–402. [CrossRef]

37. Chen, W.W.; Balaj, L.; Liao, L.M.; Samuels, M.L.; Kotsopoulos, S.K.; Maguire, C.A.; LoGuidice, L.; Soto, H.; Garrett, M.; Zhu, L.D.; et al. Beaming and droplet digital pcr analysis of mutant idh1 mrna in glioma patient serum and cerebrospinal fluid extracellular vesicles. *Mol. Ther.-Nucleic Acids* **2013**, *2*, e109. [CrossRef]
38. Dressman, D.; Yan, H.; Traverso, G.; Kinzler, K.W.; Vogelstein, B. Transforming single DNA molecules into fluorescent magnetic particles for detection and enumeration of genetic variations. *Proc. Natl. Acad. Sci. USA* **2003**, *80*, 8817–8822. [CrossRef]
39. Kumaresan, P.; Yang, C.J.; Cronier, S.A.; Blazej, R.G.; Mathies, R.A. High-throughput single copy DNA amplification and cell analysis in engineered nanoliter droplets. *Anal. Chem.* **2008**, *80*, 3522–3529. [CrossRef]
40. Chen, J.; Xu, X.; Huang, Z.; Luo, Y.; Tang, L.; Jiang, J.H. BEAMing LAMP: Single-molecule capture and on-bead isothermal amplification for digital detection of hepatitis C virus in plasma. *Chem. Commun.* **2018**, *54*, 291–294. [CrossRef]
41. Abate, A.R.; Chen, C.H.; Agresti, J.J.; Weitz, D.A. Beating Poisson encapsulation statistics using close-packed ordering. *Lab Chip.* **2009**, *9*, 2628–2631. [CrossRef] [PubMed]
42. Lee, D.H.; Park, J.K. Reduction in microparticle adsorption using a lateral interconnection method in a PDMS-based microfluidic device. *Electrophoresis* **2013**, *34*, 3119–3125. [CrossRef] [PubMed]
43. Edd, J.F.; Di Carlo, D.; Humphry, K.J.; Köster, S.; Irimia, D.; Weitz, D.A.; Toner, M. Controlled encapsulation of single-cells into monodisperse picolitre

- drops. *Lab Chip*. **2008**, *8*, 1262–1264. [CrossRef]
44. Wu, L.; Chen, P.; Dong, Y.; Feng, X.; Liu, B.F. Encapsulation of single cells on a microfluidic device integrating droplet generation with fluorescence-activated droplet sorting. *Biomed. Microdevices* **2013**, *15*, 553–560. [CrossRef]
45. Lagus, T.P.; Edd, J.F. High-throughput co-encapsulation of self-ordered cell trains: Cell pair interactions in microdroplets. *RSC Adv*. **2013**, *3*, 20512–20522. [CrossRef]
46. Ghaemi, R.; Dabaghi, M.; Attalla, R.; Shahid, A.; Hsu, H.H.; Selvaganapathy, P.R. Use of flame activation of surfaces to bond PDMS to variety of substrates for fabrication of multimaterial microchannels. *J. Micromech. Microeng.* **2018**, *28*, 087001. [CrossRef]
47. Kreutz, J.E.; Munson, T.; Huynh, T.; Shen, F.; Du, W.; Ismagilov, R.F. Theoretical design and analysis of multivolume digital assays with wide dynamic range validated experimentally with microfluidic digital PCR. *Anal. Chem.* **2011**, *83*, 8158–8168. [CrossRef]
48. Roberts, C.C.; Rao, R.R.; Loewenberg, M.; Brooks, C.F.; Galambos, P.; Grillet, A.M.; Nemer, M.B. Lab on a Chip Comparison of monodisperse droplet generation in flow-focusing devices with hydrophilic and hydrophobic surfaces. *Lab Chip*. **2012**, *12*, 1540–1547. [CrossRef]
49. Lee, W.; Walker, L.M.; Anna, S.L. Role of geometry and fluid properties in droplet and thread formation processes in planar flow focusing. *Phys. Fluids* **2009**, *21*, 032103. [CrossRef]
50. Chen, I.J.; Wu, T.; Hu, S. A hand-held, power-free microfluidic device for

- monodisperse droplet generation. *MethodsX* **2018**, *5*, 984–990. [CrossRef]
51. ten Klooster, S.; Sahin, S.; Schroën, K. Monodisperse droplet formation by spontaneous and interaction based mechanisms in partitioned EDGE microfluidic device. *Sci. Rep.* **2019**, *9*, 7820. [CrossRef] [PubMed]
  52. Selck, D.A.; Karymov, M.A.; Sun, B.; Ismagilov, R.F. Increased robustness of single-molecule counting with microfluidics, digital isothermal amplification, and a mobile phone versus real-time kinetic measurements. *Anal. Chem.* **2013**, *85*, 11129–11136. [CrossRef] [PubMed]
  53. Sun, B.; Shen, F.; McCalla, S.E.; Kreutz, J.E.; Karymov, M.A.; Ismagilov, R.F. Mechanistic evaluation of the pros and cons of digital RT-LAMP for HIV-1 viral load quantification on a microfluidic device and improved efficiency via a two-step digital protocol. *Anal. Chem.* **2013**, *85*, 1540–1546. [CrossRef] [PubMed]
  54. Sun, B.; Rodriguez-Manzano, J.; Selck, D.A.; Khorosheva, E.; Karymov, M.A.; Ismagilov, R.F. Measuring fate and rate of single- molecule competition of amplification and restriction digestion, and its use for rapid genotyping tested with hepatitis C viral RNA. *Angew. Chemie Int. Ed.* **2014**, *53*, 8088–8092. [CrossRef]
  55. Schoepp, N.G.; Schlappi, T.S.; Curtis, M.S.; Butkovich, S.S.; Miller, S.; Humphries, R.M.; Ismagilov, R.F. Pathogen-specific Phenotypic Antibiotic Susceptibility Test Directly from Clinical Samples in as Fast as 30 Minutes Using Digital LAMP Quantification. *Sci. Transl. Med.* **2017**, *3693*, 1–20.
  56. Luo, K.; Chang, W.; Lee, G. An Integrated Array-Based Emulsion Droplet

- Microfluidic Device for Digital Loop-Mediated Isothermal Amplification (LAMP) Analysis. In Proceedings of the 2016 IEEE 11th Annual International Conference on Nano/Micro Engineered and Molecular Systems (NEMS), Sendai, Japan, 17–20 April 2016; pp. 17–20.
57. Gansen, A.; Herrick, A.M.; Dimov, I.K.; Lee, L.P.; Chiu, D.T. Digital LAMP in a sample self-digitization (SD) chip. *Lab Chip*. **2012**, *12*, 2247. [CrossRef] [PubMed]
58. Xu, P.; Zheng, X.; Tao, Y.; Du, W. Cross-Interface Emulsification for Generating Size-Tunable Droplets. *Anal. Chem.* **2016**, *88*, 3171–3177. [CrossRef]
59. Kim, H.; Choi, I.H.; Lee, S.; Won, D.-J.; Oh, Y.S.; Kwon, D.; Sung, H.J.; Jeon, S.; Kim, J. Deterministic bead-in-droplet ejection utilizing an integrated plug-in bead dispenser for single bead-based applications OPEN. *Sci. Rep.* **2017**, *7*, 46260. [CrossRef]
60. Iwai, K.; Sochol, R.D.; Lin, L. A Bead-in-Droplet Solution Exchange System via Continuous Flow Microfluidic Railing. In Proceedings of the IEEE International Conference on Micro Electro Mechanical Systems (MEMS), Taipei, Taiwan, 20–24 January 2013; pp. 1203–1206. [CrossRef]
61. Wang, C.H.; Lien, K.Y.; Wu, J.J.; Lee, G.B. A magnetic bead-based assay for the rapid detection of methicillin-resistant *Staphylococcus aureus* by using a microfluidic system with integrated loop-mediated isothermal amplification. *Lab Chip*. **2011**, *11*, 1521–1531. [CrossRef]
62. Price, A.K.; Macconnell, A.B.; Paegel, B.M. Microfluidic Bead Suspension

- Hopper. *Anal. Chem.* **2014**, *86*, 5039–5044. [CrossRef]
63. Vashist, S.K.; Luong, J.H.T. Antibody Immobilization and Surface Functionalization Chemistries for Immunodiagnostics. In *Handbook of Immunoassay Technologies: Approaches, Performances, and Applications*; Elsevier: Amsterdam, The Netherlands, 2018; pp. 19–46. [CrossRef]
64. Sassolas, A.; Hayat, A.; Marty, J.L. Immobilization of enzymes on magnetic beads through affinity interactions. *Methods Mol. Biol.* **2013**, *1051*, 139–148. [CrossRef] [PubMed]
65. Clark, I.C.; Abate, A.R. Microfluidic bead encapsulation above 20 kHz with triggered drop formation. *Lab Chip.* **2018**, *18*, 3598–3605. [CrossRef] [PubMed]
66. Collins, D.J.; Neild, A.; de Mello, A.; Liu, A.Q.; Ai, Y. The Poisson distribution and beyond: Methods for microfluidic droplet production and single cell encapsulation. *Lab Chip.* 2015, *15*, 3439–3459. [CrossRef]
67. Shintaku, H.; Kuwabara, T.; Kawano, S.; Suzuki, T.; Kanno, I.; Kotera, H. Micro cell encapsulation and its hydrogel-beads production using microfluidic device. *Microsyst. Technol.* 2006, *13*, 951–958. [CrossRef]
68. Zilionis, R.; Nainys, J.; Veres, A.; Savova, V.; Zemmour, D.; Klein, A.M.; Mazutis, L. Single-cell barcoding and sequencing using droplet microfluidics. *Nat. Publ. Gr.* 2016, *12*, 44–73. [CrossRef]
69. Klein, A.M.; Mazutis, L.; Akartuna, I.; Tallapragada, N.; Veres, A.; Li, V.; Peshkin, L.; Weitz, D.A.; Kirschner, M.W. Droplet barcoding for single-cell transcriptomics

- applied to embryonic stem cells. *Cell* 2015, 161, 1187–1201. [CrossRef] [PubMed]
70. Kramer, T.; Rödiger, S. Absolute Quantification of Nucleic Acids on a Planar Droplet Digital PCR Array. 2016, 10–11. Available online: [https://www.researchgate.net/publication/303895837\\_Absolute\\_Quantification\\_of\\_Nucleic\\_Acids\\_on\\_a\\_Planar\\_Droplet\\_Digital\\_PCR\\_Array?channel=doi&linkId=575b178108ae414b8e46774e&showFulltext=true](https://www.researchgate.net/publication/303895837_Absolute_Quantification_of_Nucleic_Acids_on_a_Planar_Droplet_Digital_PCR_Array?channel=doi&linkId=575b178108ae414b8e46774e&showFulltext=true) (accessed on 5 November 2022). [CrossRef]
71. Rodiger, S.; Schierack, P.; Shroder, C. A Highly Versatile Microscope Imaging Technology Platform for the Multiplex Real-Time Detection of Biomolecules and Autoimmune Antibodies. *Adv. Biochem. Eng. Biotechnol.* 2013, 133, 35–74. [CrossRef]
72. Rödiger, S.; Liebsch, C.; Schmidt, C.; Lehmann, W.; Resch-Genger, U.; Schedler, U.; Schierack, P. Nucleic acid detection based on the use of microbeads: A review. *Microchim. Acta* 2014, 181, 1151–1168. [CrossRef]
73. Begolo, S.; Zhukov, D.V.; Selck, D.; Li, L.; Ismagilov, R.F. The pumping lid: Investigating multi-material 3D printing for equipment-free, programmable generation of positive and negative pressures for microfluidic applications. *Lab Chip.* 2014, 14, 4616–4628. [CrossRef]
74. Weigl, B.; Domingo, G.; LaBarre, P.; Gerlach, J. Towards non- and minimally instrumented, microfluidics-based diagnostic devices. *Lab Chip.* 2008, 8, 1999–2014. [CrossRef]
75. Sanchez Noriega, J.L.; Chartrand, N.A.; Valdoz, J.C.; Cribbs, C.G.; Jacobs, D.A.; Poulson, D.; Viglione, M.S.; Woolley, A.T.; Van Ry, P.M.; Christensen, K.A.; et

- al. Spatially and optically tailored 3D printing for highly miniaturized and integrated microfluidics. *Nat. Commun.* 2021, 12, 5509. [CrossRef] [PubMed]
76. Sajeesh, P.; Sen, A.K. Particle separation and sorting in microfluidic devices: A review. *Microfluid Nanofluid.* 2014, 17, 1–52. [CrossRef]

### 3.5 Supplementary Information

## **Picolitre droplet generation and dense bead-in-droplet encapsulation via microfluidic devices fabricated via 3D printed molds**

Tochukwu D. Anyaduba<sup>1,2</sup>, Jonas A. Otoo<sup>1</sup>, Travis S. Schlappi<sup>1,\*</sup>

<sup>1</sup> Riggs School of Applied Life Sciences, Keck Graduate Institute, 535 Watson Drive, Claremont, CA 91711, USA

<sup>2</sup> Abbott Rapid Diagnostics, 4545 Towne Center Ct, La Jolla, San Diego, CA 92121

\* Correspondence: [Travis\\_Schlappi@kgi.edu](mailto:Travis_Schlappi@kgi.edu)

## **Picoliter droplet generation and dense bead-in-droplet encapsulation via microfluidic devices fabricated via 3D printed molds**

Tochukwu D. Anyaduba<sup>1,2</sup>, Jonas A. Otoo<sup>1</sup>, Travis S. Schlappi<sup>1,\*</sup>

<sup>1</sup> Riggs School of Applied Life Sciences, Keck Graduate Institute, 535 Watson Drive, Claremont, CA 91711, USA

<sup>2</sup> Abbott Rapid Diagnostics, 4545 Towne Center Ct, La Jolla, San Diego, CA 92121

\* Correspondence: [Travis\\_Schlappi@kgi.edu](mailto:Travis_Schlappi@kgi.edu)

Chapter 2 Supplementary Information

**Section 1:** Syringe with mixer to overcome sedimentation effect of dense beads.

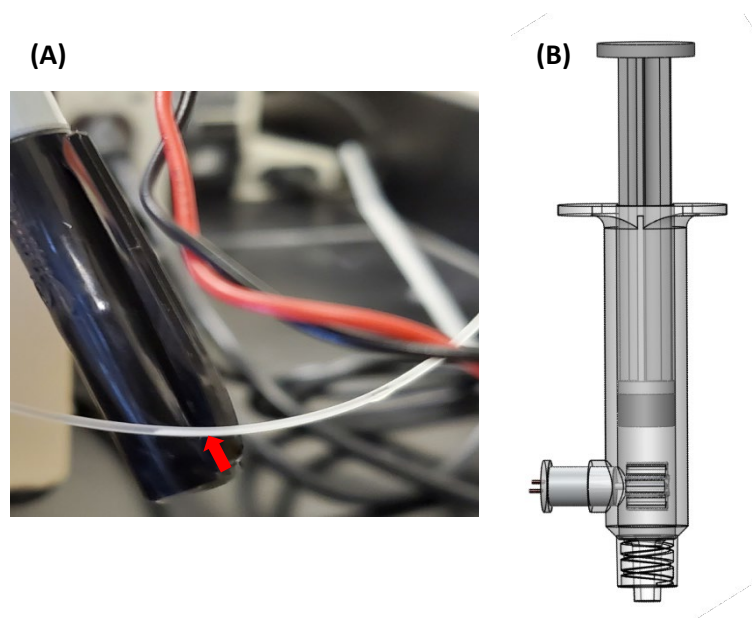


*Figure S 3.1 . (A) Tube connecting syringe containing bead suspension to the droplet generation cartridge; red arrow shows region of bead sedimentation. (B) Syringe design for mechanical resuspension and homogenization of dense particles for vertical delivery. The DC motor is powered using a 3V battery.*

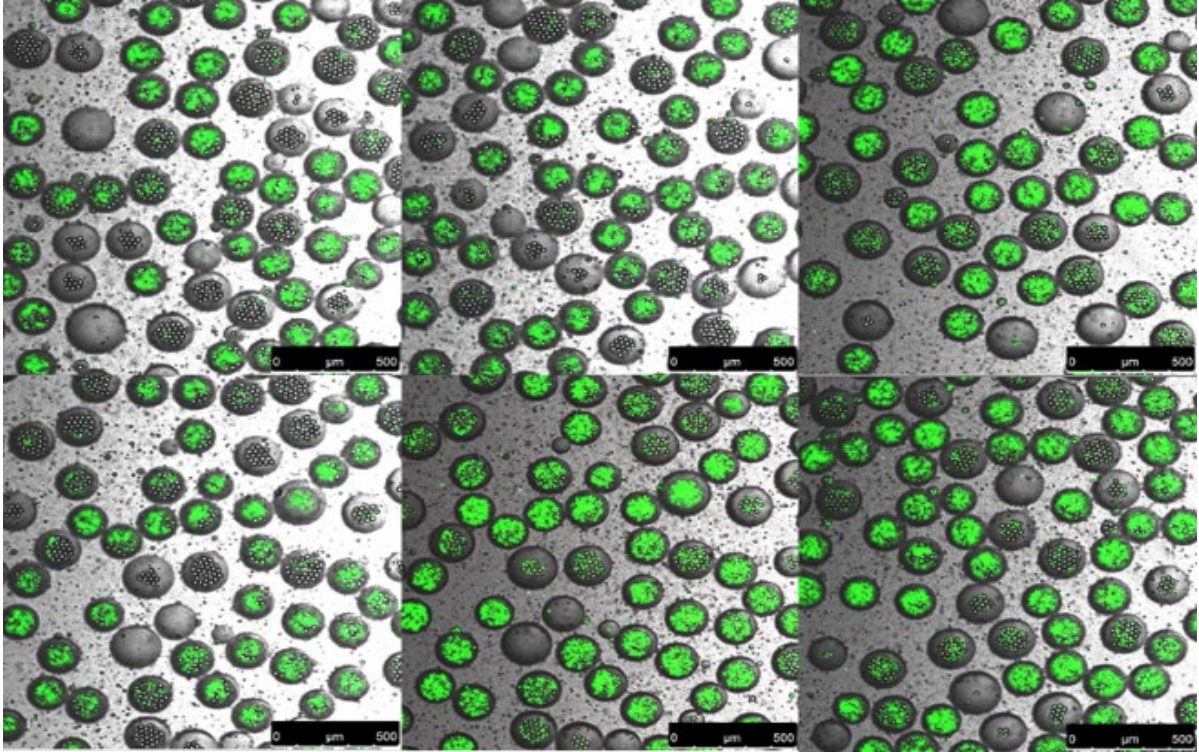


Figure S 3.2 Without the syringe mixer in Fig. S1, bead sedimentation happens in the syringe and tubing, leading to the encapsulation of multiple beads per droplet.

**Section 2:** Capillary number calculations for picoliter-scale droplet generation design.

From Figure 5 of Reference [44],  $\frac{r_d}{D_h} = 0.053 \cdot Ca^{-0.38}$ , with  $r_d$  = droplet radius,  $D_h$  = hydraulic diameter, and  $Ca$  = capillary number. The range of  $\frac{r_d}{D_h}$  studied in this work was 0.2 to 2. Using this equation,  $2 > \frac{r_d}{D_h} > 0.73$  corresponds to  $Ca < .001$ , and  $0.2 < \frac{r_d}{D_h} < 0.73$  corresponds to  $Ca > .001$ .

$$\text{A } 100 \text{ pL droplet has } r_d = \left( \frac{100 \text{ pL}}{\frac{4}{3}\pi} \right)^{1/3} = 28.8 \mu\text{m}.$$

Therefore, in the  $Ca > .001$  regime,  $0.2 < \frac{r_d}{D_h} < 0.73 \rightarrow D_h > \frac{28.8\mu m}{0.73} = 39.3\mu m$

$$\rightarrow D_h < \frac{28.8\mu m}{0.2} = 144\mu m.$$

In the  $Ca < .001$  regime,  $2 > \frac{r_d}{D_h} > 0.73 \rightarrow D_h < \frac{28.8\mu m}{0.73} = 39.3\mu m$

$$\rightarrow D_h > \frac{28.8\mu m}{2} = 14.4\mu m.$$

Capillary number calculation using Equation (6) from Reference [44]:

$$\mu_{ave} = \left( \frac{1}{2\mu_o} + \frac{1}{2\mu_i} \right)^{-1} = 1.766 \text{ cp}$$

$$Ca = \frac{\mu_{ave}(2Q_o + Q_i)}{\sigma h w_{or}} = 0.148$$

$$\mu_{oil} = 30 \text{ cp}; \mu_{water} = .91 \text{ cp}; Q_o = 100 \mu\text{L}/\text{min}; Q_i = 1 \mu\text{L}/\text{min};$$

$$\sigma = 4 \text{ mN}/\text{m}; h = 100 \mu\text{m}; w_{or} = 100 \mu\text{m}$$

### **Section 3:** Poisson prediction of positive droplet percentage

The input DNA concentrations as measured by NanoDrop were 0,  $1.0 \cdot 10^7$ ,  $2.5 \cdot 10^7$ ,  $5.0 \cdot 10^7$ ,  $4.0 \cdot 10^8$  DNA copies/mL. From previous digital LAMP experiments, we estimated that the LAMP efficiency compared to PCR for our LAMP primers was ~10% and the droplet sizes generated from the device were ~300 pL. With these estimations for LAMP efficiency and droplet size, we then used Equation (2) from Reference [43] to calculate the percentage of positive droplets expected at each input DNA concentration.

$$\frac{b}{n} = e^{-v\lambda} \rightarrow Pos\% = 1 - \frac{b}{n} = 1 - e^{-v\lambda}$$

where  $b$  = # of negative droplets,  $n$  = # of total droplets,  $v$  = droplet volume in mL, and  $\lambda$  = DNA concentration in copies/mL.

For example, at  $2.5 \cdot 10^7$  copies/mL, Equation (2) predicts 53% of droplets will be positive:

$$Pos\% = 1 - e^{-v \cdot (\lambda \cdot eff)} = 1 - e^{-(3 \cdot 10^{-7}) \cdot (2.5 \cdot 10^7) \cdot 0.1} = 52.8\%$$

**Section 4:** Effect of Glycerol on LAMP Amplification

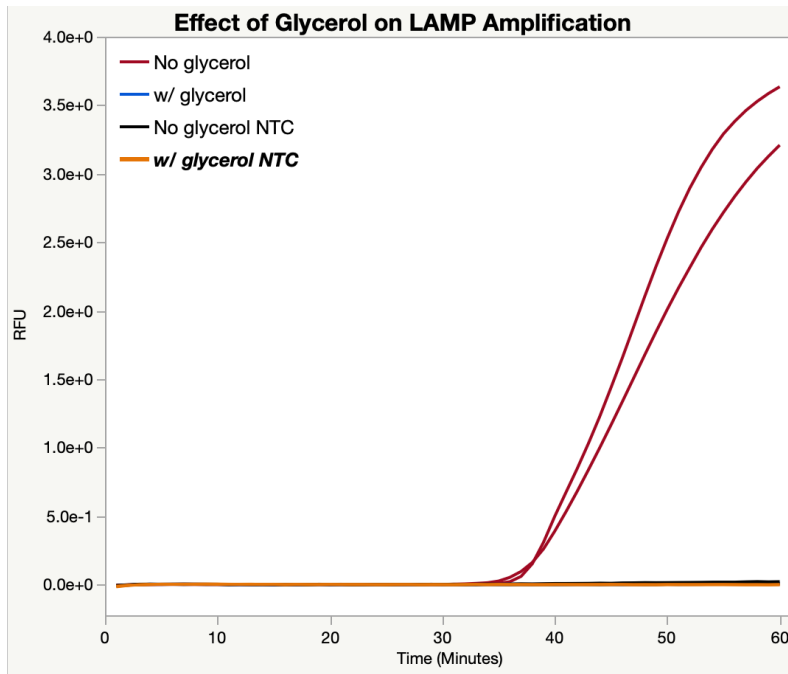


Figure S 3.3 . Denser fluids, such as glycerol, may improve bead buoyancy but it inhibits LAMP amplification (blue trace vs red trace). Bead Density =  $1.18 \text{ g/cm}^3$ , Glycerol Density =  $1.26 \text{ g/cm}^3$ .

**Section 4:** Pitfalls Of 3D Printing Fabrication of Microfluidic Cartridges

The pitfalls of 3D printing fabrication of microfluidics cartridges fall under to categories.

### 1. Equipment-dependent Pitfalls

One of the challenges attendant to using 3D printing for microfluidics is the limitation of the printer's resolution. We found that despite the advancements in 3D printing, especially desktop SLA printers, it is difficult to print channels with widths less than 50  $\mu\text{m}$ . More so, the printing of master molds at higher resolutions (for example, 25  $\mu\text{m}$  layer height) forces the printer to run for prolonged hours, thus, giving room for misaligned prints. This misalignment creates micro-channels in the molded PDMS, thereby causing leakage in the final cartridge (figure S4). Another consequence of the printer limitations is the difficulty in printing well-defined edges. This impacts flow focusing more as there is always a characteristic curvature at the flow junction (figure S5).

### 2. Procedural Pitfalls

As shown in figure S6, batch-to-batch variations in channel dimensions constitute a significant limitation of this system. This often comes from the post-print cleaning of master molds. Inadequately cleaned edges (especially around the flow channels) and other dead spaces may lead to increased channel dimensions once the left-over Stereolithographic (SLA) printer resin cures.

Variations in channel dimension also occur when PDMS get trapped in the edges of the printed molds. If the cured PDMS is not peeled off completely from the mold, there is always a risk of losing the channel wall definitions, which, in turn would affect the fluidic chip channel dimensions. More so, the idea behind the use of a 3D-printed mold is

to encourage the reuse of the molds. However, with the build-up of residual PDMS on the mold, the channel dimensions continuously increase with continued reuse.

Improperly cleaned molds also create a very rough finish on the molds which in turn are imprinted on the PDMS structures causing them to have frosted/ unclear appearance. In our experience, frosted PDMS casts do not bond properly onto the glass substrate (figure S7).

If the PDMS is not completely cured, attempts to peel them off the mold creates irregularities in the channel dimension and definition. In most cases, the channel may become occluded, tapered, or collapse due to efforts to bind the molded PDMS on the glass substrates.

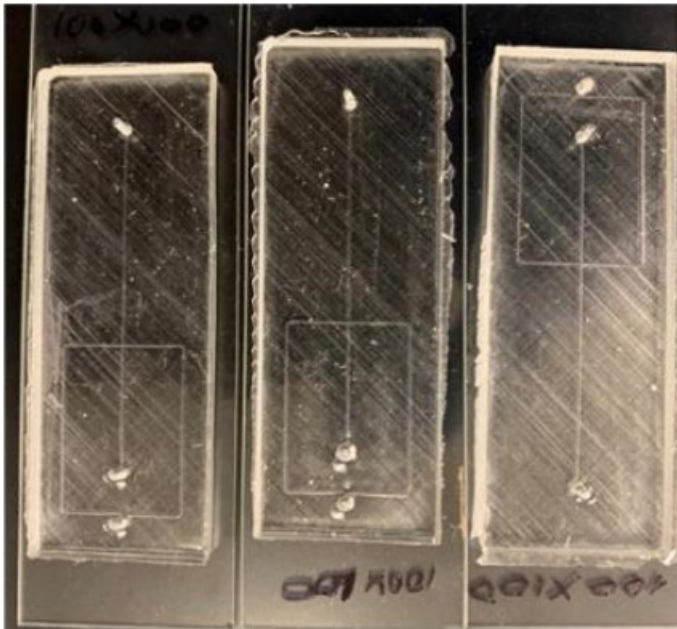


*Figure S 3.4 Microcapillary lines imprinted by 3D printed mold. This is often due to printer-head misalignment that often occurred during prolonged prints.*

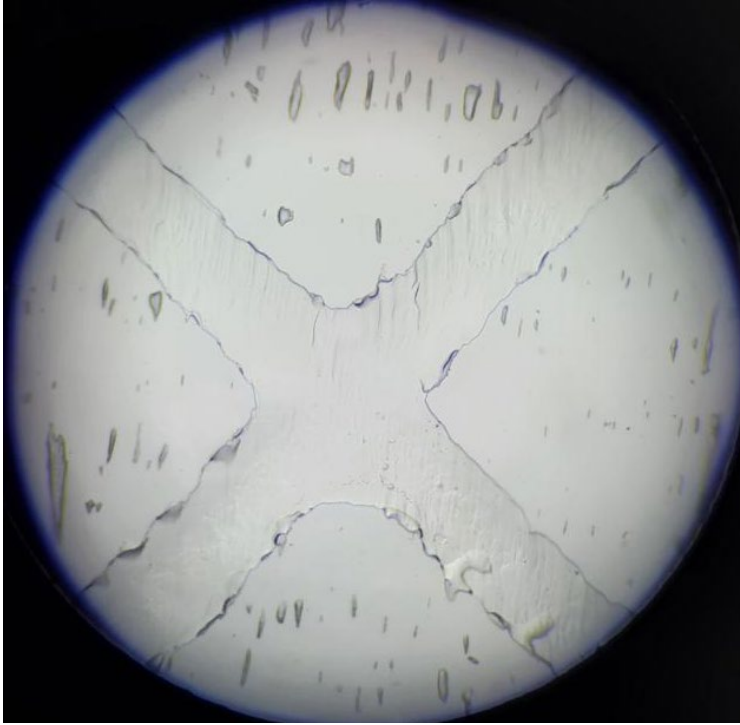


*Figure S 3.5 Micrograph showing curved vertices imprinted from 3D-printed mold*

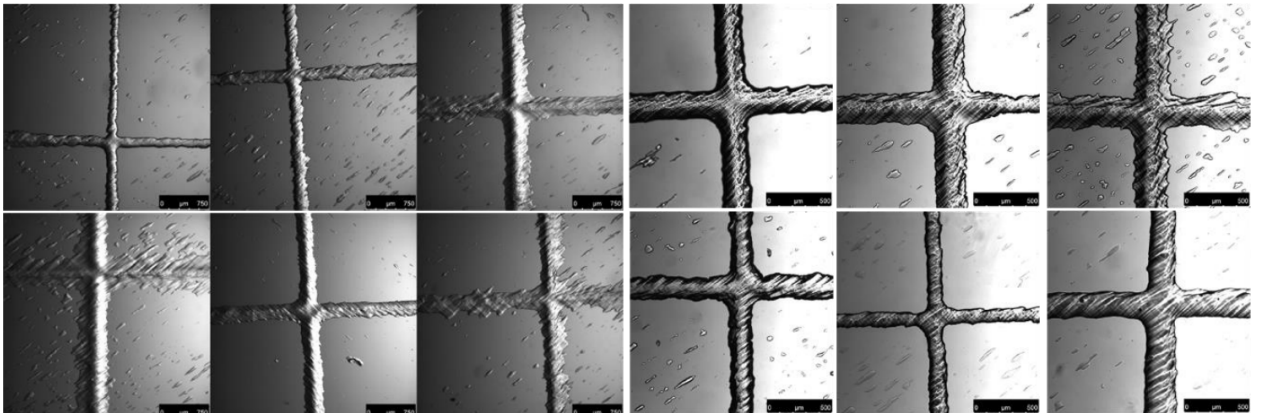


*Figure S 3.6 Irregularities in chamber dimensions due to myriad factors, including incompletely cured PDMS and build-up PDMS deposit due to mold reuse. Note that the displayed images contain channels designed to have widths of 50 and 100  $\mu\text{m}$*

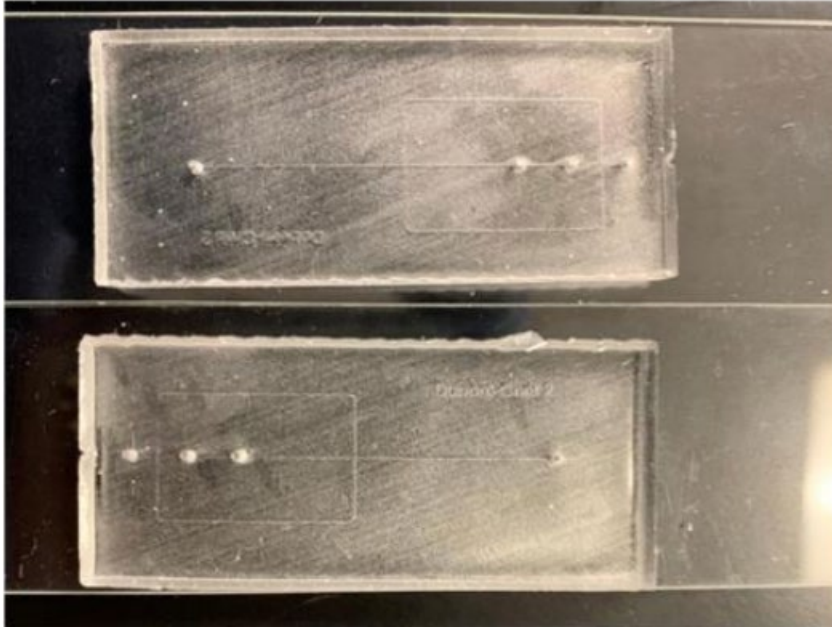


*Figure S 3.7 Frosted PDMS molded on improperly cleaned 3D printed mold*

# Chapter 4 Primer payload with microparticles for pathogen identification using Polythymidine-modified LAMP primers in droplet LAMP

Jonas A. Otoo, Tochukwu D. Anyaduba, Katie Wilson, Travis S. Schlappi\*

## Abstract

The development of accurate and accessible molecular diagnostics poses major complexity and cost hurdles. There is a need for molecular diagnostics that are suitable for point-of-care settings. Isothermal microfluidic assays have the potential to be integrated and developed into point-of-care diagnostic devices. We have developed a droplet microfluidic LAMP assay for pathogen identification via a primer payload mechanism. We achieve primer payload by attaching biotinylated and polyadenylated oligo-nucleotides to streptavidin coated microparticles. Polythymidine engineered primers were conjugated to the polyadenylated oligonucleotides and the primers were used to sequester their target DNA from solution. The functionalized microparticles were then encapsulated in droplet emulsions of LAMP reagents for amplification. We tested our assay with three UTI pathogens and demonstrated amplification of the target DNA in droplets.

## 4.1 Introduction

With the exacerbation of epidemics and pandemics around the world and the increasing rates of antibiotic resistance, the need for rapid and accurate molecular diagnostics is increasingly important. In order for diagnostics to address disease control needs, they need to be decentralized and affordable. Lateral flow antigen tests are among the most affordable kinds of diagnostic tests; however, their results can be subjective and they are not as

accurate as molecular tests<sup>1,2</sup>. On the other hand, molecular tests have relatively higher sensitivity and specificity. They are however, more expensive and even more complex to manufacture.

An approach to leverage the accuracy of molecular diagnostics and the affordability and simplicity of lateral flow device is through the use of microfluidics. Microfluidics has been a rapidly growing field that involves the manipulation of small fluid volumes in microscale devices. The field has tremendous potential for the development of new diagnostic tools, particularly for point-of-care testing and personalized medicine. Microfluidic devices have several advantages over traditional diagnostic methods, including high sensitivity, rapid turnaround time, and low cost<sup>3,4</sup>. They also have the potential to integrate multiple assays into a single device, making them ideal for multiplexed testing. In particular, they are becoming increasingly popular in the field of point-of-care testing, where they offer the potential for decentralized, fast, and accurate diagnosis in resource-limited settings. Microfluidics has also been applied to the development of microscale laboratories-on-a-chip, where entire diagnostic workflows can be integrated into a single device, enabling near real-time analysis of complex samples.

The introduction of digital microfluidics in the early 2000s broke ground for the development of digital NATs (dNAATs). Among other digital NATs, digital PCR (dPCR) offers advantages such as accurate single copy detection, high sensitivity, and absolute quantification<sup>5</sup>. Digital NATs use very small volumes of reagents and enable high throughput by compartmentalizing reactions into many discrete nL or pL volumes. While dPCR has all the added advantages of dNAATs, the challenges with PCR are still present.

Isothermal dNAATs provide an alternative method for dNAATs, that do not require thermal cycling.

In this research, we have developed a pathogen identification assay by using a microparticles for primer payload into microcompartments for isothermal amplification. We achieve isothermal amplification by a variation of Loop-Mediated Isothermal Amplification (LAMP), called droplet digital LAMP (ddLAMP).

LAMP is an isothermal amplification assay that was developed by Notomi et. al<sup>6</sup>, in 2000. LAMP utilizes 4 to 6 primers that are designed to hybridize to 4 to 6 distinct regions of the target sequence and initiate amplification. Four (forward inner primer or FIP, forward outer primer or FOP, backward inner primer or BIP and backward outer primer or BOP) out of the 6 primers are essential for the reaction to take place. The other two primers, (forward loop primer or LoopF and backward loop primer or LoopB) are optional, as the reaction can proceed in their absence. They however, increase the reaction sensitivity and specificity, and reduce the reaction time<sup>6,7</sup>. The recognition of the 4 to 6 sequences of the target makes the LAMP reaction highly selective to its target. Furthermore, the LAMP reaction is faster than, PCR, and demonstrates a higher sensitivity to conventional PCR. In addition, LAMP reactions are more robust than PCR reactions. This is because PCR reactions are more sensitive to the presence of non-target sequences and impurities, compared to LAMP reactions<sup>8-10</sup>.

There are, however, certain disadvantages of LAMP compared to PCR. LAMP amplicons are a heterogenous mixture of strands with varying lengths and loops, and hence, are very challenging to employ for post amplification processes such as sequencing. In addition, the

number of primers used in LAMP assays make it extremely difficult to develop multiplex LAMP reactions without reduced analytical sensitivity and the possibility of non-specific amplification, due to the fact that every additional target will require 4 to 6 primers<sup>6,11</sup>. To overcome this challenge, some studies employ sample splitting methods for multiplex LAMP reactions<sup>12,13</sup>. However, sample splitting reduces the number of target copies available per reaction, and hence, can cause a reduction in sensitivity of the assay.

Droplet digital LAMP (ddLAMP) allows for a highly parallel execution of LAMP reactions using the droplets as individual reaction chambers<sup>14</sup>. The use of the microparticles also facilitates the potential for multiplexing LAMP, circumventing the challenge of having too many primers in a single reaction. This work will overcome that challenge by using the microparticles to isolate the primers via payload mechanism. The isolated primers will then be used to capture their target nucleic acid and deliver them into the droplet for clonal isothermal amplification. This process will enable higher order multiplexing. Primer carrying microparticles can be differentially fluorescently barcoded for each specific target. Multiplexing offers advantages such as increased efficiency, and improved accuracy of diagnostic tests.

Some studies have demonstrated creative ways to achieve multiplex LAMP assays. Dong et al.<sup>15</sup> and Tanner et al.<sup>16</sup> developed molecular probes for identifying the various targets in the LAMP assay. Jang et al.<sup>17</sup> and Kim et al.<sup>18</sup> demonstrated a one pot multiplex reaction for the detection of SARS-CoV-2 and SARS-CoV virus respectively. Examples of space division multiplexing was implemented by Fang et al.<sup>19</sup> and Nguyen et al.<sup>13</sup> for a LAMP assay. Liang et al.<sup>20</sup> demonstrated a multiplex LAMP method which used barcodes coupled with nicking endonuclease-mediated pyrosequencing for target identification.

Nevertheless, some tradeoffs arise. These tradeoffs include the limitation of the additional costs of developing probes for each target, the reduction in sensitivity and specificity as primers compete for target, and the reduction in sensitivity as a result of spatial separation of targets.

Here, we present a droplet based digital LAMP assay using polystyrene microparticles for primer payload delivery into the droplets, for detection of some common UTI pathogen nucleic acids (figure S4.1).

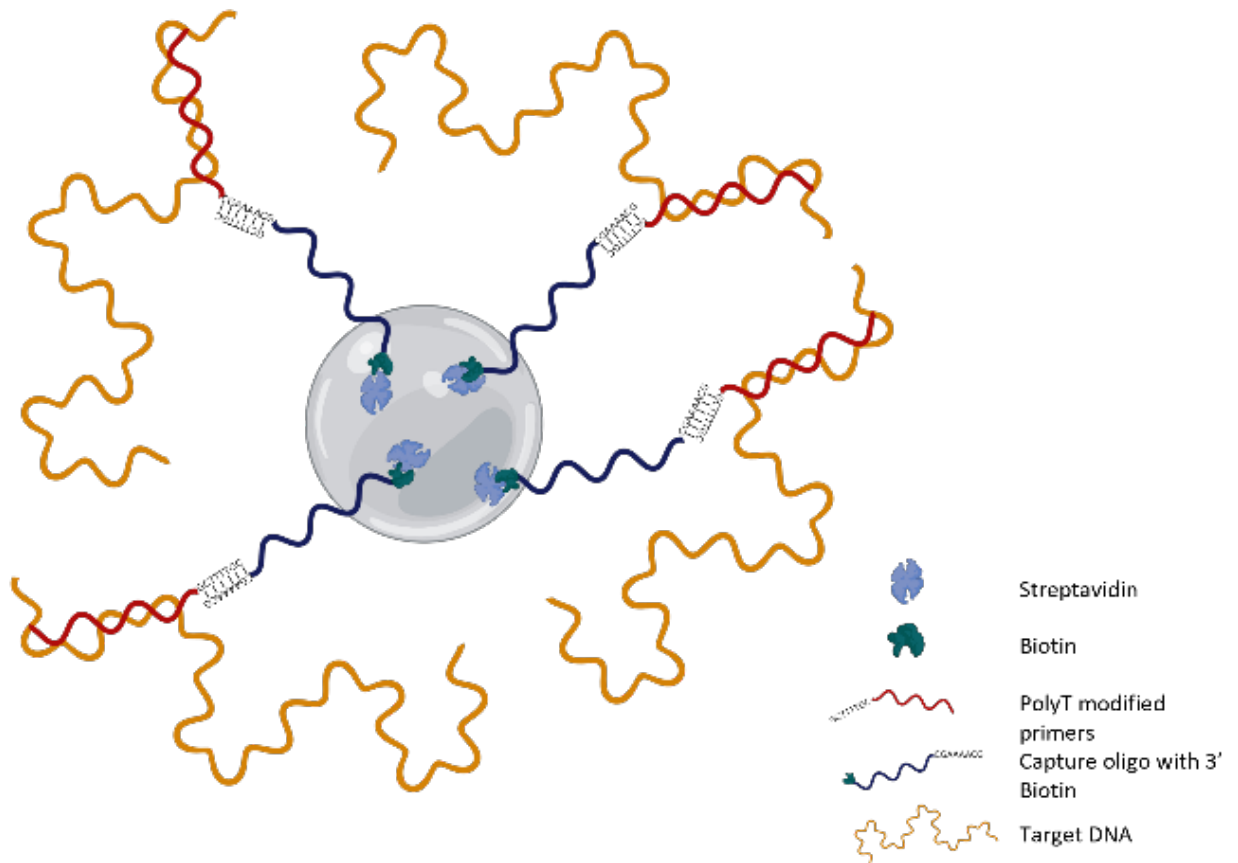


*Figure 4.1 Schematic of functionalized microparticle for primer payload mechanism.*

## 4.2 Experimental section

### 4.2.1 Reagents and equipment

Mineral oil (Sigma Aldrich M3516-1L), Triton X-100 (Fisher Biotech), ABIL EM 90 (Evonik, Germany), Polydimethylsiloxane (PDMS) and curing agent mixture (SLYGARD 184 Silicone Elastomer Base and SLYGARD 184 Elastomer Curing Agent, Isopropanol, BST 2.0, dNTP, Nuclease-free water, E. coli primers (IDT), P. aeruginosa primers (IDT), GBS primers (IDT), MgSO<sub>4</sub>, IsoAmp buffer, Evagreen dye (ThermoFisher), Tween 20, Transparent carboxylate 40 um Polystyrene microparticles (Spherotech), Transparent 40 um Polystyrene microparticles (Spherotech), Generic capture oligo (IDT), TBST buffer, TBSET buffer, 2 mL Sterile centrifuge tubes, Formlabs 3D printer, OMAX light microscope, MD35 AmScope microscope camera, Leica TCS SP5 confocal microscope, All primers were purchased from IDT, USA.

### 4.2.2 Microfluidic cartridge fabrication

The microfluidic cartridge was fabricated per the protocol in Anyaduba et. al.<sup>21</sup>

### 4.2.3 Polythymidine (polyT) LAMP primer design

E. coli LAMP primer sequences were obtained from Schoepp et al.<sup>22</sup> P. aeruginosa and group B streptococcus (GBS) LAMP primer sequences were designed using NEB LAMP primer design tool (New England BioLabs, USA). The Polythymidine (polyT) primers were design by appending a polyT 5'GCT TTT GC sequence on the 5' ends of FOP, BOP, LOOPF and LOOPB primers of the targets, E. coli, P. aeruginosa and GBS. The polyT sequence was inserted in the middle of the FIP and BIP primers (Table S 4.1).

#### *4.2.4 Comparison of 5' PolyT modified FIP and BIP with middle PolyT modified FIP and BIP LAMP*

A mastermix of 153 uL was prepared with the following components; 18uL of isothermal amplification buffer, 10.8 uL of MgSO<sub>4</sub>, 7.2 uL of BST DNA polymerase, 25.2 uL of dNTPs, 1.8 uL of Evagreen dye and 90 uL of nuclease-free water. The mastermix was aliquoted into 3 tubes (A, B, and C), 51 uL each. An amount of 3 uL of E. coli primer mix was added to tube A. An amount of 3 uL of 5'polyT E. coli primer mix was added to tube B. An amount of 3 uL of 5'polyT (polyT modification of FIP and BIP in the middle of sequence) E. coli primer mix was added to tube C. Each tube was aliquoted into two tubes of 27 uL each for positive DNA reaction versus no template control (NTC) reaction. An amount of 3 uL of E. coli DNA was added to each tube positive tube. An amount of 3 uL of nuclease-free water was added to each tube NTC tube. The reactions were run in triplicates of 10 uL, using Roche wells in the Roche LightCycler 96, for 1 hour at 65 C. Primer dilutions were prepared as shown in (table S 4.2).

#### *4.2.5 E. coli, GBS, and P. aeruginosa PolyT primers analytical specificity LAMP*

A mastermix of 153 uL was prepared with the following components; 18uL of isothermal amplification buffer, 10.8 uL of MgSO<sub>4</sub>, 7.2 uL of BST DNA polymerase, 25.2 uL of dNTPs, 1.8 uL of Evagreen dye and 90 uL of nuclease-free water. The mastermix was aliquoted into 2 tubes (A and B), 76.5 uL each. An amount of 4.5 uL of E. coli primer mix was added to tube A. An amount of 4.5 uL of P. aeruginosa primer mix was added to tube B. Each tube was aliquoted into three tubes (1A, 1B, 1C, 2A, 2B, and 2C) of 27 uL each. Tubes 1A and 1B were both mixed with an amount of 3 uL of E. coli DNA each. Tubes 2A and 2B were both mixed with an amount of 3 uL of P. aeruginosa DNA each. Tubes

3A and 3B were both mixed with an amount of 3 uL of nuclease-free water each, for NTC. The reactions were run in triplicates of 10 uL, using Roche wells in the Roche LightCycler 96, for 1 hour at 65. This experiment was repeated for E. coli and GBS, and GBS and P. aeruginosa PolyT primers analytical specificity test.

#### *4.2.6 Droplet generation*

The protocol was adapted from Anyaduba et. al.<sup>21</sup> The microfluidic chip design was used for droplet generation by flow focusing technique. In this method, a mineral oil mixture (Sigma Aldrich M3516-1L), 0.1 wt % Triton X-100 (Fisher Biotech), and 3 wt % ABIL EM 90 (Evonik, Germany), known as the continuous phase, and a mixture of 0.1 % Tween 20 (BP337-100 Fisher Scientific) in water, known as the dispersed phase, were introduced into the cartridge using syringe pumps at 30 uL/min and 1 uL/min respectively.

#### *4.2.7 Microparticle functionalization with generic capture oligo PolyA primer*

The streptavidin-functionalized polystyrene microparticles are washed and resuspended in 200 uL of TBST. An amount of 10 uL of biotinylated capture oligo polyA with 3' biotin, primer was incubated at 60 C for 1 minute and was added to the microparticles mixture. The microparticles mixture was incubated at room temperature while shaking at 1000 g, for 1 hour. The microparticles were washed 3 times with 200 uL TBST and resuspended in 200 uL TBST. An amount of 1 uL of PolyT ATTO 633 primers which was incubated at 60 C for 1 minute, was added to a 10 uL aliquot of the functionalized microparticles. The mixture was incubated at room temperature while shaking at 1000 g, for 4 hours. The microparticles were then washed 3 times in 10 uL TBST and resuspended in 10 uL TBST. The microparticles were visualized under confocal microscopy for the fluorescence of ATTO 633 (figure 4.5 A-C).

#### *4.2.8 DNA capture test PCR*

An amount 10uL of functionalized microparticles were washed 3 times with 10 uL TBST, and suspended in 10 uL TBST. An aliquot of 1 uL of PolyT E. coli BOP primer incubated at 68 C for 1 minute. The PolyT E. coli BOP primer was added to the microparticle suspension. The mixture was incubated at 28 C 1 hour. The microparticles were washed 3 times in 10 uL TBST and resuspended in 10 uL nuclease-free water. An amount of 1.1 uL of 100 copies E. coli DNA was incubated at 95 C for 1 minute. The DNA was then added to the 10 uL microparticle suspension and the mixture was incubated at 28 C for 1 hour. The tube was labeled as S1-DNA. An aliquot of 1.1 uL of 100 copies E. coli DNA mixed 10 uL of nuclease-free water in a tube and the tube was labelled S2-DNA. A PCR mixture of 0.9 uL Evagreen, 45 uL PCR mastermix, 0.45 uL of E. coli FOP primer, 0.45 uL of E. coli FIP primer, 0.36 uL bovine serum albumin, and 33.8 uL of nuclease-free water was created. The mixture was aliquoted into 3 tubes, 27 uL each. The tubes were labeled, S1, S2 and NTC. An amount of 3 uL of the supernatant of S1-DNA was mixed into tube S1. 3 uL of the content of S2-DNA was mixed into tube S2 and 3 uL of nuclease-free water was mixed into tube NTC. The contents of tubes S1, S2 and NTC were split into 10 uL aliquots, into PCR reaction tubes. The tubes were put in the Roche LightCycler and the PCR profile was run according table S4.3.

#### *4.2.9 DNA capture by microparticles*

A primer solution (E. coli, GBS, or P. aeruginosa) was prepared according to Table 1. The primer solution was incubated at 60 C for 1 minute and added to the generic capture oligo PolyA-functionalized microparticles. The mixture was incubated at room temperature while shaking at 1000 g, for 4 hours. The microparticles were washed 3 times with 200 uL

TBST and resuspended in 200 uL TBST. An aliquot of 10 uL of the target DNA, 2ng/uL, (E. coli, GBS, or P. aeruginosa) was incubated at 95 C for 3 minutes to facilitate heat-mediated DNA strand separation. The melted DNA was immediately added to the microparticles mixture. The final DNA concentration was  $1.94 \times 10^4$  copies/uL. The mixture was gently vortexed for 2 seconds and mixture was incubated at room temperature while shaking at 1000 g, overnight. The microparticles were washed 3 times with 200 uL TBST and resuspended in 200 uL TBST. The resulting solution comprised of functionalized microparticles with captured DNA (figure 4.1). The experiment was repeated using E. coli DNA at a final concentration of  $9.71 \times 10^3$  copies/uL and 194 copies/uL.

#### *4.2.10 Microparticle encapsulation*

The mineral oil mixture was maintained as the continuous phase. The dispersed phase was a mixture of 20 um PMMA microparticle in of 0.01 % in water (or 40 um polystyrene microparticles in LAMP reagent for microparticle-in-droplet dLAMP). The dispersed phase was loaded into 3 mL syringe with a built-in impeller, powered by a 1.5 V power pack. The continuous phase and dispersed phase were run at flow rates of 50 uL/min and 1 uL/min respectively, to form droplets by flow focusing (figure 4.2).

#### *4.2.11 Microparticle-in-droplet dLAMP*

The microparticles mixture with captured DNA was used as the dispersed phase in the microparticle encapsulation protocol. The microparticle encapsulated droplets were incubated at 68 C for 1 hour for the LAMP reaction to occur. The droplets were visualized by confocal microscopy.

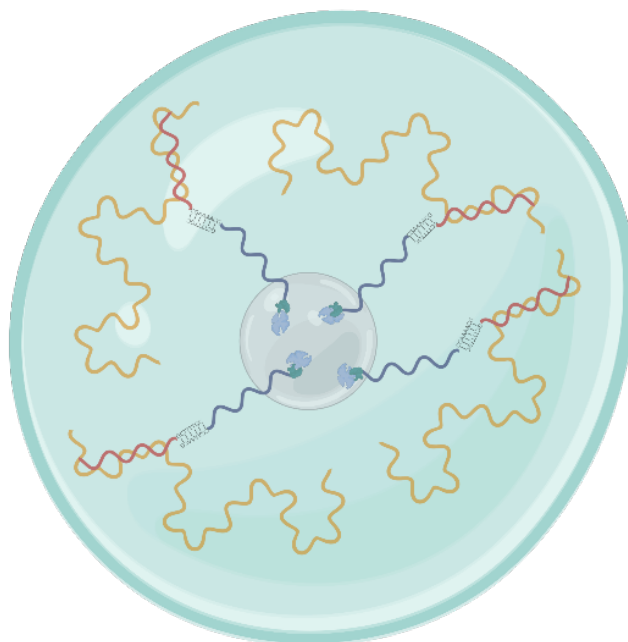


*Figure 4.2 Schematic of a functionalized microparticle with captured DNA, encapsulated in a droplet of LAMP reagents for droplet LAMP reaction.*

### 4.3 Results and discussion

#### *4.3.1 Comparison of 5' PolyT modified inner primers (FIP and BIP) with middle PolyT modified FIP and BIP LAMP*

The positive control represented the LAMP amplification curve using unmodified E. coli primers. The C<sub>q</sub> of the positive control was 7. The mean C<sub>q</sub> of the LAMP reaction using the PolyT modified E. coli primers with the FIP and BIP that has the PolyT modification in the middle of the sequence was 10 (figure 4.3). The reaction with the FIP and BIP with middle sequence modification delayed the reaction by only 3 cycles, compared to the positive control. The LAMP reaction using the PolyT modified E. coli primers with the FIP and BIP that has the PolyT modification at the 5' end of the sequence showed no amplification. This is because the 5' ends of the FIP and BIP primers are critical in the

LAMP reaction (figure S4.2). The 5' overhang of the FIP and BIP complementary to the F1 and B1 regions, respectively, of the target sequence. The 5' overhang of the FIP and BIP bind to the F1 and B1 regions, respectively, in the ninth step of the LAMP reaction, and form dumbbell structures that are an important intermediate for the continuance of the LAMP reaction. Therefore, the presence of the barcode at the 5' ends of the FIP and BIP primers inhibits the progression of the LAMP reaction past the dumbbell structure formation (figure S4.3).

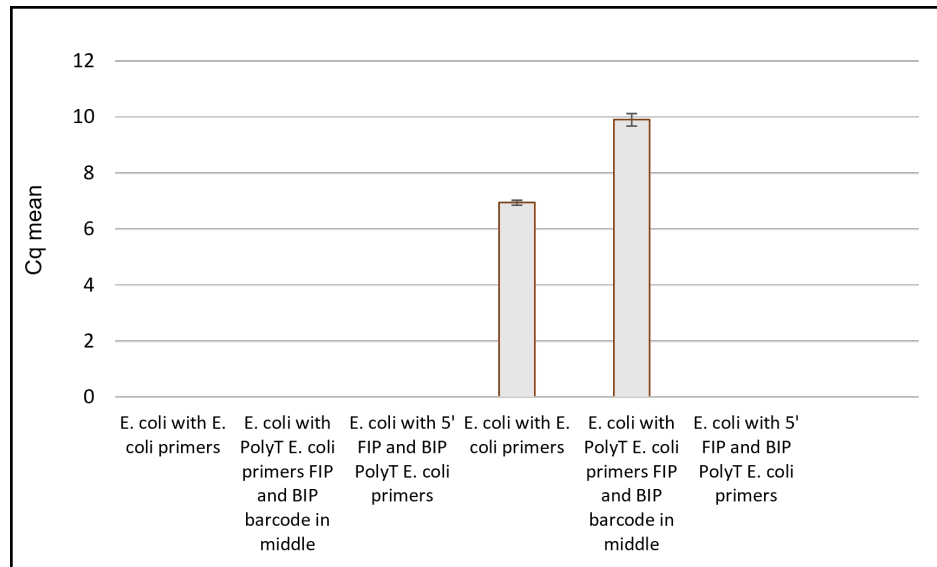


*Figure 4.3 The impact of the PolyT modification of E. coli primers on their sensitivity in a LAMP reaction. The placement of the PolyT modification in the FIP and BIP primers are crucial.*

#### 4.3.2 E. coli, GBS, and P. aeruginosa PolyT primers analytical specificity LAMP

The LAMP reaction was run to evaluate the analytical specificity of the E. coli, GBS and P. aeruginosa polyT primers (table S4.1). The positive controls for the reactions, E. coli DNA with E. coli polyT primers, GBS DNA with GBS polyT primers, and P. aeruginosa

DNA with *P. aeruginosa* primers. All the positive control reactions showed amplifications. There were no amplifications in any of the reactions with a mismatch primer-target pair. This demonstrated that there was a 100% analytical specificity of the polyT primers against these 3 targets common to UTIs.

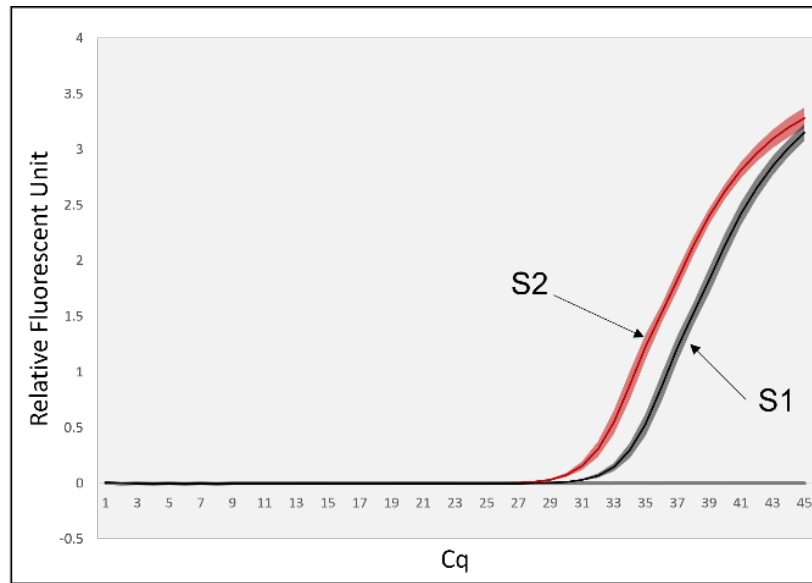


*Figure 4.4 PCR reaction testing the ability of the functionalized microparticles to capture their target DNA.*

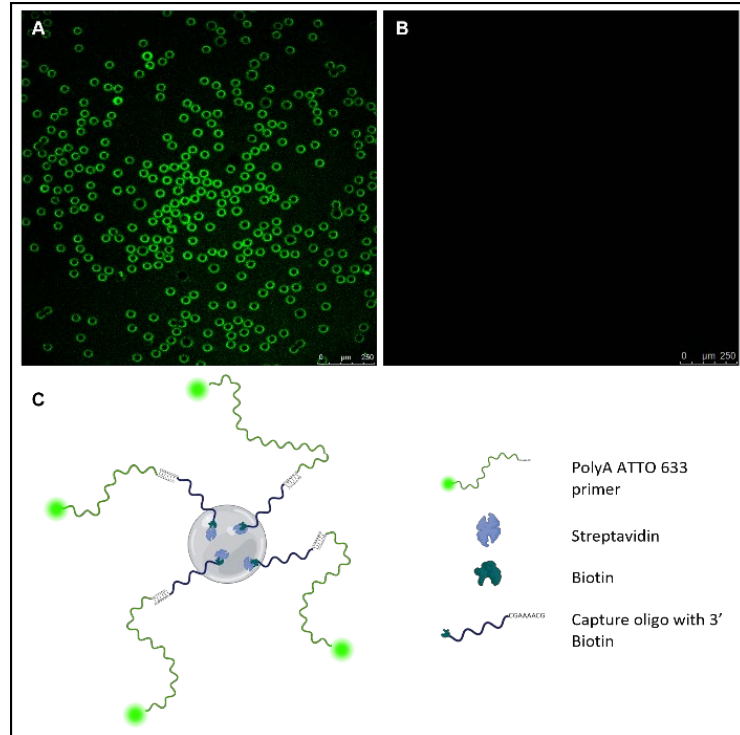


Figure 4.5 A. Pseudo-colored confocal microscopy fluorescent image of microparticles functionalized with ATTO 633 primers. B. Confocal image of microparticles that are not functionalized with ATTO 633 primers. C. Schematic of a microparticle functionalized with ATTO 633 polyT primers.

#### 4.3.3 Microparticle functionalization with generic capture oligo PolyA primer

The presence of the green pseudo-colored fluorescence on the microparticles (figure 4.5 A and B) showed that they the ATTO 633 primers were successfully sequestered from solution and concentrated onto the microparticles. The fluorescence observed is the fluorescence of the ATTO 633 excited by a laser at 633 nm wavelength.

#### 4.3.4 DNA capture test PCR.

The positive control reaction (S1) for the DNA capture test amplification of the E. coli DNA with a Cq mean of 31 (figure 4.4). The test reaction (S2) showed amplification of E.

coli DNA with a Cq mean of 33. This demonstrated that the functionalized microparticles in S2 captured a proportion of the E. coli DNA molecules and sequestered them from the solution. There was therefore a 2-cycle delay in the S2 reaction compared to the control reaction (S1) as a result of the deficit of DNA due to the net sequestered DNA by the microparticles.

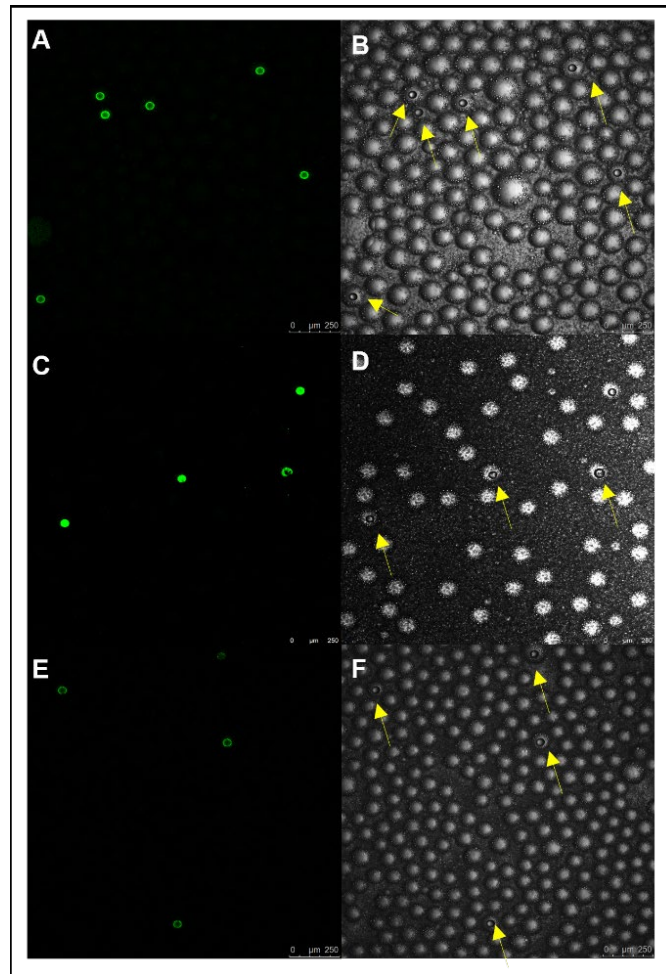


*Figure 4.6 A. Fluorescent and B. Brightfield images of droplet LAMP with microparticles functionalized with E. coli DNA and E. coli primers. C. Fluorescent and D. Brightfield images of droplet LAMP with microparticles functionalized with P. aeruginosa DNA and*

*P. aeruginosa primers. E. Fluorescent and F. Brightfield images of droplet LAMP with microparticles functionalized with GBS DNA and GBS primers.*

#### *4.3.5 Microparticle encapsulation and Microparticle-in-droplet LAMP*

The beads in the droplets fluoresced when excited with a laser at 488 nm (Evagreen Ex/Em = 500nm/530nm). The beads that were functionalized with *E. coli* primers and incubated with *E. coli* DNA at a for capture, showed fluorescence when visualized by confocal microscopy (figure 4.6 A and B). Similarly, the beads that were functionalized with *P. aeruginosa* primers and incubated with *P. aeruginosa* DNA for capture, showed fluorescence when visualized by confocal microscopy (figure 4.6 C and D). Furthermore, in the experiment where microparticles were functionalized with GBS primers, and incubated with GBS DNA, there was fluorescence when the microparticles were visualized under the confocal microscope (figure 4. 6 E and F). This indicates that the target DNA was captured on the beads and amplified in the droplets.

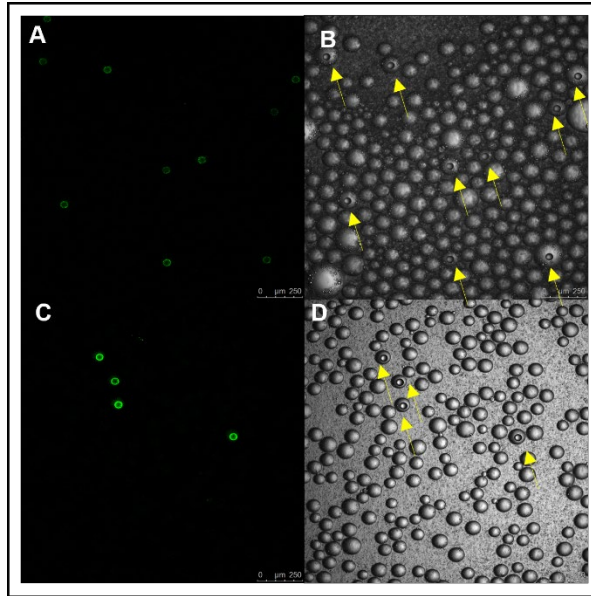


*Figure 4.7 A. Fluorescent and B. Brightfield images of droplet LAMP with microparticles functionalized with E. coli DNA (194 copies/uL) and E. coli primers. A. Fluorescent and B. Brightfield images of droplet LAMP with microparticles functionalized with E. coli DNA ( $9.71 \times 10^3$  copies/uL) and E. coli primers.*

The microparticle-in-droplet LAMP experiment was repeated using a final E. coli DNA concentration of  $9.71 \times 10^3$  copies/uL and 194 copies/uL (figure 4.7 A-D). The fluorescence on the microparticles when functionalized with E. coli DNA at a concentration of  $9.71 \times 10^3$  copies/uL, was readily observable. At E. coli DNA concentration of 194 copies/uL, the microparticle-in droplet assay showed a positive results for E. coli detection. However, the fluorescence was not as bright as the assay with E. coli DNA concentration of  $9.71 \times 10^3$  copies/uL.

In a cross-reactivity test, beads that were functionalized with E. coli primers and incubated with GBS DNA for capture, did not show any amplification (figure 4.8 A and B). Also, beads that were functionalized with GBS primers and incubated with E. coli DNA for

capture, did not show any amplification (figure 4.8 C and D). We also repeated the cross-reactivity test between *E. coli* and *P. aeruginosa*, and GBS and *P. aeruginosa* targets. There was no cross amplification. This demonstrated that the beads were extremely specific to their target and there was no cross-reactivity (figure 4.8 E to L).

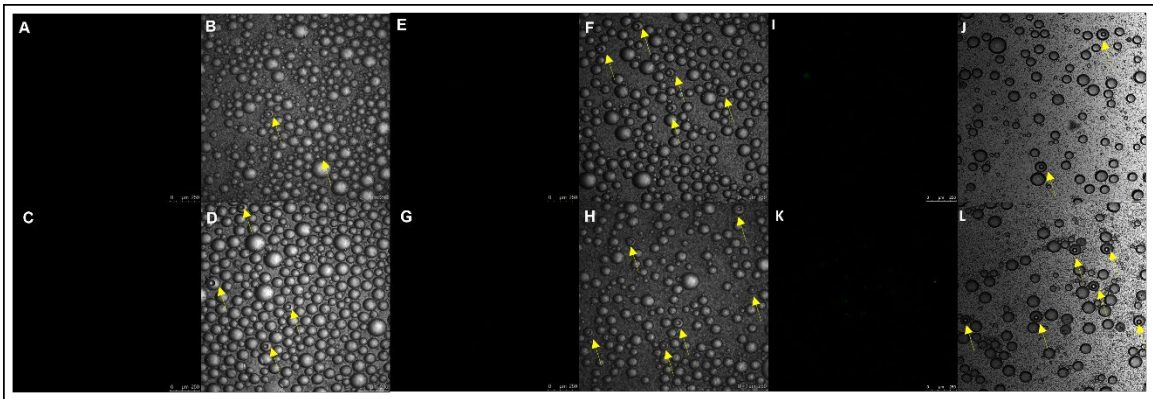


*Figure 4.8 A. Fluorescent and B. Brightfield images of droplet LAMP with microparticles functionalized with GBS DNA ( $1.94 \times 10^4$  copies/uL) and E. coli primers. C. Fluorescent and D. Brightfield images of droplet LAMP with microparticles functionalized with E. coli DNA ( $1.94 \times 10^4$  copies/uL) and GBS primers. E. Fluorescent and F. Brightfield images of droplet LAMP with microparticles functionalized with P. aeruginosa DNA ( $1.94 \times 10^4$  copies/uL) and GBS primers. G. Fluorescent and H. Brightfield images of droplet LAMP with microparticles functionalized with GBS DNA ( $1.94 \times 10^4$  copies/uL) and P. aeruginosa primers. I. Fluorescent and J. Brightfield images of droplet LAMP with microparticles functionalized with E. coli DNA ( $1.94 \times 10^4$  copies/uL) and P. aeruginosa primers. K. Fluorescent and L. Brightfield images of droplet LAMP with microparticles functionalized with P. aeruginosa DNA ( $1.94 \times 10^4$  copies/uL) and E. coli primers.*

#### 4.4 References

- (1) Gourgeon, A.; Soulier, A.; Audureau, É.; Khouider, S.; Galbin, A.; Langlois, C.; Bouvier-Alias, M.; Rodriguez, C.; Chevaliez, S.; Pawlotsky, J.-M.; Fourati, S. Performance of 22 Rapid Lateral Flow Tests for SARS-CoV-2 Antigen Detection and Influence of “Variants of Concern”: Implications for Clinical Use. *Microbiol Spectr* **2022**, *10* (4), e01157-22. <https://doi.org/10.1128/spectrum.01157-22>.
- (2) Di Nardo, F.; Chiarello, M.; Cavalera, S.; Baggiani, C.; Anfossi, L. Ten Years of Lateral Flow Immunoassay Technique Applications: Trends, Challenges and Future Perspectives. *Sensors* **2021**, *21* (15), 5185. <https://doi.org/10.3390/s21155185>.
- (3) Ye, X.; Li, Y.; Wang, L.; Fang, X.; Kong, J. All-in-One Microfluidic Nucleic Acid Diagnosis System for Multiplex Detection of Sexually Transmitted Pathogens Directly from Genitourinary Secretions. *Talanta* **2021**, *221*, 121462. <https://doi.org/10.1016/j.talanta.2020.121462>.
- (4) Pandey, C. M.; Augustine, S.; Kumar, S.; Kumar, S.; Nara, S.; Srivastava, S.; Malhotra, B. D. Microfluidics Based Point-of-Care Diagnostics. *Biotechnol. J.* **2018**, *13* (1), 1700047. <https://doi.org/10.1002/biot.201700047>.
- (5) Falzone, L.; Musso, N.; Gattuso, G.; Bongiorno, D.; Palermo, C. I.; Scalia, G.; Libra, M.; Stefani, S. Sensitivity Assessment of Droplet Digital PCR for SARS-CoV-2 Detection. *International Journal of Molecular Medicine* **2020**, *46* (3), 957–964. <https://doi.org/10.3892/ijmm.2020.4673>.
- (6) Notomi, T. Loop-Mediated Isothermal Amplification of DNA. *Nucleic Acids Research* **2000**, *28* (12), 63e–663. <https://doi.org/10.1093/nar/28.12.e63>.

- (7) Nagamine, K.; Hase, T.; Notomi, T. Accelerated Reaction by Loop-Mediated Isothermal Amplification Using Loop Primers. *Molecular and Cellular Probes* **2002**, *16* (3), 223–229. <https://doi.org/10.1006/mcpr.2002.0415>.
- (8) Mayboroda, O.; Katakis, I.; O’Sullivan, C. K. Multiplexed Isothermal Nucleic Acid Amplification. *Analytical Biochemistry* **2018**, *545*, 20–30. <https://doi.org/10.1016/j.ab.2018.01.005>.
- (9) Kermekchiev, M. B.; Kirilova, L. I.; Vail, E. E.; Barnes, W. M. Mutants of Taq DNA Polymerase Resistant to PCR Inhibitors Allow DNA Amplification from Whole Blood and Crude Soil Samples. *Nucleic Acids Res* **2009**, *37* (5), e40. <https://doi.org/10.1093/nar/gkn1055>.
- (10) Francois, P.; Tangomo, M.; Hibbs, J.; Bonetti, E.-J.; Boehme, C. C.; Notomi, T.; Perkins, M. D.; Schrenzel, J. Robustness of a Loop-Mediated Isothermal Amplification Reaction for Diagnostic Applications. *FEMS Immunol Med Microbiol* **2011**, *62* (1), 41–48. <https://doi.org/10.1111/j.1574-695X.2011.00785.x>.
- (11) Moonga, L. C.; Hayashida, K.; Kawai, N.; Nakao, R.; Sugimoto, C.; Namangala, B.; Yamagishi, J. Development of a Multiplex Loop-Mediated Isothermal Amplification (LAMP) Method for Simultaneous Detection of Spotted Fever Group Rickettsiae and Malaria Parasites by Dipstick DNA Chromatography. *Diagnostics* **2020**, *10* (11), 897. <https://doi.org/10.3390/diagnostics10110897>.
- (12) Li, N.; Lu, Y.; Cheng, J.; Xu, Y. A Self-Contained and Fully Integrated Fluidic Cassette System for Multiplex Nucleic Acid Detection of Bacteriuria. *Lab Chip* **2020**, *20* (2), 384–393. <https://doi.org/10.1039/C9LC00994A>.

- (13) Nguyen, H. Q.; Bui, H. K.; Phan, V. M.; Seo, T. S. An Internet of Things-Based Point-of-Care Device for Direct Reverse-Transcription-Loop Mediated Isothermal Amplification to Identify SARS-CoV-2. *Biosensors and Bioelectronics* **2022**, *195*, 113655. <https://doi.org/10.1016/j.bios.2021.113655>.
- (14) Rane, T. D.; Chen, L.; Zec, H. C.; Wang, T.-H. Microfluidic Continuous Flow Digital Loop-Mediated Isothermal Amplification (LAMP). *Lab Chip* **2015**, *15* (3), 776–782. <https://doi.org/10.1039/c4lc01158a>.
- (15) Dong, Y.; Zhao, Y.; Li, S.; Wan, Z.; Lu, R.; Yang, X.; Yu, G.; Reboud, J.; Cooper, J. M.; Tian, Z.; Zhang, C. Multiplex, Real-Time, Point-of-Care RT-LAMP for SARS-CoV-2 Detection Using the HFman Probe. *ACS Sens.* **2022**, *7* (3), 730–739. <https://doi.org/10.1021/acssensors.1c02079>.
- (16) Tanner, N. A.; Zhang, Y.; Evans, T. C. Simultaneous Multiple Target Detection in Real-Time Loop-Mediated Isothermal Amplification. *BioTechniques* **2012**, *53* (2), 81–89. <https://doi.org/10.2144/0000113902>.
- (17) Jang, W. S.; Lim, D. H.; Yoon, J.; Kim, A.; Lim, M.; Nam, J.; Yanagihara, R.; Ryu, S.-W.; Jung, B. K.; Ryoo, N.-H.; Lim, C. S. Development of a Multiplex Loop-Mediated Isothermal Amplification (LAMP) Assay for on-Site Diagnosis of SARS CoV-2. *PLOS ONE* **2021**, *16* (3), e0248042. <https://doi.org/10.1371/journal.pone.0248042>.
- (18) Kim, J. H.; Kang, M.; Park, E.; Chung, D. R.; Kim, J.; Hwang, E. S. A Simple and Multiplex Loop-Mediated Isothermal Amplification (LAMP) Assay for Rapid Detection of SARS-CoV. *BioChip J* **2019**, *13* (4), 341–351. <https://doi.org/10.1007/s13206-019-3404-3>.

- (19) Fang, X.; Chen, H.; Yu, S.; Jiang, X.; Kong, J. Predicting Viruses Accurately by a Multiplex Microfluidic Loop-Mediated Isothermal Amplification Chip. *Anal. Chem.* **2011**, *83* (3), 690–695. <https://doi.org/10.1021/ac102858j>.
- (20) Liang, C.; Chu, Y.; Cheng, S.; Wu, H.; Kajiyama, T.; Kambara, H.; Zhou, G. Multiplex Loop-Mediated Isothermal Amplification Detection by Sequence-Based Barcodes Coupled with Nicking Endonuclease-Mediated Pyrosequencing. *Anal. Chem.* **2012**, *84* (8), 3758–3763. <https://doi.org/10.1021/ac3003825>.
- (21) Anyaduba, T.; Otoo, J.; Schlappi, T. Picoliter Droplet Generation and Dense Microparticle-in-Droplet Encapsulation via Microfluidic Devices Fabricated via 3D Printed Molds. *Micromachines* **2022**, *13* (11), 1946. <https://doi.org/10.3390/mi13111946>.
- (22) Schoepp, N. G.; Schlappi, T. S.; Curtis, M. S.; Butkovich, S. S.; Miller, S.; Humphries, R. M.; & Ismagilov, R. F. (2017). Rapid pathogen-specific phenotypic antibiotic susceptibility testing using digital LAMP quantification in clinical samples. *Science translational medicine*, *9*(410), eaal3693.

#### 4.5 Supplementary Information

## Primer payload with microparticles for pathogen identification using Polythymidine modified LAMP primers in droplet LAMP (dLAMP)

Jonas A. Otoo, Tochukwu D. Anyaduba, Katie Wilson, Travis S. Schlappi\*

Table S 4-1 Primer Sequences

Detail	Sequence
P. aeruginosa polyT FIP	TCG CCC ACT TCG CGC AGT GGG AAC TTT <b>GCT TTT TTT GCTTT</b> CCG TCG CCA CAA CAA GG
P. aeruginosa polyT BIP	GAC CGA TGG CTC CGG CAC CGA ATT <b>GCT TTT TTT GCTTC</b> AAC TGA AGT GGA TGT TGC TGA
P. aeruginosa polyT FOP	<b>GCT TTT TTT GCCCA</b> TGA ACT ACG CCT GAC CA
P. aeruginosa polyT BOP	<b>GCT TTT TTT GCCGC</b> TTG GCC AGG ATG TCC
P. aeruginosa polyT LoopF	<b>GCT TTT TTT GCGCC</b> GTG GTG GTA GAC CTG T
P. aeruginosa polyT LoopB	<b>GCT TTT TTT GCGTT</b> CAC TTC AAG CCG TCC CCG
E. coli polyT FIP	CGG TTC GGT CCT CCA GTT AGT GTT TT <b>GCT TTT TTT GC</b> C CCG AAA CCC GGT GAT CT
E. coli polyT FOP	<b>GCT TTT TTT GCGGC</b> GTT AAG TTG CAG GGT AT
E. coli polyT BIP	TAG CGG ATG ACT TGT GGC TGG TT <b>GCT TTT TTT GC</b> T TTC GGG GAG AAC CAG CTA TC
E. coli polyT BOP	<b>GCT TTT TTT GCTCA</b> CGA GGC GCT ACC TAA
E. coli polyT LoopF	<b>GCT TTT TTT GCGTG</b> AAA GGC CAA TCA AAC C
E. coli polyT LoopB	<b>GCT TTT TTT GCACC</b> TTC AAC CTG CCC ATG
5' modified E. coli polyT BIP	<b>GCT TTT TTT GCCCG</b> TTC GGT CCT CCA GTT AGT GTT TTC CCG AAA CCC GGT GAT CT
GBS polyT FOP	<b>GCT TTT TTT GC</b> GTGGGGAGCAAACAGGATT
GBS polyT BOP	<b>GCT TTT TTT GC</b> CCTGGTAAGGTTCTTCGCG
GBS polyT FIP	CGGCGACTAAGCCCGGAAAGTTTT <b>GCT TTT TTT GC</b> GTAGTCCACGCCGTAAACG
GBS polyT BIP	CTGGGGAGTACGACCGCAAGTTTT <b>GCT TTT TTT GC</b> CATGCTCCACCGCTTGTG
GBS polyT LoopF	<b>GCT TTT TTT GC</b> GGCCTAACACCTAGCACTCA
GBS polyT LoopB	<b>GCT TTT TTT GC</b> GTTGAAACTCAAAGGAATTGACGG
5' modified E. coli polyT FIP	<b>GCT TTT TTT GCTAG</b> CGG ATG ACT TGT GGC TGG TTT TTC GGG GAG AAC CAG CTA TC
Capture oligo with 3' Biotin	GCA AAA AAA GCA AAA GTC AC/3Bio/

PolyT sequences shown in red.

*Table S 4-2 Primer dilution for 100 uL final volume*

<b>Primer/Reagent</b>	<b>Volume (uL)</b>
FIP	32
BIP	32
BOP	4
FOP	4
LoopF	8
LoopB	8
Nuclease-free water	12

All primer stock solutions are 100uM in concentration.

*Table S 4-3 PCR profile*

<b>Step</b>	<b>Temperature</b>	<b>Duration</b>
Initial Denaturation	95 C	2 min
Denaturation	95 C	15 s
Annealing	61 C	30 s
Elongation	72 C	30 s
Melt Curve	95 C – 55 C – 95 C	NA

Denaturation, Annealing and Elongation steps were cycled 45 times

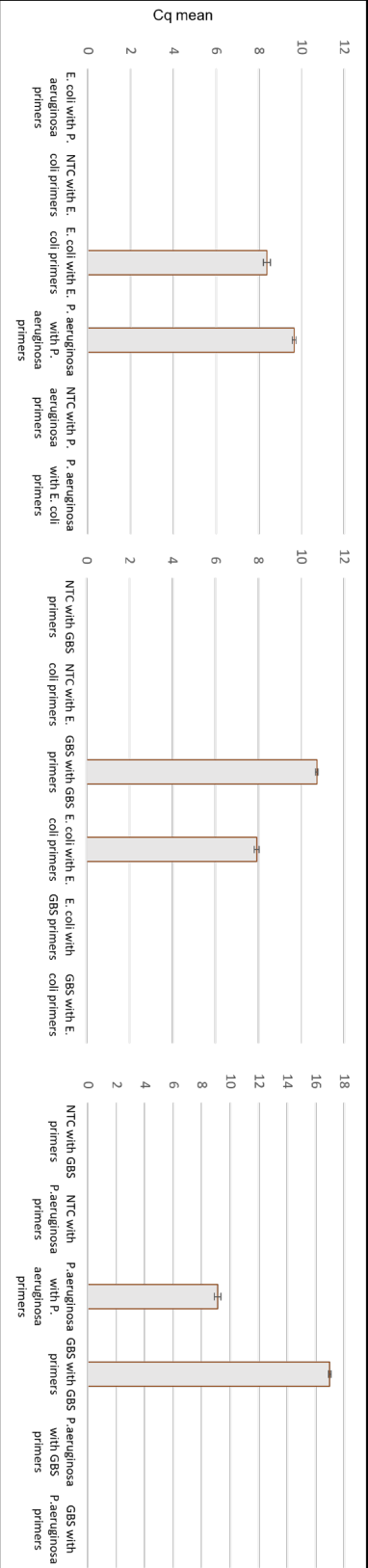


Figure S 4.1 Testing the analytical specificity of *E. coli* polyT primers and *P. aeruginosa* polyT primer. B. Testing the analytical specificity of *E. coli* polyT primers and GBS polyT primer. C. Testing the analytical specificity GBS polyT primers and *P. aeruginosa* polyT primer.

## Loop-Mediated Isothermal Amplification (LAMP)

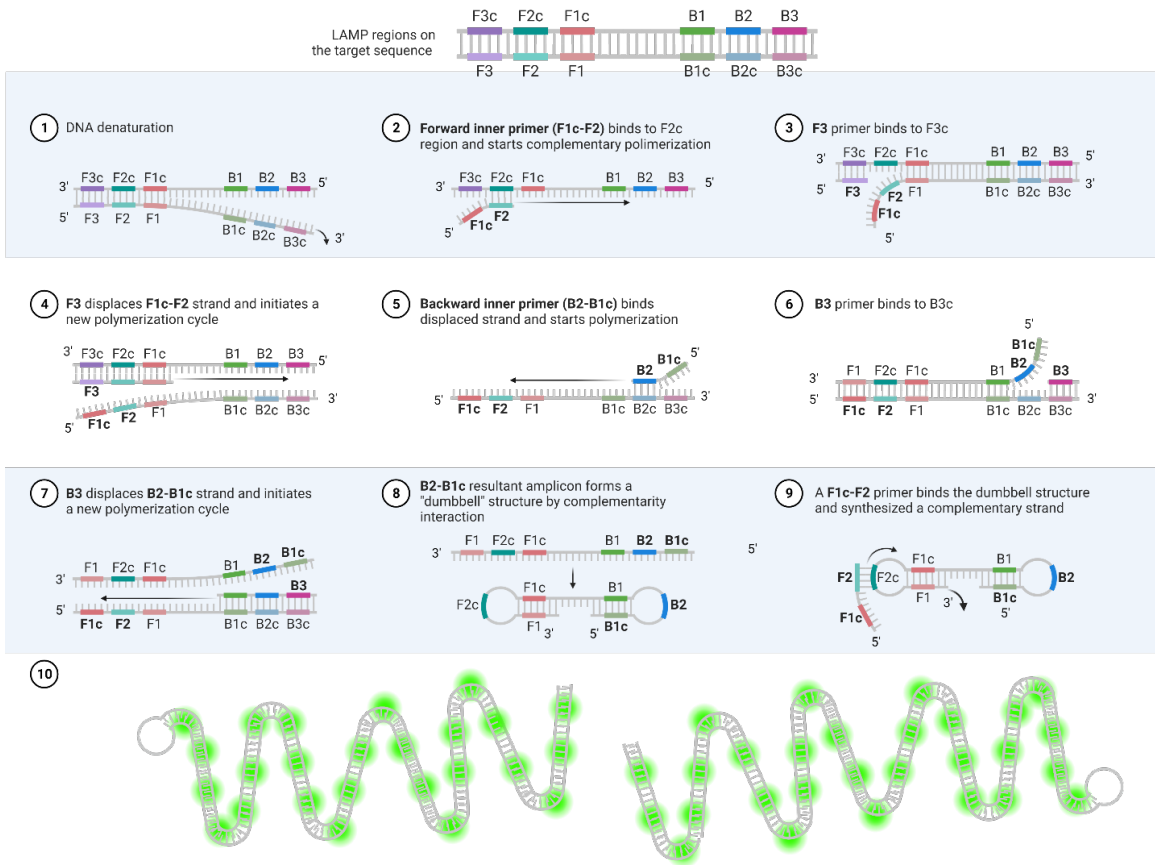


Figure S 4.2 Schematic LAMP reaction

## Loop-Mediated Isothermal Amplification (LAMP)

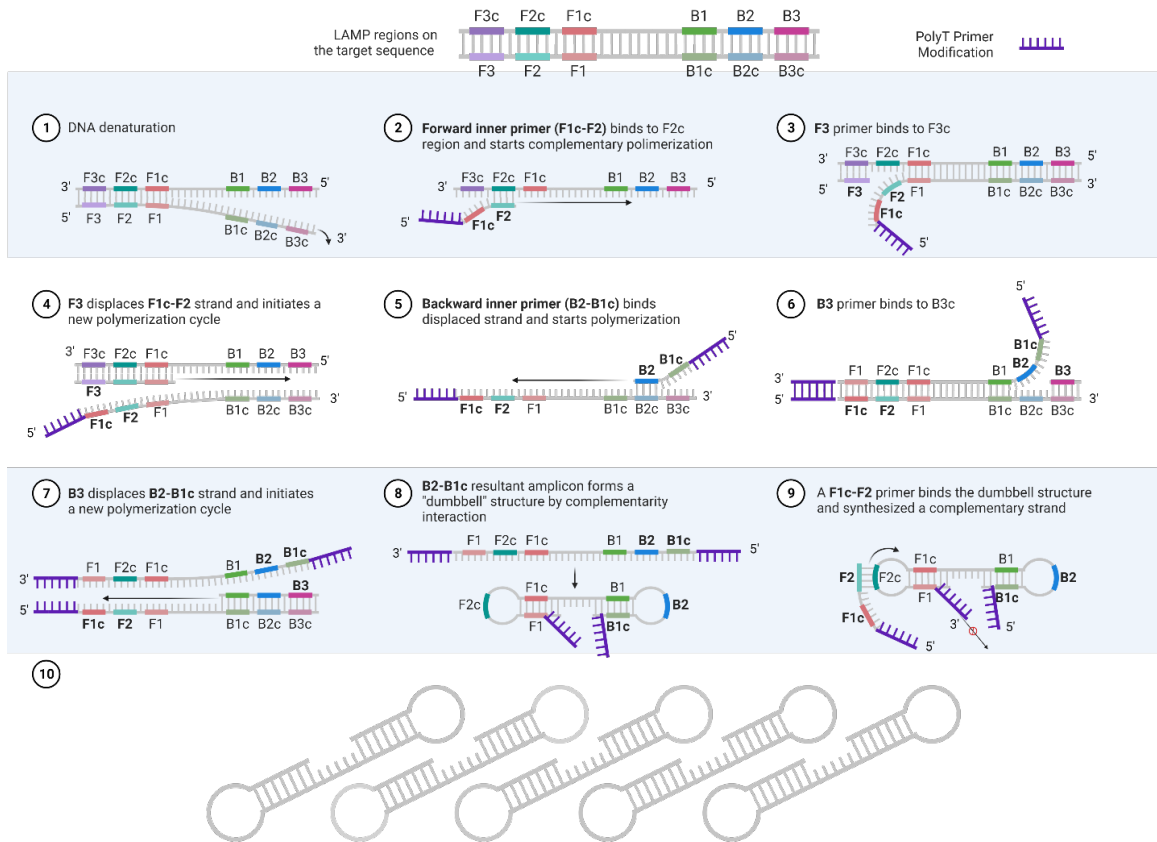
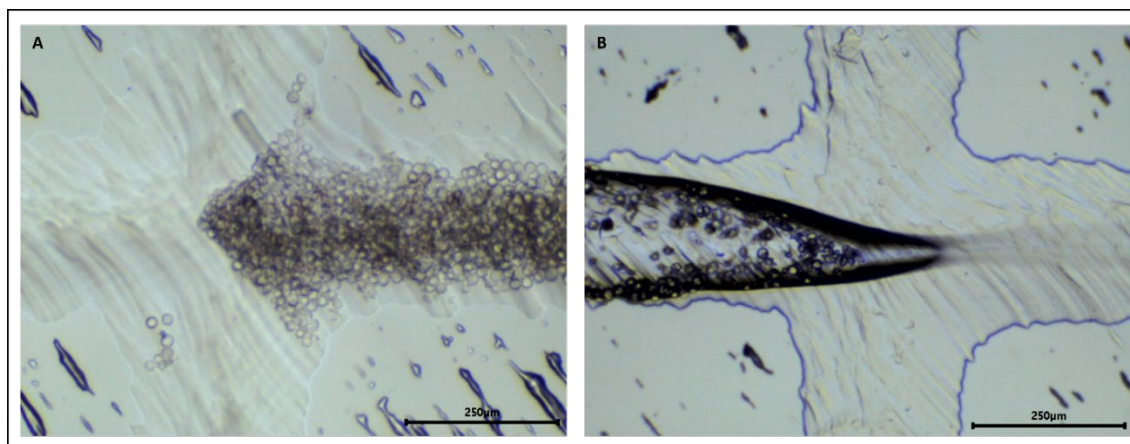


Figure S 4.3 Schematic of LAMP reaction with PolyT primers. The reaction stops at step 9 when the PolyT modification of FIP and BIP are placed at the 5' end.

## Chapter 5 Challenges and Other Projects

### 5.1 PMMA beads encapsulation

My initial experiments with bead encapsulation involved using PMMA beads with a size of 20  $\mu\text{m}$  obtained from PolyAn, Germany. PMMA has a density of 1.18  $\text{g}/\text{cm}^3$ , which caused the beads to settle in the microfluidic cartridge's syringe, tubes, and channels during the encapsulation process. The bead encapsulation was performed according to the method stated in section 3.2.5. To overcome this issue, measures such as increasing the flow rate and impeller speed were implemented to push the PMMA beads through the cartridge. However, increasing the flow rate resulted in bead accumulation and cartridge clogging (figure 5.1 A), leading to high pressure buildup that damaged the syringe and cartridge. Increasing the impeller speed also led to increased agitation and bead collision, causing breakage of the beads (figure 5.1 B).



*Figure 5.1 A. Microfluidic cartridge channel clogged with 20  $\mu\text{m}$  PMMA beads. B. Broken PMMA beads in the microfluidic cartridge channel going into being encapsulated into droplets.*

To address the issue of bead breakage, I utilized computer-aided design and 3D printing technology to create a backward-pointing blade impeller made of silicone, a softer material. Although this solution worked, it did not resolve the problems of bead sedimentation and channel blockage. As a result, I switched to using 40  $\mu\text{m}$  polystyrene beads, which have a density range of 0.96-1.05  $\text{g}/\text{cm}^3$ . The lower density of the polystyrene beads meant that a higher flow rate was not necessary for them to move through the cartridge's tubes and channels. Furthermore, I employed the use of a density matching reagent (OptiPrep, Stemcell Technologies, USA) to keep the particles suspended and the mixture homogenous. At a 16.5% Optiprep concentration, the microparticle sedimentation rate was successfully slowed and the mixture remained homogenous figure (5.2 A and B). I was also able to achieve single bead-in-droplet encapsulation without the use of our syringe mixer (figure 5.2 C).

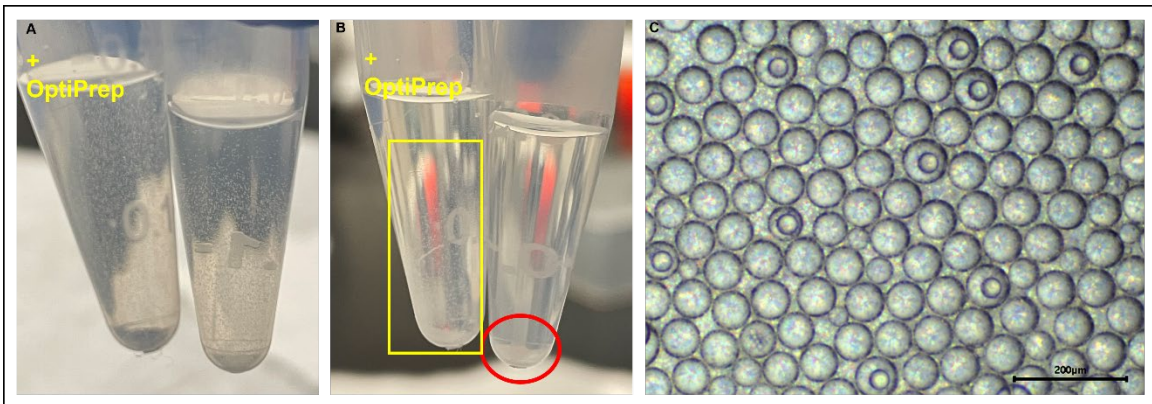


*Figure 5.2 A. Comparing the sedimentation rate of microparticles in 16.5% Optiprep in water versus microparticles in just water. B One hour into comparing the sedimentation rate of microparticles in 16.5% Optiprep in water versus microparticles in just water. C. Microparticle-in-droplet encapsulation with 16.5% Optiprep.*

## 5.2 Gel beads primer payload delivery

The objective of this project was to produce dissolvable polyacrylamide hydrogel beads for use as a primer payload. We synthesized the gel beads according to the method by Wang et al, with one modification. [1] We eliminated the barcoding step. We postulated that we could load primers into the matrix of polyacrylamide hydrogel beads, which would act as carriers for DNA capture and delivery into droplet emulsions for amplification. To release the primer and DNA into the droplets, the polyacrylamide hydrogel would be dissolved with DTT. Additionally, we proposed to use dyes to color-code the gel beads according to specific DNA targets, which would aid in multiplex pathogen identification. We successfully synthesized the polyacrylamide hydrogel and demonstrated that we could dissolve the hydrogel beads with DTT at a concentration that did not inhibit LAMP. However, the hydrogels we synthesized using our channel dimensions were too large for our intended application, with minimum sizes larger than our ideal size of approximately 40  $\mu\text{m}$  in diameter (figure 5.3). We hypothesize that using smaller channels will facilitate the synthesis of hydrogels of the desired diameter.

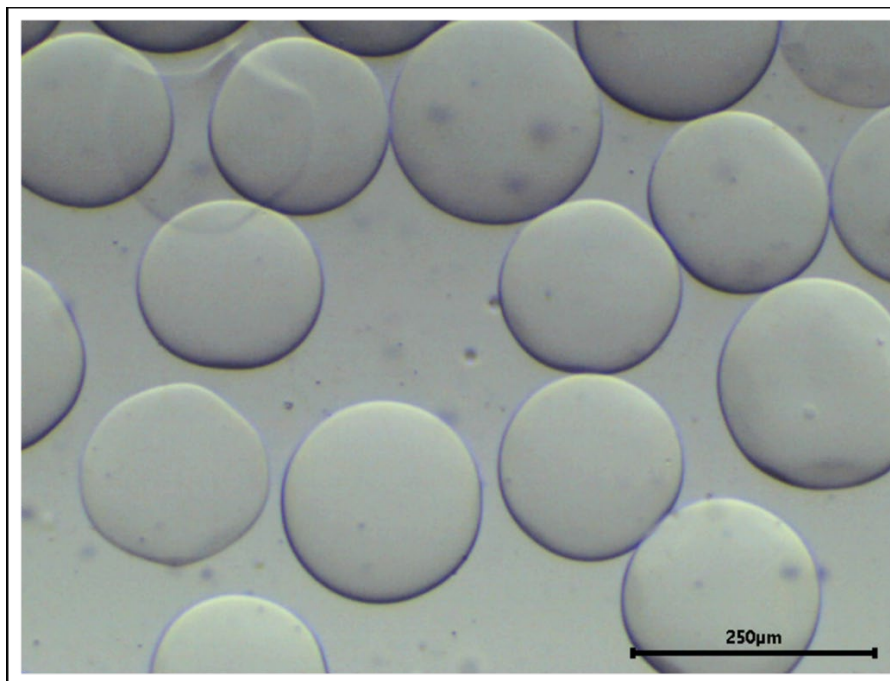


*Figure 5.3 Dissolvable polyacrylamide gel beads.*

### 5.3 Colorimetric droplet LAMP

The objective of this project was to create a colorimetric droplet LAMP assay that could be read visually without the use of complicated equipment like a confocal microscope. We prepared a LAMP master mix using the dLAMP protocol from section 3.2.3, but with a modification where Eriochrome black T (EBT) was used as the indicator dye instead of EvaGreen. We used a mixture of 2 weight % 008-FluoroSurfactant (RAN Biotechnologies, USA) in HFE7500 instead of mineral oil. During the LAMP reaction, pyrophosphates produced by nucleotide incorporation form precipitates with  $Mg^{2+}$  ions, depleting the  $Mg^{2+}$  ions from the solution. EBT (purple) releases its  $Mg^{2+}$  ions into the solution, leading to a color change from purple to blue. However, we did not observe a visual color change with the droplet LAMP when using EBT as the indicator dye (figure 5.4 A). This is likely due to the small size of the droplets and the low concentration of EBT. According to Beer-

Lambert's law, the color intensity is directly proportional to the length of the light path (in this case, the droplet diameter) and the concentration of the EBT. We realized that at higher concentrations of beyond 0.1mM, EBT started to inhibit the LAMP reaction.

$$A = \epsilon cl \quad \text{Beer-Lambert equation}$$

$A$  = Absorbance

$\epsilon$  = Molar absorptive coefficient

$c$  = Concentration

$l$  = Optical path length

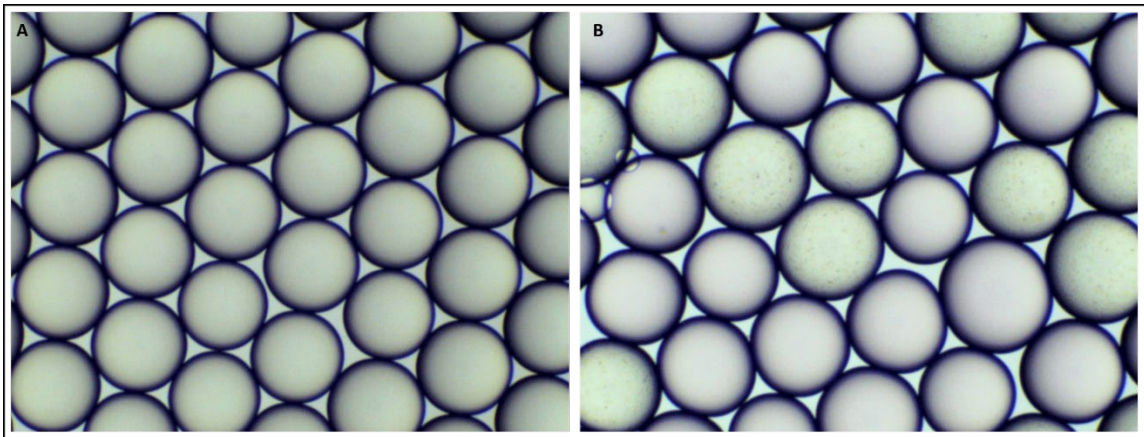


*Figure 5.4 A. Droplet LAMP using Eriochrome Black T (EBT) as indicator showing no color change. B. Droplet LAMP using NEB colorimetric LAMP master mix, showing faint pink (no DNA amplification) droplets and faint yellow (presence of DNA amplification) droplets.*

An attempt was made to conduct colorimetric LAMP by employing the WarmStart® Colorimetric LAMP 2X Master Mix (New England BioLabs, USA) reagent as the master

mix, using the dLAMP protocol according section 3.2.3. This particular reagent is sensitive to the pH changes that occurs during a LAMP reaction and manifests a color transition from pink to yellow. A distinction in color was observed between the negative and positive droplets (figure 5.4 B). Nevertheless, due to the picoliter scale diameter of the droplets, the visual perception of the color intensity was not readily discernible.

#### 5.4 Multiplexed bead-in-droplet LAMP

Having demonstrated the proof of concept that our assay is able to achieve primer payload delivery and DNA amplification via droplet LAMP, we attempted to execute a multiplex reaction. The first challenge was obtaining 40 um streptavidin coated fluorescent beads. We were unable to find a vendor with off the shelf 40 um streptavidin coated fluorescent beads in their catalogue. A few companies were willing to custom produce the beads for us at up to \$10,000 per vial. We resorted to using 40 um carboxylate beads with the plan to coat them with streptavidin in-house, via 1-Ethyl-3-(3-dimethylaminopropyl)carbodiimide (EDC) chemistry method adapted from Kurdekar et al, [2]. We were successful in coating carboxylate transparent beads with streptavidin. We tested the streptavidin coated beads with biotinylated fluorescent probes (ATTO 633 probe). The fluorescence of the beads when observed under confocal microscopy denoted that they streptavidin on the beads bonded to the biotin on the biotinylated ATTO 633 probe (figure 5.5 A and B).

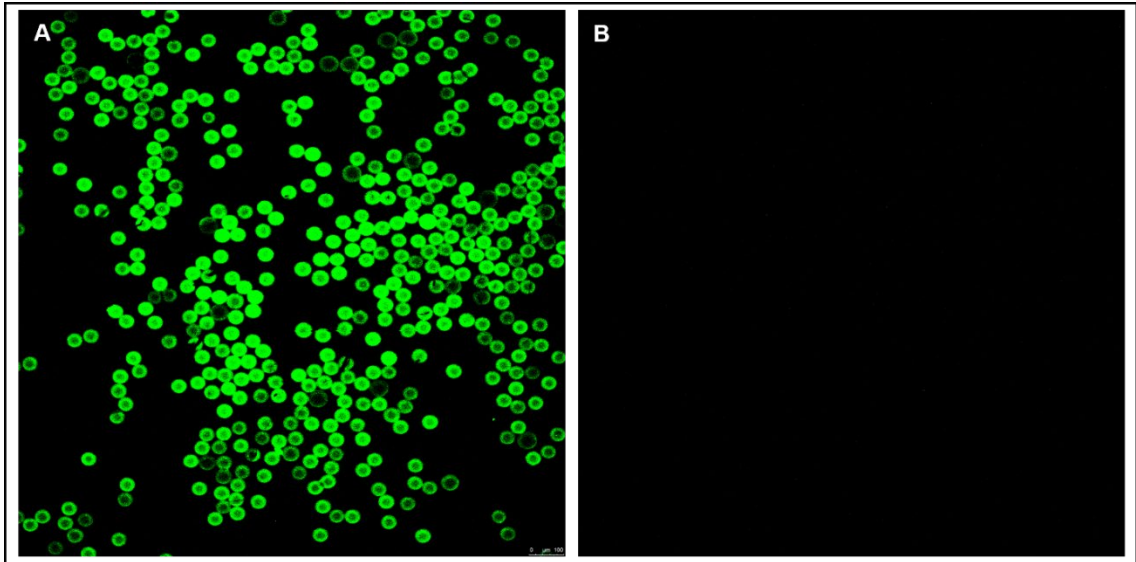


*Figure 5.5 A. Streptavidin coated beads functionalized with biotinylated ATTO 633 primers and visualized under confocal microscopy. B. Non-functionalized bead visualized under fluorescent microscopy, for negative control.*

However, the attempt to coat the fluorescent beads with streptavidin posed challenges. The fluorescent material on the surface of the beads, increased its hydrophobicity. This caused the beads to come of solution and to form a precipitate on the sides of the reaction tubes (figure 5.6). The fluorescent beads also had an increased buoyancy and hence, they floated on the surface of the reagents in the reaction tube.

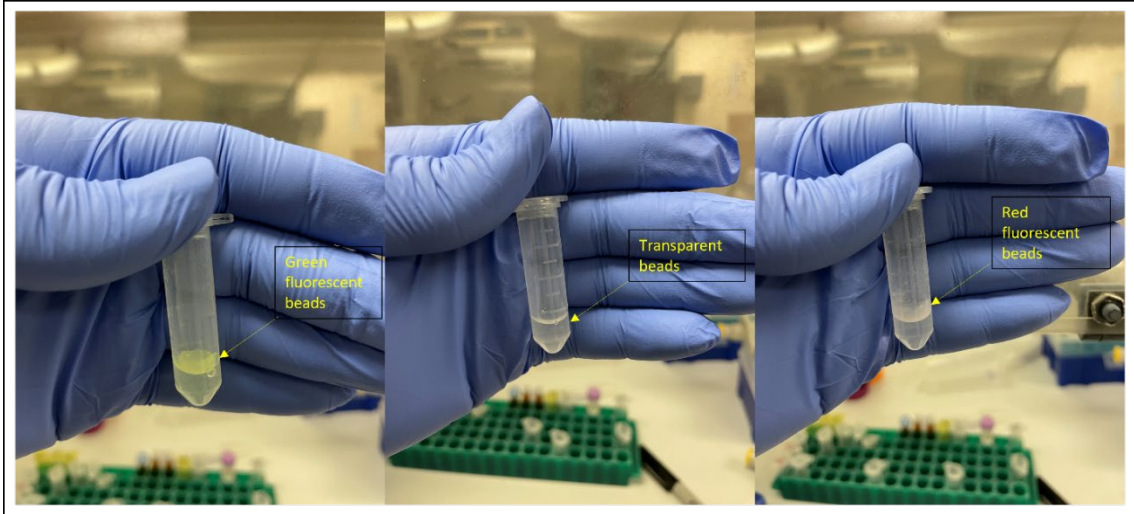


*Figure 5.6 Depicting the behavior of fluorescent beads in the reaction tube compared to the transparent beads.*

## 5.5 Reference

- [1] Y. Wang *et al.*, “Dissolvable Polyacrylamide Beads for High-Throughput Droplet DNA Barcoding,” *Adv. Sci.*, vol. 7, no. 8, p. 1903463, Apr. 2020, doi: 10.1002/advs.201903463.
- [2] A. D. Kurdekar, L. A. Avinash Chunduri, C. S. Manohar, M. K. Haleyurgirisetty, I. K. Hewlett, and K. Venkataramaniah, “Streptavidin-conjugated gold nanoclusters as ultrasensitive fluorescent sensors for early diagnosis of HIV infection,” *Sci. Adv.*, vol. 4, no. 11, p. eaar6280, Nov. 2018, doi: 10.1126/sciadv.aar6280.

## Chapter 6 Conclusion

### 6.1 Conclusion

There were three main aims of this project. They were;

- To develop processes for isothermal nucleic acid amplification in droplet-bead emulsions.
- To create a POC-compatible microfluidic cartridge to execute the processes.
- To conduct preliminary verification of the device using extracted DNA.

#### *6.1.1 Develop processes for isothermal nucleic acid amplification in droplet-bead emulsions*

We successfully developed an assay for isothermal nucleic acid amplification in droplet-bead emulsions. With inspiration from overhang PCR and mRNA sequencing technique, we modified LAMP primers with a polythymidine selection sequence that facilitated primer payload and DNA target delivery into picolitre-scale droplets for amplification by LAMP.

#### *6.1.2 Create a POC-compatible microfluidic cartridge to execute the processes*

We developed a low cost microfluidic cartridge for droplet generation. Computer-aided design (CAD) techniques was used to design a mold which was printed using a 3D printer. The 3D-printed mold was used to cast PDMS for fabrication of a microfluidic cartridge by bonding onto glass slides, using flame treatment surface activation.

#### *6.1.3 Preliminary verification of the device using extracted DNA*

Preliminary verification of the assay and device was conducted using extracted DNA targets. DNA of three common UTI pathogens, *E. coli*, *P. aeruginosa*, and Group B

Streptococcus, were used to verify the assay and device. Our assay was also successful in detecting E. coli DNA at a concentration of 194 copies/uL.

## 6.2 Recommendation

The cross-reactivity experiments demonstrate that our assay has high analytical specificity. A potential future continuation of this project is to explore the use of microparticles with different fluorescent signatures. The fluorescent signatures of the microparticles may serve as barcodes for different pathogens in order to achieve a one pot, higher order multiplexing pathogen identification, without sample splitting.

Furthermore, a potential future direction of this project will be to optimize the assay in order to eliminate complex equipment such as a thermal cycler and confocal microscope, through the use of a simple heater and the development of a colorimetric detection method. It is also important that the reagents are optimized so that they are viable at room temperature and would not require refrigeration.

Finally, another potential future direction of this project, will be to explore the integration of the microfluidic device to execute the various steps of the assay. Integrating the steps from sample preparation through amplification, to detection, will enable this assay and device satisfy the REASSURED criteria by the WHO. This will make it truly suitable for POC setting.